AFCRL-63-701

SEISMIC WAVES GENERATED BY CHEMICAL EXPLOSIONS

Carl Kisslinger, Emil J. Mateker, Jr., and Thomas V. McEvilly

SAINT LOUIS UNIVERSITY
INSTITUTE OF TECHNOLOGY
3621 Olive Street, St. Louis, Missouri

FINAL REPORT

AF 19(604)-7402
Project 8652
Task 865201

31 July 1963

Prepared

for

Air Force Cambridge Research Laboratories
Office of Aerospace Research
United States Air Force
Bedford, Massachusetts

WORK SPONSORED BY ADVANCED RESEARCH PROJECTS AGENCY

PROJECT VELA-UNIFORM

ARPA Order No. 180-61, Amendment 2
Project Code No. 8100, Task 2

AFCRL-63-701

(5) 4538 00

(6) SEISMIC WAVES GENERATED BY CHEMICAL EXPLOSIONS.

(10) by Carl Kisslinger, Emil J Mateker, Jr., and Thomas V. McEvilly.

Saint Louis University
Institute of Technology
3621 Olive Street, St. Louis, Missouri

FINAL REPORT

AF 19(604)-7402
Project 8652
Task 865201

31 July 1963

Prepared
for

AIR FORCE CAMBRIDGE RESEARCH LABORATORIES
OFFICE OF AEROSPACE RESEARCH
UNITED STATES AIR FORCE
BEDFORD, MASSACHUSETTS

WORK SPONSORED BY ADVANCED RESEARCH PROJECTS AGENCY

PROJECT VELA-UNIFORM

(16) Proj. 8653; ARPA Order No. 180-61, Amendment 2
Project Code No. 8100, Task 2

NOTICES

Requests for additional copies by Agencies of the Department of Defense, their contractors, and other Government agencies should be directed to the:

DEFENSE DOCUMENTATION CENTER (DDC)
CAMERON STATION
ALEXANDRIA, VIRGINIA.

Department of Defense contractors must be established for DDC services or have their 'need-to-know' certified by the cognizant military agency of their project or contract.

All other persons and organizations should apply to the:

U. S. DEPARTMENT OF COMMERCE
OFFICE OF TECHNICAL SERVICES
WASHINGTON 25, D. C.

Table of Contents

List of Figures

List of Tables

SEISMIC WAVES GENERATED BY CHEMICAL EXPLOSIONS

Summary and Recommendations.

This report describes the results of research on some fundamental properties of seismic waves generated by chemical explosions. The work was carried out between August 1, 1960 and July 31, 1963. In the course of the program, seismograms from some 160 small charges, one 500 pound surface burst, one 100 ton surface charge, and a buried charge of 10 tons were recorded at close range. The experiments involving the small charges were designed to elucidate a variety of aspects of the generation of seismic waves by explosive sources. The principal subjects investigated were:

1) The properties of source functions obtained by phase equalization of dispersed surface waves recorded at close range;
2) The effect on surface waves of distributing the charge in space and time;
3) The effect of source depth on the properties of the compressional and Rayleigh waves;
4) The effect of the medium at the shot on the properties of the seismic signal;
5) The properties of the horizontally polarized shear waves generated by an explosion.

Most of the objectives of the work were accomplished. In some cases the techniques employed were not totally adequate to completely solve the problem under investigation. On the other hand, some interesting areas for further study are suggested by some of the results.

Some of the principal conclusions of the work are:

1) Even at close range, the spectrum of the observed surface waves may be so narrow that the computed source function is oscillatory. The peak of the spectrum may remain at the same frequency over a wide range of charge sizes, suggesting that the shot-point medium and the geologic layering may exert an influence on the radiated surface waves that overrides the expected effect of yield. The difficulty of interpreting the calculated source function in terms of simple force systems acting at the origin is clearly demonstrated by the results.

2) When a distributed explosion is fired so that there is no interaction of the component detonations in the non-linear region around each charge, simple superposition will give the radiation of the Rayleigh wave. Time delays associated with the spatial distribution, as well as those between detonations must be taken into account. The orientation of maxima and minima of Rayleigh wave

amplitudes may be controlled as desired by this technique. Superposition is simplified in this case because the radiation of Rayleigh waves from a single point charge is completely symmetric at the test site at which the experiments were conducted, eliminating the necessity of considering an azimuthally dependent amplitude function in the motion synthesis. The distribution of Love waves around a point charge is complicated, so that numerical superposition of the output from a number of charges is difficult. The gross properties of the Love waves from a distributed charge seem to be explained by simple superposition.

3) The effect of shot depth on the body wave properties cannot be separated easily from the effect of changing material properties with depth. The amplitude measured directly above the source from a series of 0.5 pound shots in clay approximated a decay law of $d^{-1.5}$. The prolonged, oscillating P-motion observed from shots at various depths in clay is the result of the combined effect of the primary reflections from the near-surface boundaries and the oscillatory nature of the P-wave emanating from the source.

The effect on the Rayleigh wave of increasing the shot depth is to decrease the amplitude. High-gain filtered records from shots at various depths in

clay contain long period motion in the region immediately over the source. The period is that of the Rayleigh wave observed at distance. The presence of long period motion directly over the source supports a hypothesis similar to that proposed by Dix for the generation of long waves from an explosion.

4) Horizontally polarized shear waves are always produced by a buried explosion. The portion of the total seismic energy that is transmitted in this form is primarily a function of the medium, with shots in competent brittle materials producing proportionally larger shear waves.

Love waves are radiated with marked azimuthal variation of amplitude, marked by nodal lines and clear-cut reversal in polarity of the entire waveform in different directions outward from the source. The waves are thought to be produced directly by the shot as a result of non-linear processes, such as cracking, in the highly stressed material near the explosion.

SH motion is also produced by mode conversion at non-horizontal boundaries and apparent SH motion may result from compressional head waves refracted at dipping interfaces. Short period transverse horizontal motion is often seen beginning with very

small amplitude at the same time as, or immediately after, the onset of the first compressional motion. The origin of this motion is unexplained. It is found on the records from small explosions in this research, as well as seismograms of events from the Nevada Test Site.

The shear body wave propagating directly from the source has been recorded at locations directly above buried shots. It is identified by particle motion and velocity.

Recommendations. The experiments carried out under this project and the analysis of the data have served to elucidate a number of properties of explosion-generated seismic waves. When a seismologist has obtained a record of the ground motion due to any seismic source, he knows that the record contains valuable information concerning the physics of the wave-generating mechanism, and wave propagation, as well as data pertinent to the determination of the properties of the medium through which the waves have traveled to the seismograph. The decision as to the best manner in which to proceed to extract this information is often a difficult one. A variety of methods were applied in this work, and the results are of value in evaluating the various approaches.

Even though the records have been analyzed in detail for the particular phenomenon under study in each case, they

undoubtedly contain much more information that can be exploited in future work. At this time, there seems to be no point in further extensive experimental programs using small charges unless a true breakthrough in instrumentation provides a means of gaining new data, especially in the high-stress region near the shot. On the other hand, specific experiments designed to test particular hypotheses will be very desirable, and these small charges provide an inexpensive and rapid means of collecting the data. Currently, under Contract AF 19(628)-1689, model studies using very small explosive charges are being conducted, and these may prove to be a superior method of gathering information.

It is recommended that a series of experiments in which the charge size is increased several orders of magnitude over those used here be considered under the VELA-Uniform program. In particular, a sequence of one thousand pound spherical or short cylindrical high-explosive charges, fired at depths from 1000 feet below the surface, at intervals, up to a shot on the free surface, and even 10 feet or so above the surface, would be of great value. The site for such an experimental series should be in a region of flat topography, underlain by flat-lying beds, with no significant structural changes over an area of many square miles. A site in the Great Plains seems most promising. If such a series is conducted, it should be heavily instrumented, and will require the cooperative participation of

several laboratories.

A further recommendation is that all underground nuclear shots be recorded with three-component seismographs at short range and many azimuths. The value of such data for studying wave generation is made abundantly clear by the results of this research.

CHAPTER 1

INTRODUCTION

Studies of fundamental properties of seismic waves generated by explosions, and of some of the parameters affecting these properties, have been carried out by the Department of Geophysics and Geophysical Engineering of St. Louis University, under Contract AF 19(604)-7402.

An understanding of the mechanism by which a buried explosion generates seismic waves, and the manner in which the variable factors involved in the detonation affect wave generation is essential to the solution of one of the critical aspects of the VELA-Uniform effort, viz., the identification of a recorded seismic event as an earthquake or an explosion. In full-scale tests, instrumentation to measure the response of the earth in the zone of elastic behavior usually must be so far out that ordinary variations in geology and topography between the source and the recording site play an important role in determining the character of the seismogram. In the face of a number of undetermined variable parameters, the isolation of the effect of any one is difficult. While small chemical explosions can never be a complete substitute for full-scale tests in seismological research, they do offer the possibility of scaling down the experiment so that it is practical to have uniform known geology from shot point to seismograph.

In this research, over a period of three years, a

total of some 160 small charges, 0.25 to 15 pounds at positions from 38 meters below the surface to 3 meters above it, have been fired and the resulting ground motion measured at distances of 0 to 250 meters. All seismograms were recorded on the earth's surface, although subsurface measurements would have been desirable in some cases. The media in which the shots were fired were loess, clay, alluvium, sandstone, and limestone. Details of the experiments, instrumentation, description of the test sites, and field procedures are presented in Chapter II.

One of the criteria suggested for distinguishing between an earthquake and an explosion is the character of the source function found by phase equalization of dispersed surface waves. Although details of the time history of the force applied at the source cannot be recovered in this way, the initial polarity and type of force (impulse, step, etc.,) can in principle be determined. The properties of the source functions obtained under a variety of conditions for shots in soil have been investigated, and are described in Chapter III.

In an earthquake, especially one of large magnitude in which a fault length of hundreds of kilometers may be involved, a point source is an inadequate representation of the wave-generating mechanism, and the effect on the seismic signal of the moving source must be taken into account in a careful analysis. To simulate a moving source,

several shots were fired in which the charge was distributed in a number of holes and fired sequentially. The resulting radiation patterns of Rayleigh waves are described in Chapter IV, while the effect on Love waves is presented in Chapter V on explosion-generated SH motion.

Early in the research, it was established that horizontally polarized shear waves (SH waves) are a normal result of a buried explosion fired under a wide variety of conditions. While this result is unfortunate from the viewpoint of distinguighing between explosions and earthquakes, it has stimulated further thought by several investigators on the nature of a contained explosion as a seismic source. An explosion is essentially a center of compression with spherical symmetry, but this model is inadequate to explain the details of the resulting seismic waves.

The effect of source depth on the generation of compressional and Rayleigh waves, and some observations on the effect of the medium around the shot are discussed in Chapter VI.

Two large chemical explosions, one of 100 tons of TNT fired as an experiment of the Canadian Defense Research Board at the Suffield Experimental Station, and one of 10 tons of Tovex fired near Poplar Bluff, Missouri, were recorded as part of the research program. The results are discussed in the Appendix.

The assistance of the staff of the Suffield Experimental

Station, Ralston, Alberta, and in particular Mr. G.H.S. Jones, seismologist, in carrying out the observations at their test site is gratefully acknowledged. Gratitude is also expressed to the managements of the Alpha Portland Cement Company quarry, Lemay, Missouri, and Pioneer Silica Company, Augusta, Missouri, for permission to carry out experiments in their quarries.

CHAPTER II

THE EXPERIMENTAL PROGRAM

All of the field experiments carried out under the research program are summarized in Table I. The experiments are organized according to the test site at which they were conducted. For all except the tests at Suffield Experimental Station (SES) the explosive used was forty per cent gelatin dynamite, in one-half pound sticks, eight inches long by one and one-eighth inch diameter. At SES, Nitrone was used. In the Table, the column headed "Array" describes the disposition of the instrumentation as follows: "P" indicates a profile in line with the shot point, and the numbers following give the range of shot-to-detector distances covered by the profile; "A" indicates azimuthal coverage at a fixed distance from the shot point, and the numbers following give the angle subtended by the array and the distance.

Description of the Test Sites.

Four test sites were used. A wider variety of media was originally planned, but detailed knowledge of the geology and the properties of the waves at a site are of such importance in interpreting the experiments, it was judged advisable to concentrate the effort into these few sites. The materials selected are representative of media in which test explosions are likely to be fired, although data for shots in crystalline igneous rocks would have been useful. The results for the shots in compact crystalline limestone

are probably applicable to chemical explosions in igneous intrusives of fine to medium texture. Because the equation of state of the material in the range of hydrodynamic behavior is important in determining the response to a nuclear shot, caution must be observed in carrying over the results for carbonate rocks to aggregates of feldspar and quartz.

Florissant Test Site. The Florissant Test Site is an open field on the grounds of St. Stanislaus Seminary, Florissant, Missouri. Located in T 47 N, R 6 E, in St. Louis County, the site is roughly a mile from the Missouri River. The surface material is loess, underlain by Pleistocene silts and clays. The bedrock is Mississippian limestone, at a depth of 33 to 45 meters. Clay densities of 1.2 to 2.0 gm/cm^3 occur above the water table, and about 2.2 gm/cm^3 below. At about 25 meters depth the clay changes from stiff to very stiff (Kisslinger, 1959).

Alpha Test Site. The Alpha Test Site is the quarry operated by the Alpha Portland Cement Company in Lemay, Missouri. It is located in the northeast quarter of Section 26, T 44 N, R 6 E, St. Louis County. The exposed limestone is the St. Louis formation, of Middle Mississippian age. The rock is a dense, hard limestone, varying from lithographic to finely crystalline in texture. Chert nodules are widespread. Over part of the quarry floor the surface rock is almost purely calcitic, in other parts it

is dolomitic. The average density is 2.67 gm/cm^3. (Kisslinger, 1953).

Augusta Test Site. The Augusta Test Site is a quarry in the St. Peter sandstone, located along the bluffs of the Missouri River in T 44 N, R 1 E, St. Charles County, Missouri. The St. Peter sandstone is a very pure silica sand of Middle Ordovician age. The well-rounded grains are poorly cemented. The grain size is uniform, 0.12 - 0.25 mm. The density is 1.8 to 2.0 gm/cm^3.

In order to avoid interference with quarrying operations, all of the experiments were confined to one bench, some 300 meters long and 20 to 50 meters wide. About 25 meters of sandstone lay under the level at which the tests were conducted.

Suffield Test Site. The Suffield Test Site is on and adjacent to the Watching Hill Blast Range of the Suffield Experimental Station of the Canadian Defense Research Board, Ralston, Alberta. It is located approximately 25 miles northwest of Medicine Hat, in T 17 N and T 18 N, R 5 W. At the site, approximately 64 meters of silts and clays, interbedded with gravels, overlay the Cretaceous Foremost formation. The Foremost is made up of brackish-water deposits of interbedded light gray sandstones, dark gray shales and coal seams, pale yellow silts, and rusty-colored concretionary banks. The densities of the surface silts and clays are low, less than 2 gm/cm^3. (Russell and Landes, 1940; Crock-

ford, 1949).

Instrumentation.

The project can be divided into two phases on the basis of the instruments employed. During the first year, five Sprengnether three-component portable seismographs were available. For the last two years (starting with shot point 48), a sixth standard Sprengnether, a very low-magnification Sprengnether, and a 12 channel low frequency electronic refraction system were added.

The Sprengnether Three-Component Portable Seismograph. This instrument was the primary tool of this research program. It is a simple mechanical-optical seismograph, incorporating all three components, the timer, and camera into one easily emplaced box. (Figure 1). Some modification of the standard instrument was required to meet the needs of the project. A system was developed so that all units could be turned on from a single remote control point and various methods of putting the shot firing time on each record were tried. The zero-time device was never completely reliable, and it is fortunate that much of this work required waveforms rather than very precise travel times. During the last two years of the work, better timing was obtained by tying the first breaks to the records from the high-gain refraction system.

The natural undamped period of all seismometer elements is 0.75 second, and all components are damped to 0.55 crit-

FIGURE I

SPRENGNETHER THREE-COMPONENT

PORTABLE SEISMOGRAPH

ical by a conventional damping vane - magnet arrangement. All but the very low magnification instrument are equipped with dual magnification, in which, by simple optical doubling, a high gain, twice the low value, is available.

The low magnification instrument, in which the mirror is mounted directly on the pendulum for each component, has a static magnification of 7.5. This proved very useful for measurements directly over shots buried as shallow as three meters, and for observations close to the 100 ton and 10 ton shots.

The standard instruments are actually of two different generations. Three of them, Numbers 3, 4 and 5, are old instruments that were reworked for the purpose of this program. They are characterized by a higher magnification of the vertical component than the horizontals. The vertical components on two of these were marked by high frequency noise which was eventually traced to the camera motor. This noise is on the records for almost all of the shots.

When the case within which the seismograph is mounted is subjected to strong shock, as in some of these close-in experiments, the panels of the case vibrate, and these parasitic vibrations show up on the seismograms. This situation was improved in two of the instruments by lining the entire inside of the case with Y-9052 Scotch Foam Vibration Damping Tape. A number of reproducibility tests were carried

out (see Table I) which aided in distinguishing between true ground motion and instrument noise.

The static magnifications (Low) of all components in the new instruments (Numbers 1, 2, and 6) are nominally 50. More precise values were determined by tilt-test calibration. For the older instruments, the horizontal components have magnifications of about 90, and the verticals about 145. High magnifications are twice these values. When the instruments are operated on high magnification, the direction of motion on the vertical component only is reversed from the sense on low magnification.

The SIE GTR 200 Low Frequency Refraction System. A 12 channel unit identical to that developed for the crustal studies program of the United States Geological Survey was purchased from Dresser Electronics, SIE Division (Warrick, et al, 1961). The geophones selected were 1.0 cps units (EV-12) built by Electro-Technical Laboratories. The performance of the system was satisfactory for the close-in measurements program.

Six horizontal component 1 cps geophones (EV-17H) from Electro-Technical Laboratories were acquired toward the end of the contract. Because of a failure in the GTR 200 system it was not possible to make any records with these seismometers. They will prove useful in future observations to be made under a continuation of this research under another contract.

The response characteristics of the GTR 200 are given in the paper by Warrick, et al, cited above. Galvanometric recording only was used.

Data Processing.

The field records were converted to digital form almost as a routine practice. The digitalization was accomplished with a system developed by Data Instruments Co., of North Hollywood, California. The heart of the system is a unit known as the Telecordex Type 8G, which accepts the output from magnetic shaft position encoders, and puts out digital information to a typewriter or an IBM Key Punch. Two scanning devices were used, one a micrometer microscope on which shaft position encoders were mounted, the other a Type 099D4 Data Reducer from Data Instruments. The Data Reducer has a reading precision of 157 counts per centimeter of record. The microscope offers a precision of 15700 counts per centimeter of record, and was used for most of the work on the records from small explosions. The microscope also offered optical magnification of ten times, which was of great value in interpreting the small signals in many of the tests.

The digitalization process converts times and amplitudes into counts. A computer program was developed for the IBM 1620 to convert the counts back into time and to ground amplitudes. The amplitudes were computed by assuming that the seismographs were responding as true displacement meters for the frequencies involved, and the trace

amplitudes were divided by the static magnification. Time computations presented a special problem since the chart speeds were slightly different for the various seismographs, and were somewhat variable for any one instrument. The positions of the timing lines over the portion of the record to be processed were read into the computer, and the program interpolated the position of the point on the trace at which a reading was taken between two adjacent timing lines, and expressed this position as the time from the selected zero.

Those records that were to be subjected to Fourier analysis were digitalized at equal time intervals, spaced closely enough that the folding frequency was twice the highest frequency of interest. All that was required from other records was the values of peak amplitudes, time of arrival of selected phases, or sufficient detail to allow the construction of particle motion disgrams.

The following programs for the IBM 1620 were developed as part of the research:

Ground motion from digitalized seismograms

Plot ground motion

Fourier transform

Fourier synthesis of phase equalized ground motion

Phase velocities from Fourier transforms

Impulse response for given dispersion curve

Source functions by convolution

Synthesis of ripple-fired shots

Travel times for all body wave arrivals in three-layered medium.

Detailed discussions of many of the seismograms resulting from this series of tests have been presented in the series of Semi-Annual Technical Summaries that have been issued during the course of the project, as well as in scientific papers and special reports. It is not practical to present a complete review of all experimental results in this report. Rather, the main results will be presented, along with sufficient data to support the conclusions, and references will be made to previously published material where appropriate.

Table 1

SUMMARY OF FIELD PROGRAM

A. Florissant Test Site

Shot Point	Depth of Charge (m)	Charge Weight (lbs.)	Array*	Remarks
1a	1.40	.5	P: 15-60m	Loose tamping
1b	1.88	.5	P: 15-60m	No tamping
2	1.39	.5	P: 14-59m	Tight tamping
3a	1.39	.5	A: 180°, 30m	Loose tamping, instruments on hillside
3b	1.80	.5	A: 180°, 30m	No tamping, instruments on hillside
4	1.37	.5	A: 180°, 30m	Tight tamping, instruments on hillside
5a	6.00	.5	A: 360°, 25m	
5b	3.82	.5	A: 360°, 25m	
5c	3.00	.5	A: 360°, 25m	No tamping
6	1.22	1.5	P: 135-195m	
7	1.31	1.0	P: 75-135m	
8	1.31	.5	P: 15-75m	
9	1.42	1.0	Broadside	
10	1.42	1.0	Broadside	
11	1.34	.5	A: 360°, 15m	
12a	5.30	2.0	A: 360°, 25m	
12b	2.71	1.5	A: 360°, 25m	
12c	.82	1.0	A: 360°, 25m	
13	1.43	.5	A: 180°, 25m	Side of hill
14a	1.28	.5	A: 180°, 25m	Loose tamping, side of hill
14b	1.74	.5	A: 180°, 25m	No tamping, side of hill
22	1.31	.5	A: 360°, 25m	
23	1.52	1.0	A: 360°, 25m	
24	1.46	1.5	A: 360°, 25m	
25	.24	.5	A: 360°, 20m	
25p1	0	.5	A: 360°, 20m	Water-filled pit, surface shot

Table 1 (Cont'd)

A. Florissant Test Site

Shot Point	Depth of Charge (m)	Charge Weight (lbs.)	Array*	Remarks
25p2	0	.5	A: 360°, 20m	Water-filled pit, surface shot
26	.21	.25	A: 360°, 20m	
26p1	0	.25	A: 360°, 20m	Water-filled pit, surface shot
26p2	0	.12	A: 360°, 20m	Water-filled pit, Surface shot
26p3	.6	.25	A: 360°, 20m	Water-filled pit, bottom shot
31a	3.0	1.5	P: 20-110m	
31b	1.0	1.0	P: 20-110m	
32a	2.7	2.0	P: 107-227m	
32b	0.9	1.5	P: 107-227m	
33	1.1	1.0	Cluster	Reproducibility test
51a	4.1	1.5	A: 90°, 30m, 60m	Effect of depth of source on radiation pattern
51b	1.5	2.0	A: 90°, 30m, 60m	Variation of radiation pattern with distance
52a	3.7	.5	A: 90°, 30m, 60m	
52b	1.6	.5	A: 90°, 30m, 60m	
53a	4.1	1.5	A: 180°, 61m	Band pass filtering during reading
53b	1.4	1.5	A: 180°, 61m	
54a	4.0	2.0	A: 180°, 122m	
54b	1.0	2.0	A: 180°, 122m	
55a	2.0	.5	A: 360°, 25m	Effect of air-filled and water-filled cavity
55b	2.3	2.0	A: 360°, 25m	Cavity
55c	2.2	2.0	A: 360°, 25m	Cavity filled with water
56a	0	.5	A: 360°, 25m	Effect of burial near zero depth
56b		.5	A: 360°, 25m	Half buried
56c	0	.5	A: 360°, 25m	
56d		.5	A: 360°, 25m	Buried flush
56e	0	.5	A: 360°, 25m	Circular pit

Table 1 (Cont'd)

A. Florissant Test Site

Shot Point	Depth of Charge (m)	Charge Weight (lbs.)	Array*	Remarks
56f	0	.5	A: 360°, 25m	2:1 elliptic pit
56g	0	.5	A: 360°, 25m	End of elliptic pit
56h		.5	A: 360°, 25m	Bottom of elliptic pit
57	4.0	2.5	A: 360°, 25m	Check on soil moisture around shot
58	1.3	2.5	A: 180°, 213m	Radiation pattern at longer range
61	1.4	2.5 (5 caps)	A: 180°, 213m	Repeat of 58 to check on detonation of total charge
62a-h	14.6-1.2	.5 each	P-0-20m	Effect of depth on Rayleigh wave generation. 8 shots
63a-e	14.6-3.0	1.5 each	P-2.5-25m	Effect of charge weight on depth effect. 5 shots
64a-y	38.1-1.5	see Remarks	P: 0-50m	Effect of depth and log of P & S wave velocities. 1.5 lbs. at approximately 38m, 32m, 26m, 20m, 14m, 8m. 0.5 lbs. at 1.0m intervals
65	1.5-7.6	1.25 lbs. in 5 equal charges vert. stacked.	A: 360°, 30m	Sequentially fired from bottom up at 1000 ft/sec
66	1.5-7.6	1.25 lbs. in 5 equal charges vert. stacked	A: 360°, 30m	Total charge fired instantaneously
67a	1.5	Same as above	A: 360°, 30m	Line of charges fired instantaneously
67b	1.1	Same as above	A: 360°, 30m	Line of charges fired sequentially at 1000 ft/sec.
68a	1.5	Same as above	A: 360°, 30m	Line of charges fired sequentially at 500 ft/sec.

Table 1 (Cont'd)

A. Florissant Test Site

Shot Point	Depth of Charge (m)	Charge Weight (lbs.)	Array*	Remarks
68b	1.1	Same as above	A: 360°,30m	Line of charges fired sequentially at 330 ft/sec.
69a	1.5	1.25 lbs.	A: 360°,30m	Calibration shot
69b	.7	.25 lbs.	A: 360°,30m	Calibration shot
70	1.5	1.0 lbs. in 2 holes, 1.5 meters apart	A: 360°,30m	Line of charges fired sequentially at 1000 ft/sec.
71	1.5	Same as above	A: 360°,30m	Line of charges fired sequentially at 500 ft/sec.
72a	1.5	4 lbs. in 8 holes in double line	A: 360°, 30m	Double line fired from opposite ends at 1000 ft/sec.
72b	1.1	Same as above	A: 360°,30m	Double line fired from opposite ends at 500 ft/sec.
73a	38.1	4.5	P: 0-50m A: 360°,2.5m	
73b	32.0	4.5	P: 0-50m A: 360°,2.5m	
73c	25.9	4.5	P: 0-50m A: 360°,2.5m	
73d	19.8	4.5	P: 0-50m A: 360°,2.5m	
73e	.3	1.5	P: 12.5-50m	Cratering shot

Table 1 (Cont'd)

B. Alpha Test Site

Shot Point	Depth of Charge (m)	Charge Weight (lbs.)	Array*	Remarks
14X	1.43	.5	P: 12-75m	
15	1.40	.5	P: 72-135m	Crack pattern observed
15R	1.56	1.0	Cluster	Reproducibility test
16	1.22	1.0	P: 128-191m	Blew out, crack pattern observed
16R	1.40	1.5	A: 180°, 25m	Joint pattern alignment
17	1.34	.5	A: 360°, 25m	Crack pattern observed
18	.94	1.0	A,P: 90°, 20-40m	Corner shot near free faces
19	1.49	1.0	A,P: 80°, 12-29m	
20	.76	1.0	A: 180°, 20m	Free face shot, crater in face formed
21	1.16	2.0	A: 106°, 20-30m	Free face shot, face displaced but no crater
36	1.3	2.0	P: 18-118m	
37	1.2	2.5	P: 114-231m	
37X		.5	Cluster	Reproducibility, no cement
37Y		.5	Cluster	Reproducibility, cement
38	1.0	1.5	A: 120°, 30m	
39	1.0	1.5	A: 120°, 30m	
40	1.0	1.5	A: 120°, 30m	
48	3.2	2.0	A: 180°, 20m,35m	One meter from free face
49	3.2	1.5	A: 180°, 20m,35m	One meter from free face
50	.8	1.5	A: 180°, 20m,35m	Two meters from free face

Table 1 (Cont'd)

C. Augusta Test Site

Shot Point	Depth of Charge (m)	Charge Weight (lbs.)	Array*	Remarks
27	1.5	.5	A: 360°, 20m	
28	1.2	1.0	A: 360°, 20m	
29	1.6	1.5	A: 360°, 20m	
30a	3.3	1.0	A: 360°, 20m	
30b	1.2	1.0	A: 130°, 20m	
34	1.3	1.5	P: 20-110m	
34X	0.2	.5	Cluster	Reproducibility test
35	1.3	2.5	P: 105-217m	

Table 1 (Cont'd)

D. Suffield Test Site

Shot Point	Depth of Charge (m)	Charge Weight (lbs.)	Array*	Remarks
41a	3.20	2.0	A: 360°, 30.4m	
41b	1.53	2.0	A: 360°, 30.4m	
41c	-1.53	2.0	A: 360°, 30.4m	
41d	0	2.0	A: 360°, 30.4m	
42	1.53	4.0	A: 360°, 30.4m	
43a	4.88	5.0	P: 18.3-244m	
43b	2.14	5.0	P: 18.3-244m	
43c	-3.04	5.0	P: 18.3-244m	
43d	-3.04	15.0	P: 18.3-244m	
43e	0	5.0	P: 18.3-244m	
43f	0	15.0	P: 18.3-244m	
44a	5.50	10.0	P: 18.3-244m	
44b	2.28	10.0	P: 18.3-244m	
44c	-3.04	10.0	P: 18.3-244m	
44d	0	10.0	P: 18.3-244m	
44e	0	500 (TNT)	P: 140-366m	

CHAPTER III

SOURCE FUNCTIONS AND SYNTHESIS OF MOTION BY PHASE EQUALIZATION

The mechanism of seismic wave generation is one of the fundamental problems of seismology. One objective of this program of research was to gain a clearer understanding of the process by which surface waves are generated by explosions. Except in the most simple case of an elastic half-space, the motion in the source region which gives rise to the surface waves observed at distance is distorted by dispersion during propagation. In principle, the effects of dispersion and other propagation effects can be removed, and, subject to a number of assumptions, the source motion can be recovered.

Two equivalent phase equalization methods have been used with equal success. These are described by Sato (1955, 1956) and Aki (1960b). The analyses of source motion from the fundamental Rayleigh mode, the first Rayleigh shear mode, and Love waves have been carried out.

The first method is based upon the simple principle that the amplitude and phase angle of the Fourier transform of the trace of the motion at any observing station is the result of the modification of the initial amplitude and phase spectra near the origin as a result of phase shifts and amplitude changes caused by dispersion, attenuation, and recording. The Fourier amplitude and phase spectra of the observed motion are the basic data in this

technique. From the spectral data along an observed profile the phase velocity and initial phases of all components are calculated, absorption coefficients determined, and finally the motion at any distance calculated by resynthesis of the Fourier components.

Assuming cylindrical spreading of the wavefront, the motion at any distance, r, is given by

$$(1)\quad f(r,t) = \sqrt{\frac{2}{\pi}\frac{r_a}{r}} \int_0^\infty A(r,\omega)\ F(r_a,\omega) \cos(\phi(\omega)-\omega t)\,d\omega$$

where: r_a = distance to recording station
$F(r_a,\omega)$ = observed Fourier spectral amplitude
$\phi(\omega)$ = initial phase, and
$A(r,\omega)$ = attenuation function.

The attenuation function represents the absorption losses within the medium. It is assumed that these can be expressed by:

$$(2)\qquad A(r,\omega) = \exp(-R\alpha)$$

in which α can be written as $B\omega^n$, where B is an absorption coefficient and n defines the dependence of attenuation on frequency.

One of the principal assumptions in the techniques used for calculation of the source functions is that the spectrum at any observation point expresses the spectrum at the source. If, however, higher frequencies have been attenuated to the point that they are not recorded, no absorption law will replace them. The loss of the high frequency energy will make it impossible to arrive at a short rise time for the computed source function, and if the observed

spectrum is severely band-limited, the calculated motion must be oscillatory.

In the second method, first exploited by Aki, the impulse response of the layered medium is cross-correlated with the field record to obtain the motion at the source (source function). If the phase velocity curve is known, a theoretical seismogram at any distance can be calculated by

$$(3) \qquad g(t) = \int_{-\infty}^{\infty} G(\omega) \exp(i\omega t)\, d\omega$$

where $G(\omega)$ represents the combined frequency response of the earth and recording system. $|G(\omega)|$ is assumed to be unity only over a finite frequency band, say ω_1 to ω_2, and the phase of $G(\omega)$ includes shifts due to dispersion and recording. The cross-correlation of a theoretical seismogram, $g(t)$, along a particular wave path with the field record, $x_{(t)}$, for the same path will yield the source function $y(\tau)$, i.e.

$$(4) \qquad y(\tau) = \int_{0}^{\infty} g(t)\, x(t+\tau)\, dt.$$

It has been shown (Jones and Morrison, 1954) that this cross-correlation equalizes the phase angle of the record $x(t)$ to the source in the frequency range from ω_1 to ω_2.

Test Sites and Data.

The surface wave data used for the calculations of the source functions were obtained at two test sites: the Florissant site, which consists of approximately 120 feet of clay-loess overlying Mississippian limestone; and the test

site at the Suffield Experimental Station, which has about 210 feet of clay with sand and gravel lenses overlying the Cretaceous Foremost sandy shale formation (see Chapter II).

Examples of the recorded ground motions which were used for source function calculations are shown in Figures 2 and 3. Figure 2 is a profile of the three components of motion of the surface waves at Florissant (S.P. 6, 7). The motion was recorded on Sprengnether portable three-component blast seismographs. The instruments were carefully aligned with the shot point so that one horizontal component responded to radial motion and the other to tangential motion. The vertical and radial components are dominated by the fundamental Rayleigh mode which is preceded by prograde elliptic motion (Kisslinger, 1959; Gilbert, et al 1962). This prograde motion is thought to be a combination of $\bar{P}$ (a diffracted compressional wave) and the first Rayleigh shear mode. Both the prograde and retrograde events show normal dispersion across the profile. The transverse motion is identified as a Love wave, and also is normally dispersed.

Figure 3 shows the recorded motion along a profile at the Suffield test site, produced by a 10 lb. charge at a depth of 5.5 meters (S.P. 44a). The vertical and radial component motion is dominated by the fundamental Rayleigh mode at the closer distances. This event is preceded by a prograde elliptic event which has been identified as the

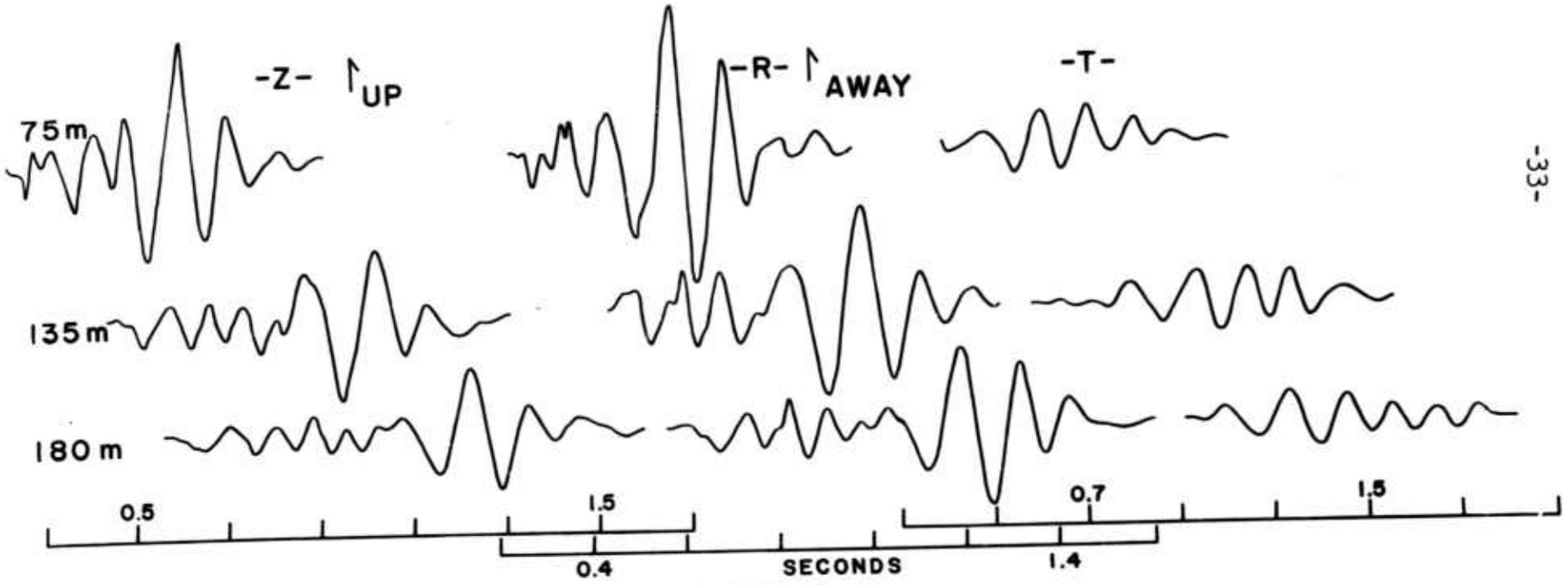

FIGURE 2

MOTION ALONG A PROFILE

-FLORISSANT-

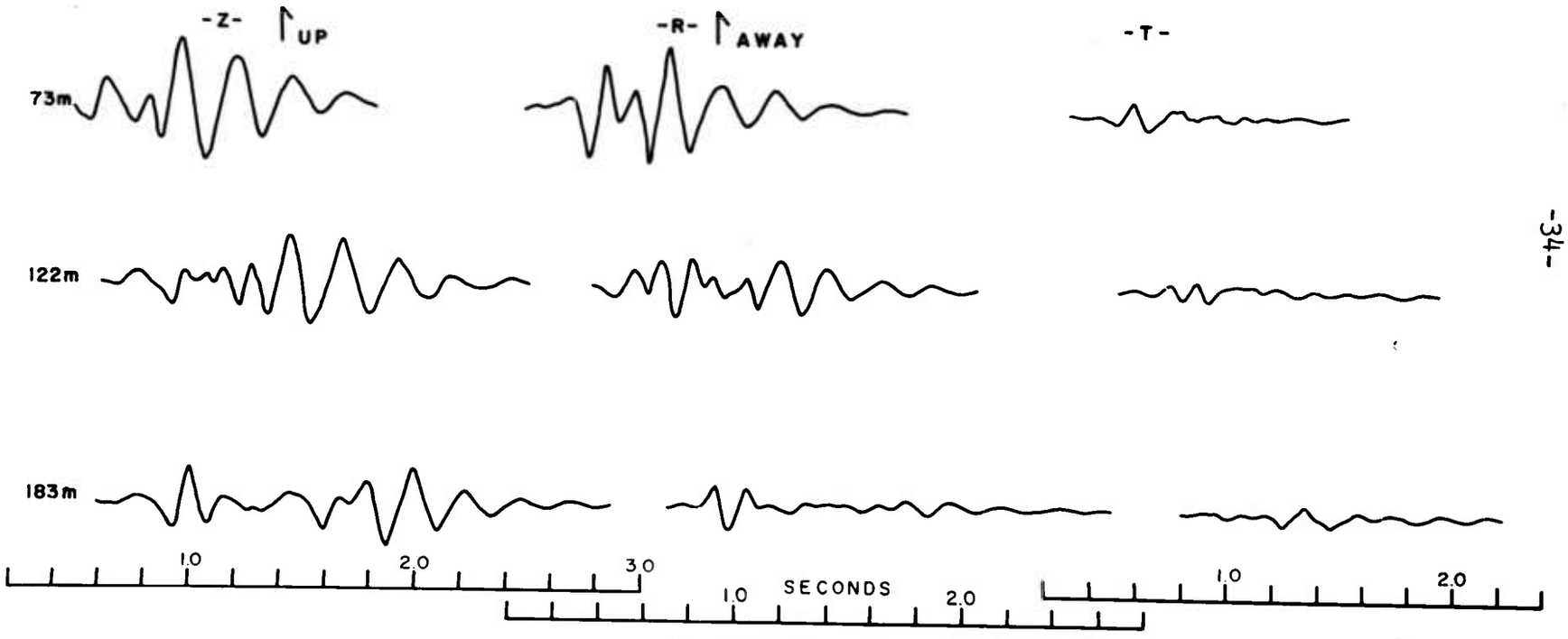

FIGURE 3

MOTION ALONG A PROFILE

-SUFFIELD-

first Rayleigh shear mode M_{21}. This identification is based upon the particle motions, Figure 4, and the phase velocity curve, Figure 8. The development of this event as it separates from the fundamental Rayleigh wave with increasing distance is well shown in Figure 3.

The Rayleigh motion, best exhibited on the vertical component, is a wave packet with almost constant frequency at all distances at which it has been observed. This does not mean that the medium, known to be layered, is not dispersive. A careful correlation of peaks and troughs shows that dispersion is exhibited as a progression of the maximum amplitude at a group velocity of approximately 90 meters per second through the constant frequency wave packet. This is demonstrated in Figure 5 in which the vertical component of the ground motion between 91 and 213 meters is plotted. The transverse motion at Suffield has been identified as a Love wave on the basis of the agreement of the observed phase velocity curve with the theoretical curve. (Figure 8). It is obvious from a comparison of Figures 2 and 3 that the long dispersed wave train of Love motion was not observed along the profile at Suffield as it was at the Florissant test site. However, it has been established (Kisslinger, et al, 1961; Stauder and Kisslinger, 1962) that Love waves are generated at both sites with an asymmetrical pattern of radiation, and it may be that the profile at Suffield

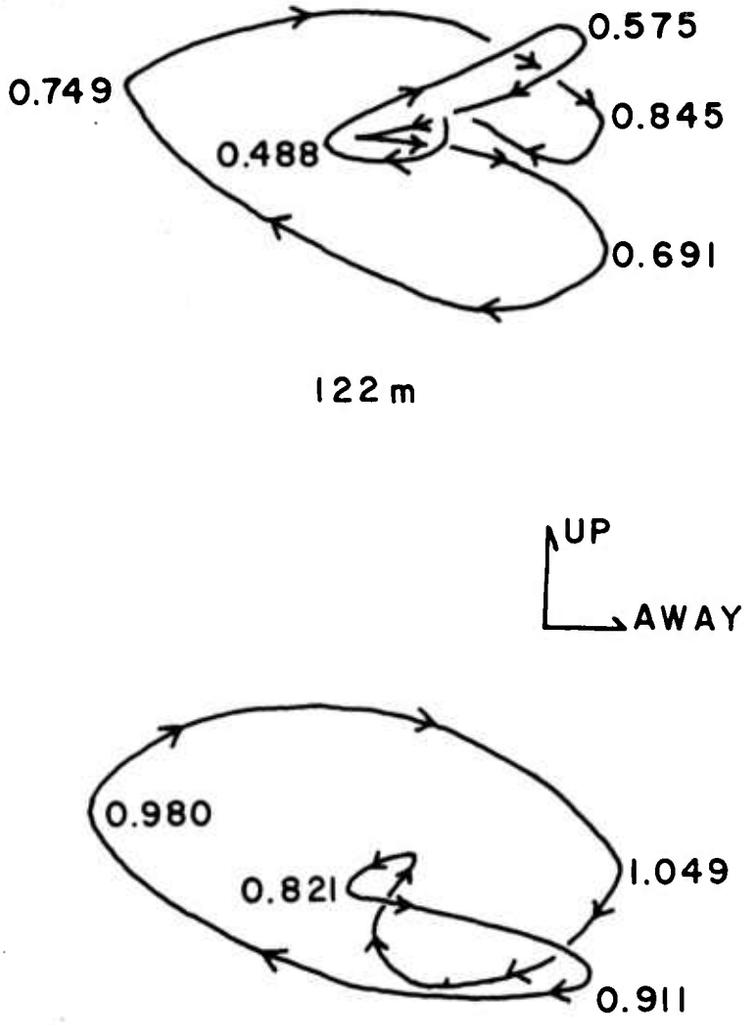

FIGURE 4
PARTICLE MOTION DIAGRAM, M_{21}
-SUFFIELD-

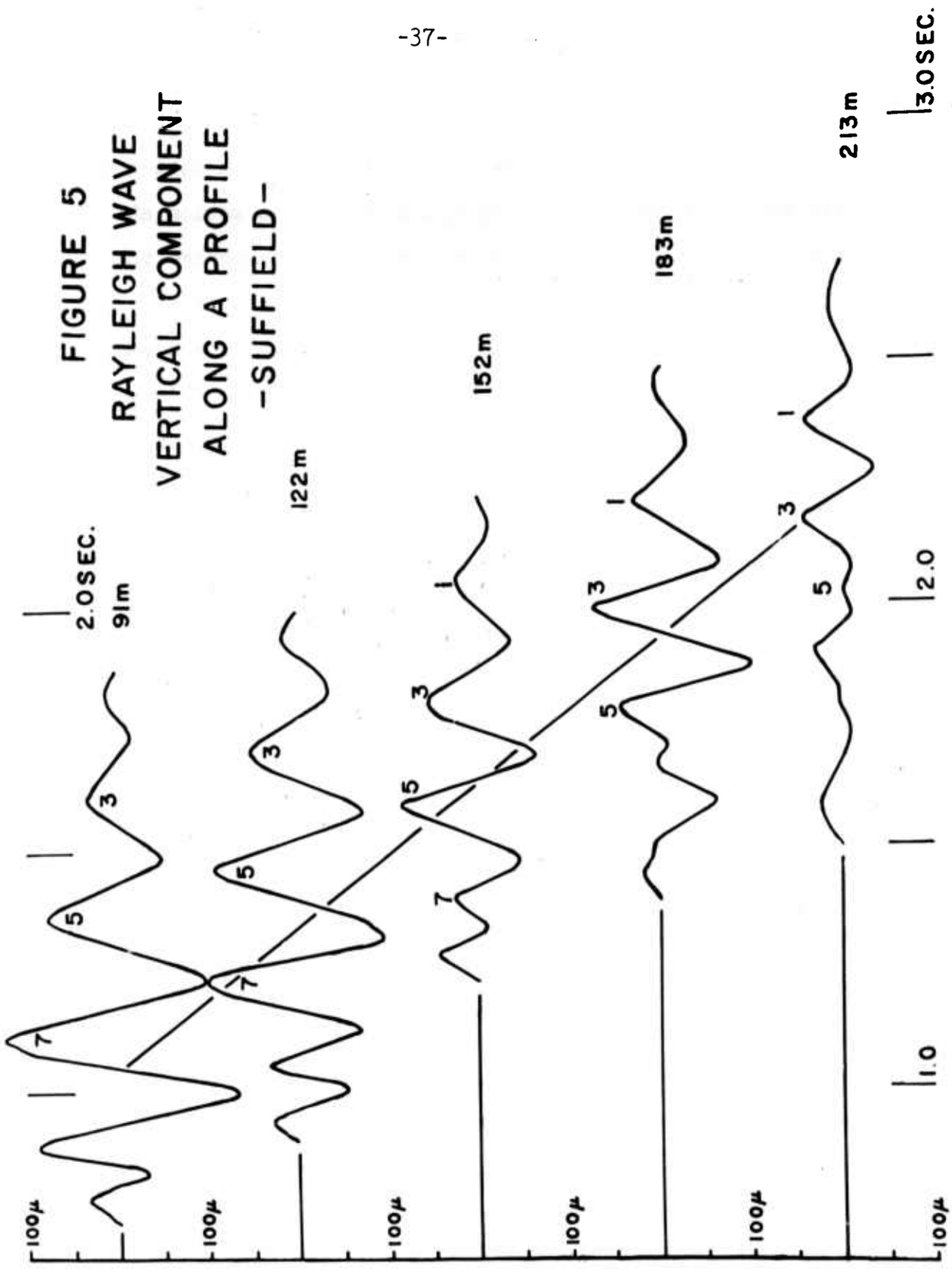
FIGURE 5
RAYLEIGH WAVE
VERTICAL COMPONENT
ALONG A PROFILE
-SUFFIELD-
2.0SEC.
91m
122m
152m
183m
213m
100μ
1.0
2.0
3.0SEC.

happened to lie near a nodal line. The Rayleigh motion at the two sites differs in two respects: 1) the motion at Suffield is a constant frequency wave packet whereas the motion at Florissant, though still exhibiting a fairly narrow spectrum (about one octave, Figure 6), is a normally dispersed wave train; 2) the vertical component dominates the Rayleigh motion at Suffield but at Florissant the radial component is bigger.

A comparison of the Fourier amplitude spectra at both sites for these surface waves is shown in Figure 6. The Rayleigh wave spectrum at Florissant is peaked at approximately 7 cps. The frequencies at which the amplitudes are 0.7 of the maximum are 4.5 and 10 cps. At Suffield the vertical spectrum is sharply peaked at 4 cps. with the half power points at 3.5 and 5 cps. Since at the distances involved here it is difficult to separate the beginning of the Rayleigh wave from the prograde event, each event affects the spectrum of the other. This is most noticeable on the radial component at Suffield, on which the Rayleigh wave is relatively small.

The theoretical and observed dispersion curves for each of these surface waves and the corresponding earth models at the two sites are shown in Figures 7 and 8. These earth models were selected as giving the best agreement with the observed fundamental Rayleigh wave curve

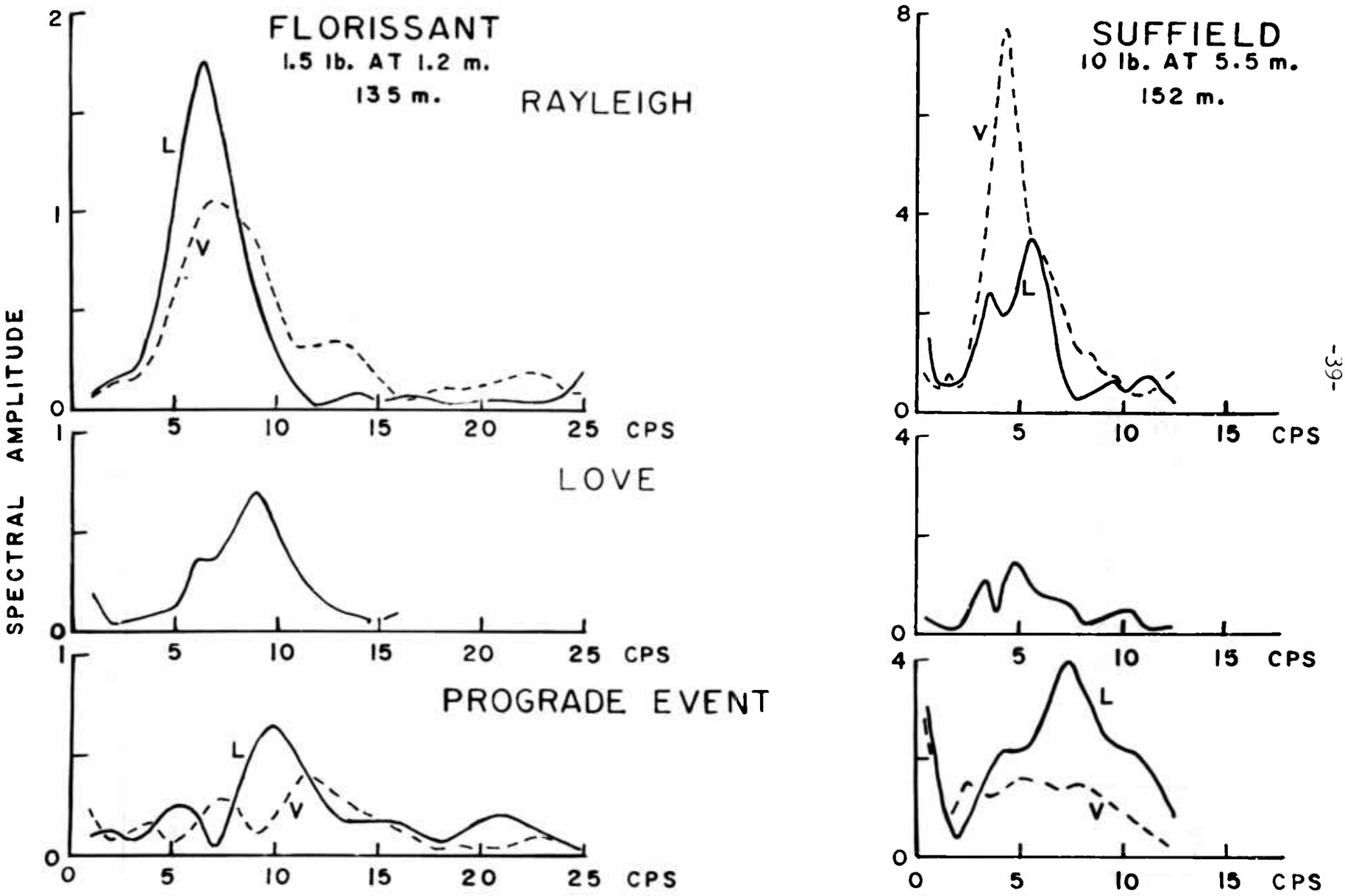

FIGURE 6. FOURIER SPECTRA, FLORISSANT AND SUFFIELD

FIGURE 7

DISPERSION CURVES, FLORISSANT

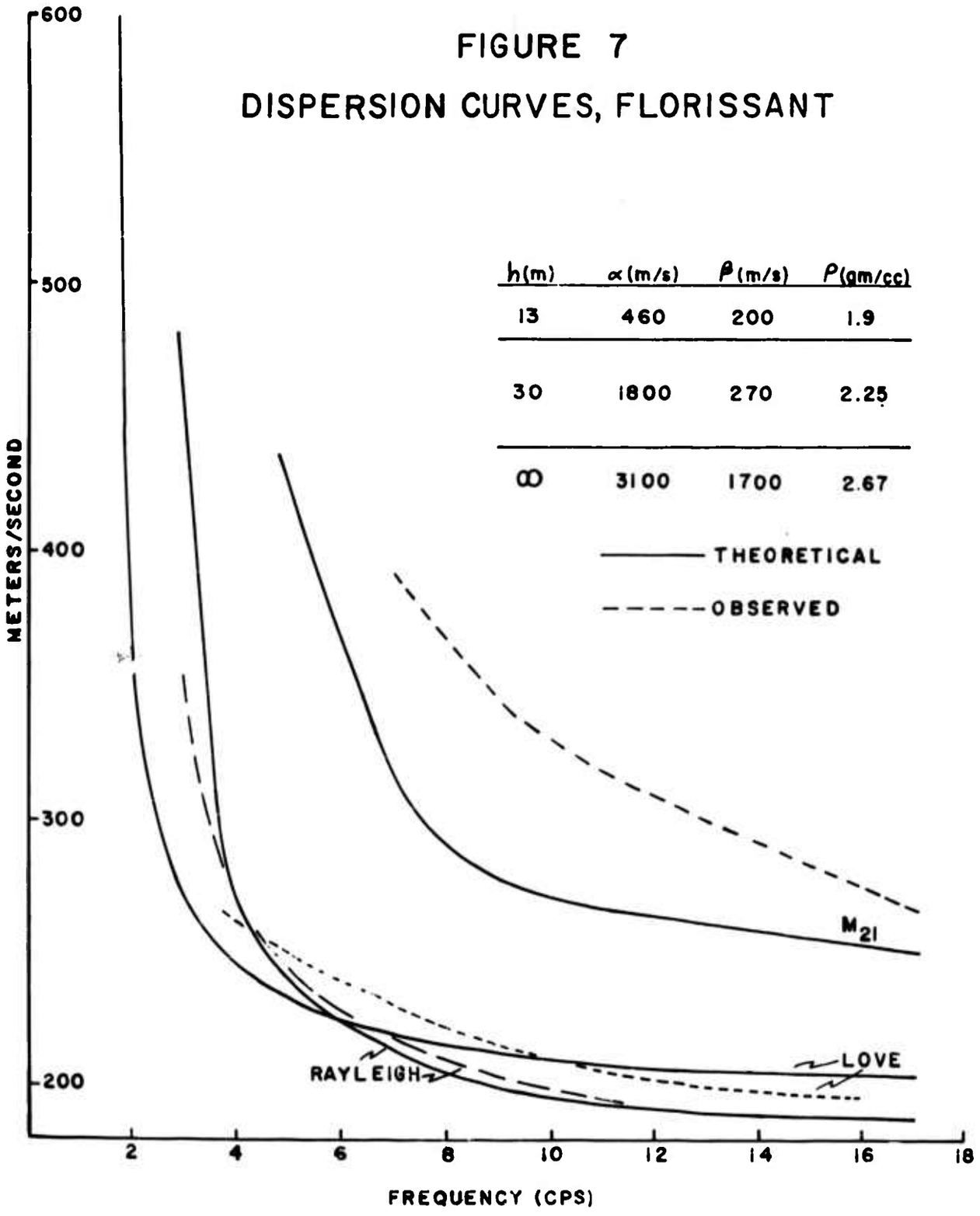

FIGURE 8

DISPERSION CURVES, SUFFIELD

h(m)	∝(m/s)	β(m/s)	ρ(gm/cc)
13.7	670	140	1.8
10.7	1680	305	2.0
40	1680	610	2.3
∞	2400	1400	2.5

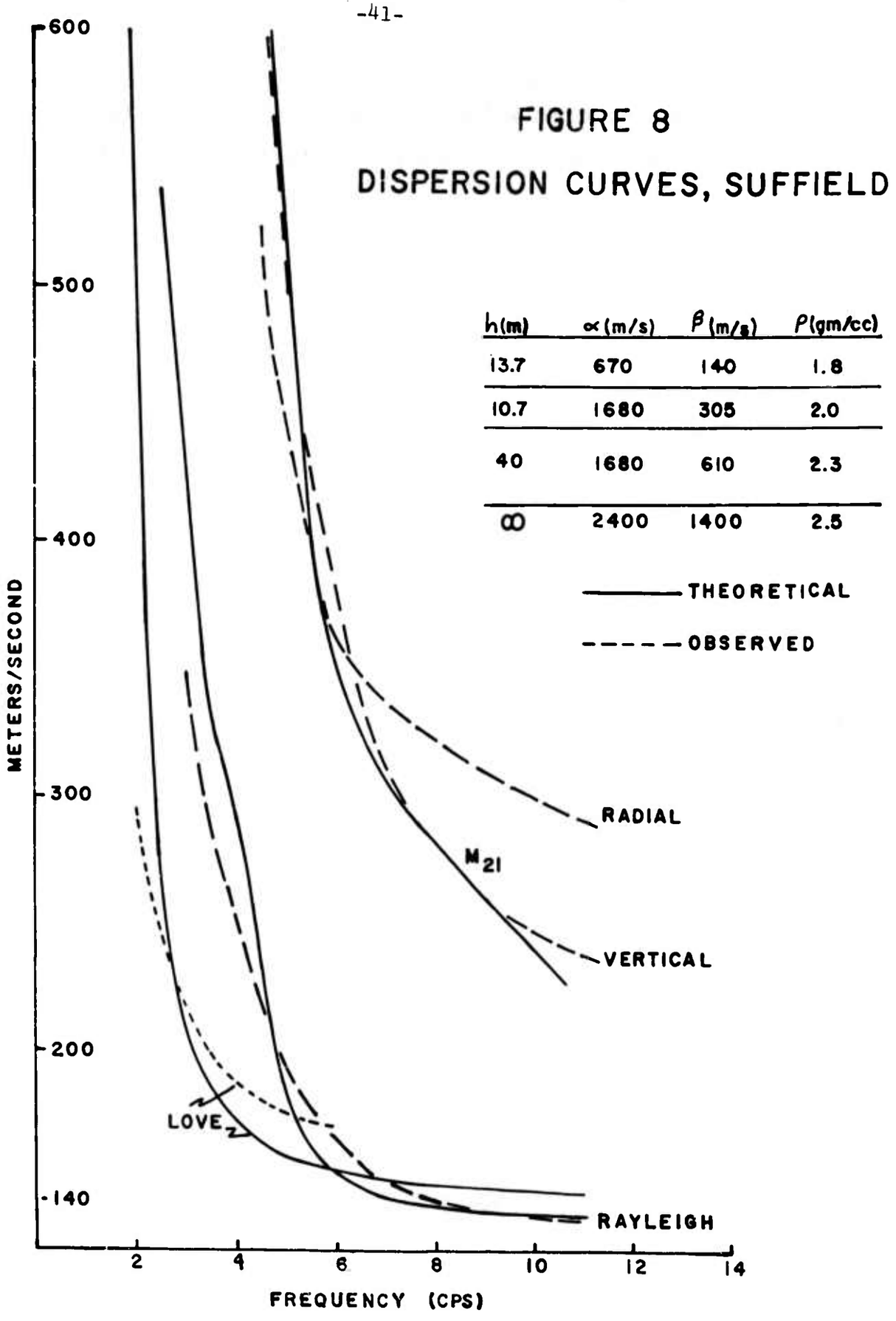

consistent with known velocity and structural data. The curves computed from these models for the other types of surface waves were then accepted as the proper theoretical curves.

Since the method of analysis yields an infinite set of possible observed phase velocity curves (Sato, 1958, Kisslinger, 1960), it is necessary to select one of these on the basis of independent information. At both sites, P and S wave velocities have been directly measured and layer thicknesses are known from refraction surveys and logs of shot holes. The earth models used for the theoretical curves fit well with the known velocities and layer thicknesses.

An interesting feature of these curves is that the Rayleigh wave phase velocity is greater than that of the Love wave over part of the frequency band of interest. An inspection of the models shows that the shear velocities in the upper layers at both sites are low. In the clays overlying the more rigid substratum the value of Poisson's ratio is quite high, ranging from approximately 0.38 to 0.49. These high values coupled with the increase of the P-wave velocity at the first boundary without a corresponding increase in the shear wave velocity cause this unusual relationship of Love and Rayleigh phase velocity curves. The high values of Poisson's ratio are characteristic of the unconsolidated surface layers and the increase in P-wave

velocity without similar changes in shear wave velocity is a characteristic of shallow water tables.

These figures also show the dispersion curves of the prograde elliptic events discussed previously. At Suffield the vertical and horizontal components of this event gave observed phase velocities which were slightly different. This is most probably due to the interference effects with other events so close to the source. However, the general agreement of these, particularly the vertical component, with the theoretical curve is quite good. At Florissant this is not the case. As already mentioned the prograde motion is thought to be a combination of $\overline{P}$ and the M_{21} mode, and the effect of this interference in the observed curve is not known.

Attenuation coefficients, α, were determined for the individual Fourier components of the fundamental Rayleigh mode from the Fourier spectral amplitude at varying distances. The values were determined from the relation

$$(5) \qquad A_r = \frac{A_o}{\sqrt{r}} \exp(-\alpha r),$$

where A_r = Fourier amplitude at distance r,
and A_o = initial amplitude.

The values determined for the two test sites are shown in Table 2. Because the variation is small over the predominant frequency range of the Rayleigh wave at both sites, an average value independent of frequency was assigned to each site for use in the synthesis calculations.

Table 2

ATTENUATION COEFFICIENTS

Suffield		Florissant	
(cps)	(meters^{-1})	(cps)	(meters^{-1})
3.5	1.0037	4.0	0.0062
4.0	0.0044	5.0	0.0075
4.5	0.0040	6.0	0.0075
5.0	0.0046	7.0	0.0078
5.5	0.0057	8.0	0.0072
		9.0	0.0078
		10.0	0.0078
		11.0	0.0088

Synthesis of Fundamental Rayleigh Mode

The synthesis studies from these data are in two categories: 1) the attempt to synthesize the motion in the source region, i.e. calculation of the source function, and 2)the synthesis of motion at distances sufficiently far from the source that the fundamental Rayleigh wave has separated from the other events such as direct and refracted body waves and higher modes.

Synthesis at Distance. The motion synthesized at 135 and 180 meters fro the observed motion at 75 meters at Florissant (Figure 2) is compared with the observed motion in Figure 9. Except for amplitude, the calculated motion agrees quite well with the observed motion. Slight differences in time for peaks and troughs are reasonably accounted for by slight inaccuracies in the phase velocity data. The smaller amplitudes on the synthesized traces are largely due to the effect of the charge size. The observed motion at 75 meters, the input to the synthesis calculation, was

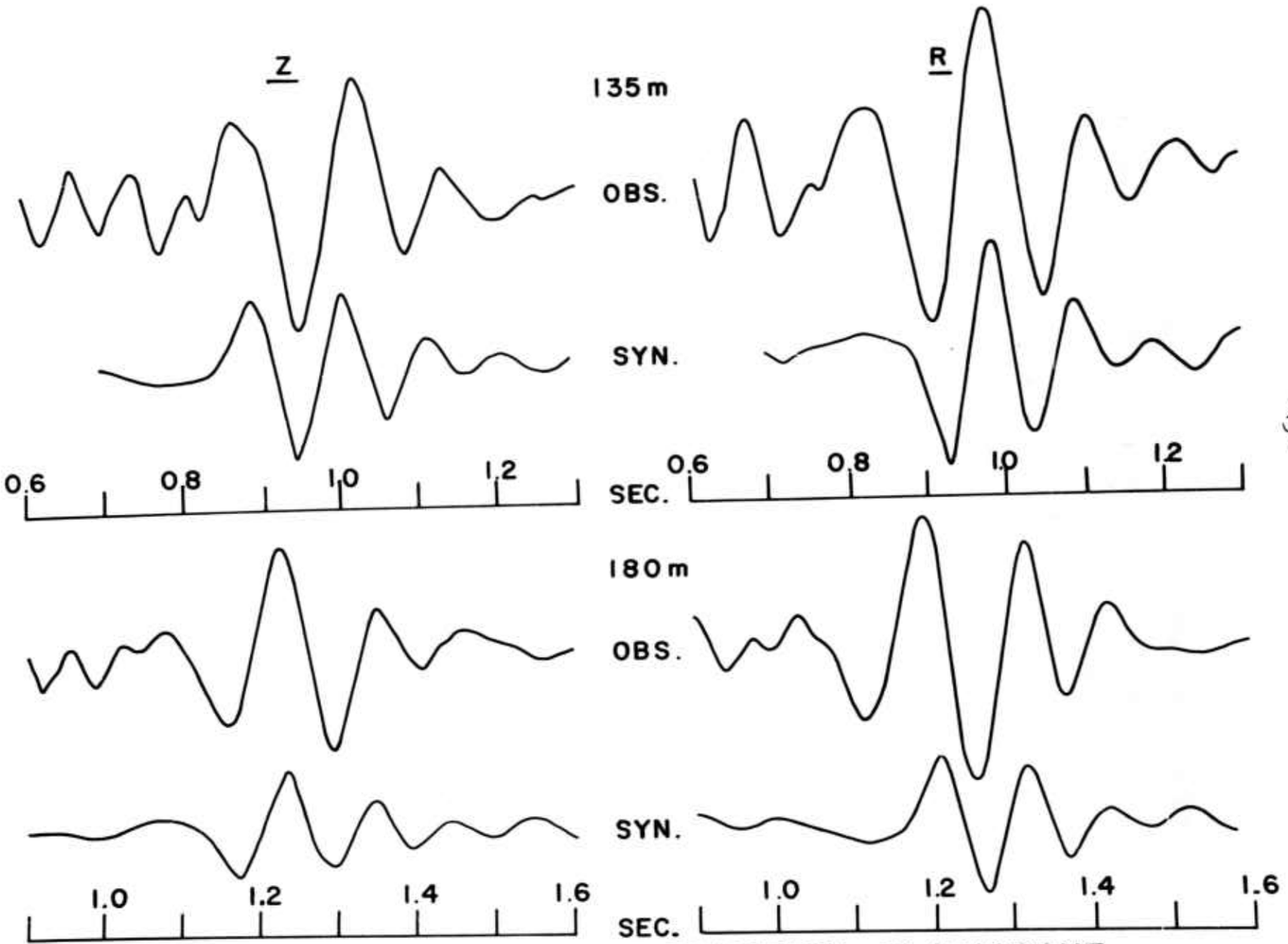

FIGURE 9. OBSERVED AND SYNTHESIZED MOTION, FLORISSANT

recorded from a smaller shot than that which produced the observed motion at 135 and 180 meters. Motion recorded at the same distance from both of these shots indicated that the vertical component of the Rayleigh motion was approximately 1.3 times greater from the larger shot. The mean value of the ratio of observed to synthesized at 135 meters is 1.46 on the vertical and 1.4 for the radial. Figure 10 illustrates the agreement of amplitude one might expect when the synthesized motion is calculated from motion recorded from the same shot. This figure shows the vertical motion synthesized at 75 and 90 meters from observed motion at 90 and 75 meters respectively. The amplitude agreement is quite good. Similar calculations for the radial motion produced the same results.

The synthesized vertical and radial motion at Suffield at 183 and 244 meters as calculated from the observed motion at 122 meters is shown in Figure 11. Again the comparisons are quite favorable, particularly the vertical components. The largest motion occurs at the same time on the synthesized and observed traces, frequencies are the same and the amplitudes are similar and die off rapidly on both sides of the maximum motion.

The observed motion from 183 meters was used to synthesize the motion at 122 meters at Suffield, the reverse of the process discussed above. The synthesized motion at 122 meters compared very favorably with the observed. This

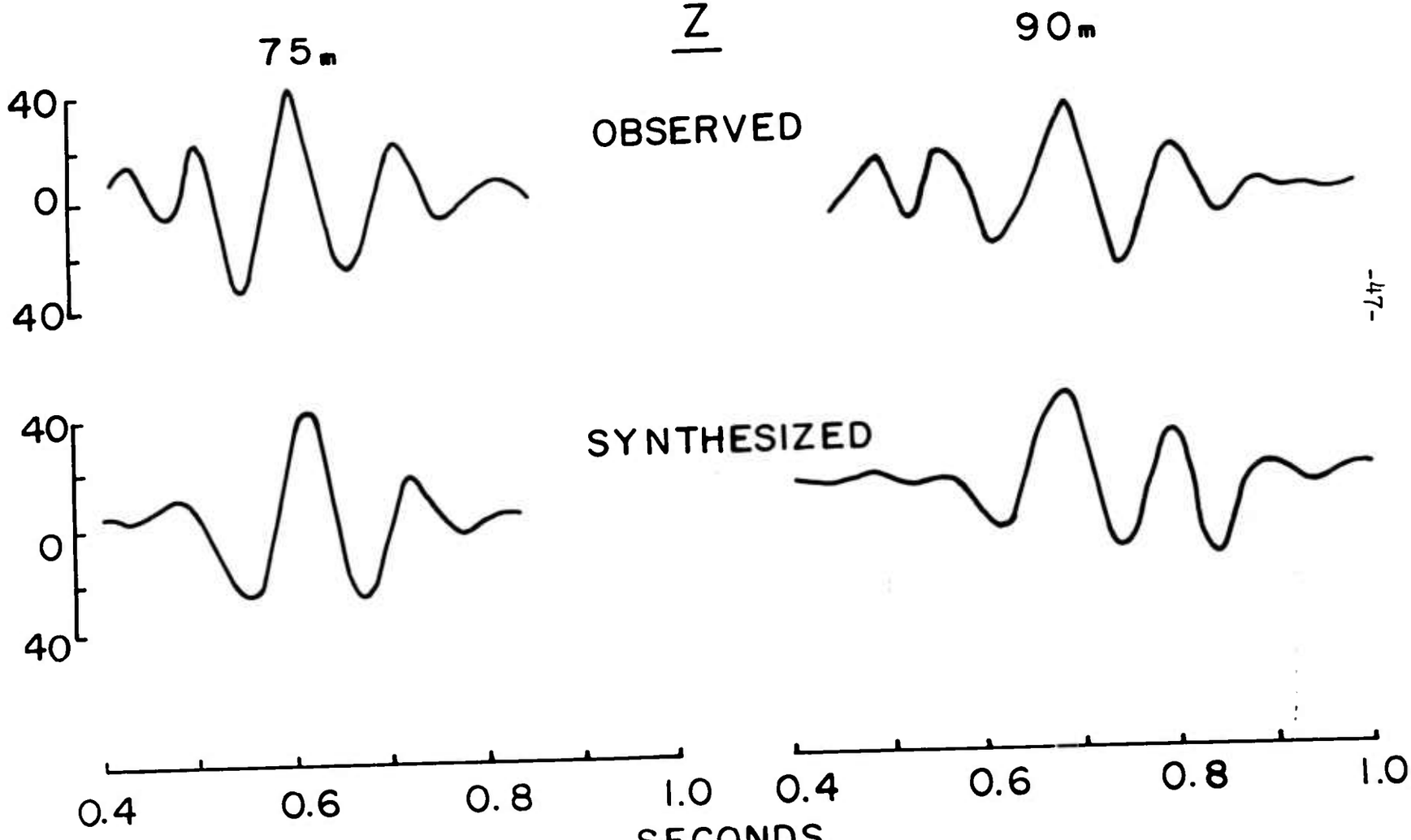

FIGURE 10. OBSERVED AND SYNTHESIZED MOTION, FLORISSANT

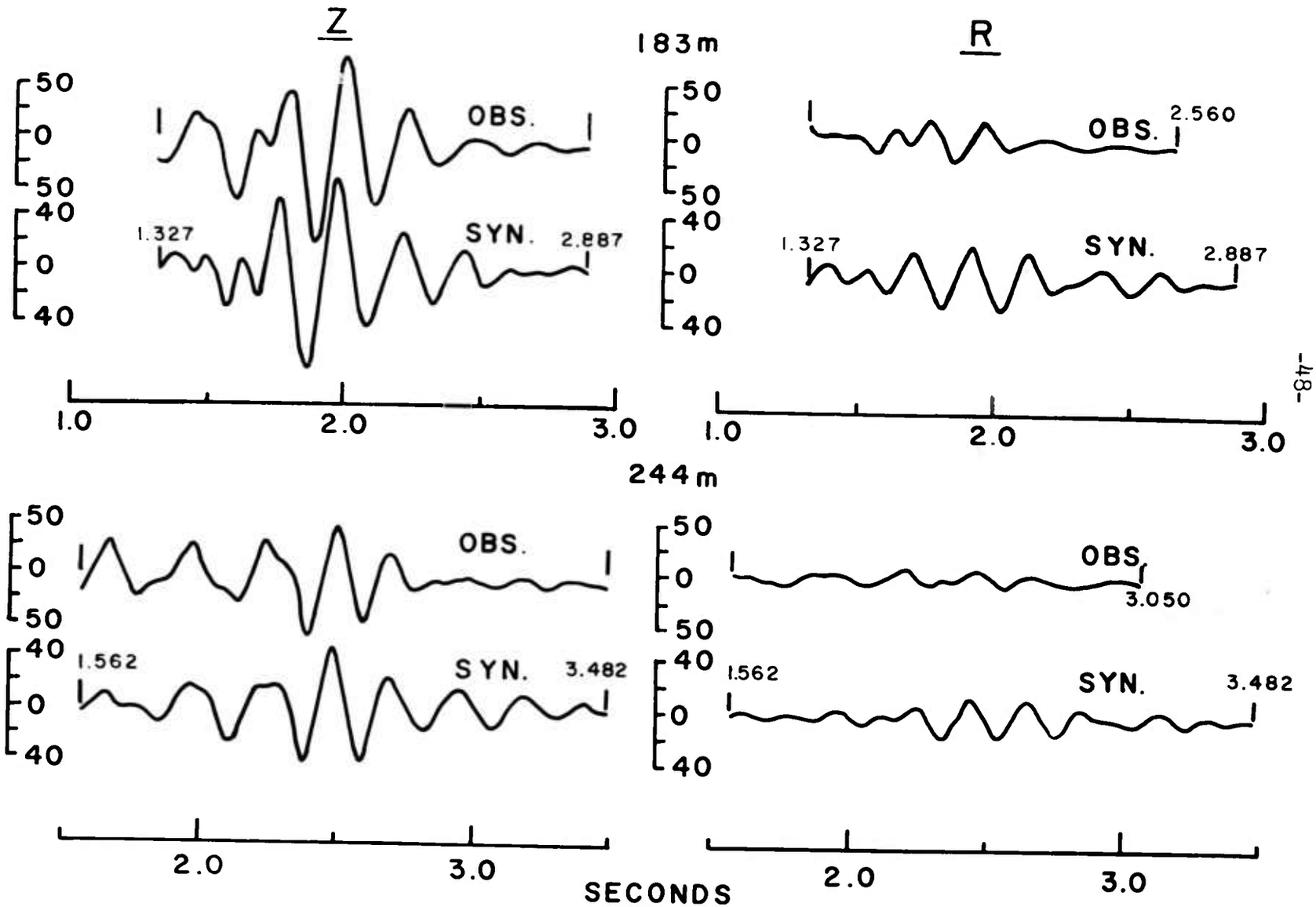

FIGURE 11. OBSERVED AND SYNTHESIZED MOTION, SUFFIELD

same test was performed at Florissant for various distance combinations with equally good results.

From these examples, it is obvious that Sato's technique of synthesis is very successful in predicting or reproducing the observed motion at any distance from the source at which the Rayleigh wave has separated from the other events on the record. This implies that the phase velocity curves must be reasonably accurate, that attenuation in this region is adequately represented by the assumptions made, and the numerical methods are satisfactory.

Synthesis in the Source Region. Before examining the calculated source functions it is instructive to consider the results of the synthesis at Suffield at 18 and 55 meters from the source. The motion, shown in Figure 12, was calculated from the observed motion at 122 meters.

At 55 meters the maximum calculated vertical motion coincides with the maximum observed motion. The onset of the fundamental Rayleigh, especially in the radial component, is somewhat obscured on the observed trace by the prograde event preceding it. The long duration of the oscillatory motion observed at this distance, slightly less than one wave length from the source, is especially to be noted.

At 18 meters, approximately one quarter wave length from the source, motion is observed for longer than one second. The frequency of this extended train is practically

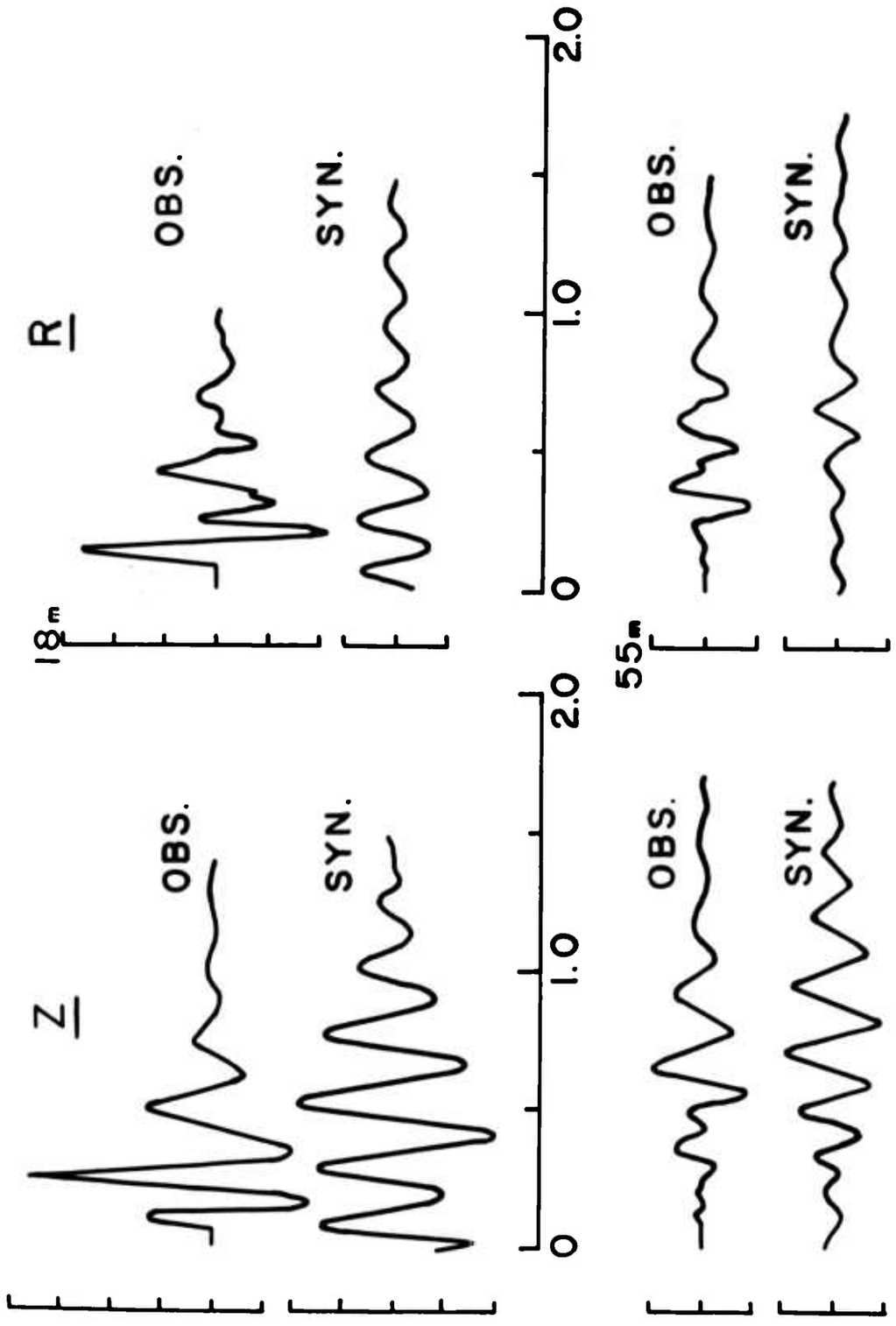

FIGURE 12. OBSERVED AND SYNTHESIZED MOTION, SHORT RANGE, SUFFIELD

constant and crests can be correlated with larger amplitude phases at greater distances (Figure 5). This motion is reproduced on the synthesized traces. A comparison of the synthesized and observed traces reveals that the maximum synthesized vertical motion is approximately 0.1 second later than the maximum motion on the observed trace. The particle motion in the radial-vertical plane, Figure 13, indicates that the fundamental Rayleigh motion begins at approximately 0.220 seconds, which corresponds to a time 0.040 seconds before the observed maximum on the vertical trace. However, in Figure 5 it was shown that the maximum energy is propagating at a group velocity of 90 meters per second. This means that the maximum Rayleigh motion should occur at about 0.2 seconds. The interference with body waves and the prograde event preceding the Rayleigh wave alters the observed traces such that the Rayleigh onset predicted from the particle motion diagram would not be accurate but would give the time at which the Rayleigh mode dominates the motion. The maximum synthesized motion on the radial component is 0.040 seconds earlier than the vertical maximum. The particle motion is elliptic retrograde. The important points to be noted here are the delays in the calculated maxima and the long duration of the synthesized and observed traces, which are particularly well shown on the vertical.

The motion calculated at the source at Suffield from

the observed motion at 122 meters is shown in Figure 14. The most striking feature is the long oscillatory nature of the source function. Figure 15 shows a comparison of the source functions calculated from different distances and different shot depths. The upper two traces are the vertical component calculated from a shot at a depth of 5.5 meters and recording distances of 122 and 183 meters respectively. The lower trace was calculated from motion observed at 153 meters from a shot at a depth of 2.3 meters. The similarity of the source functions is obvious. This shows the reproducibility to be expected from calculations from various distances, and the reproducibility of the motion from different source depths in the same medium for these cases in which the recording distances are considerably larger than the source depths.

In all of these calculations the maxima on the vertical and radial traces are approximately 0.3 seconds after origin time. The possibility that the phase velocity curves are grossly in error is ruled out when one considers the agreement between the observed and calculated motion at large distances, as previously shown and the agreement at 55 meters. Some other explanation for this delay must be sought. Before pursuing this further, let us consider the source functions at Florissant.

Figure 16 shows the radial and vertical source functions which were calculated from the observed motion at 75 and

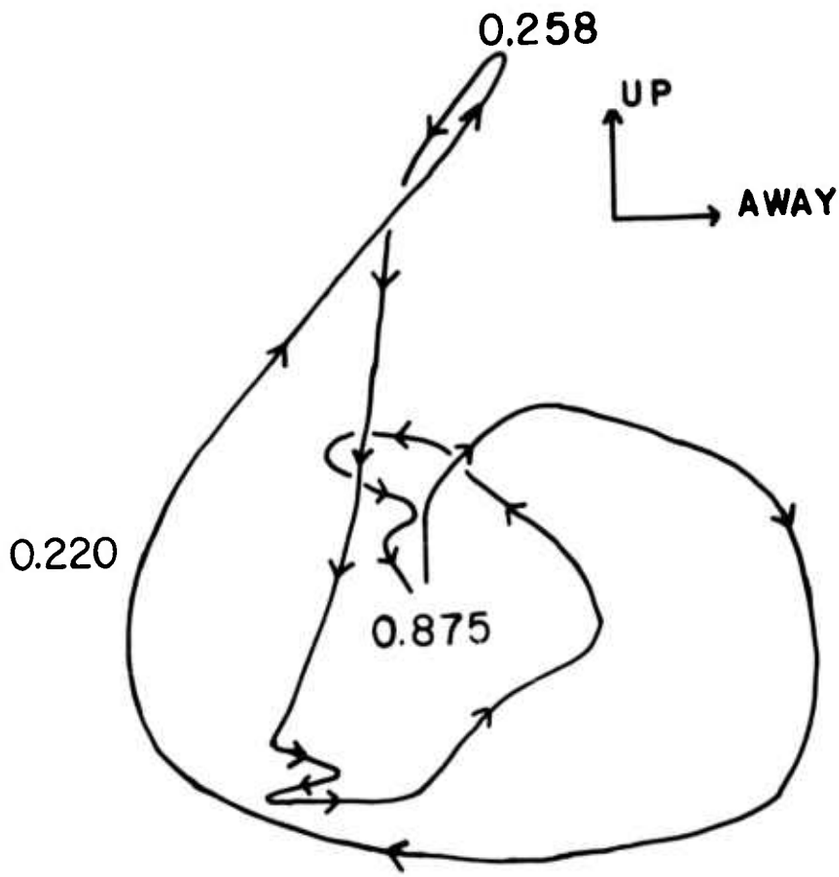

FIGURE 13

PARTICLE MOTION, SHORT RANGE

-SUFFIELD-

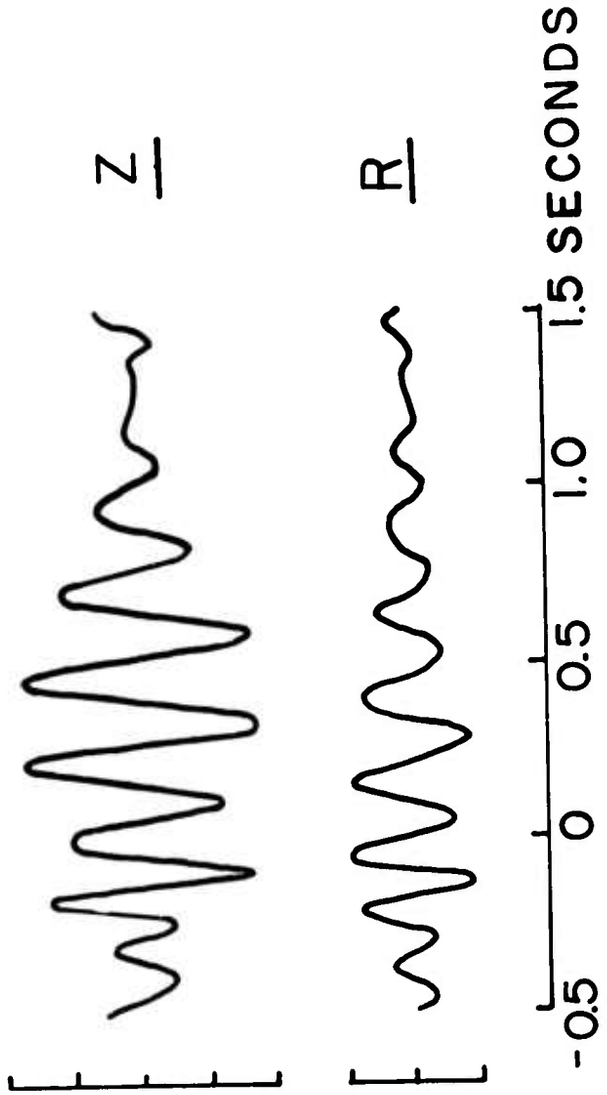

FIGURE 14

SOURCE MOTION, SUFFIELD

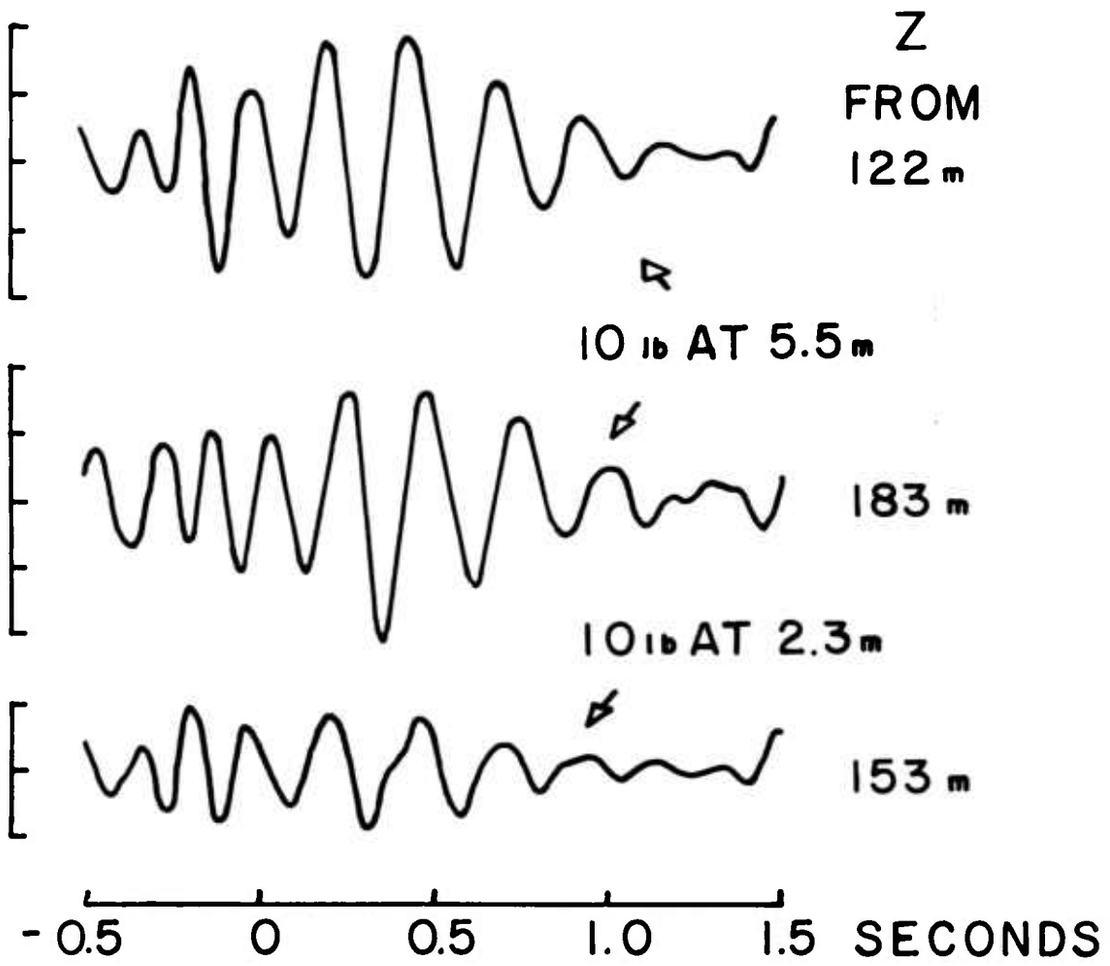

FIGURE 15. SOURCE MOTION FROM DIFFERENT DEPTHS AND DISTANCES, SUFFIELD

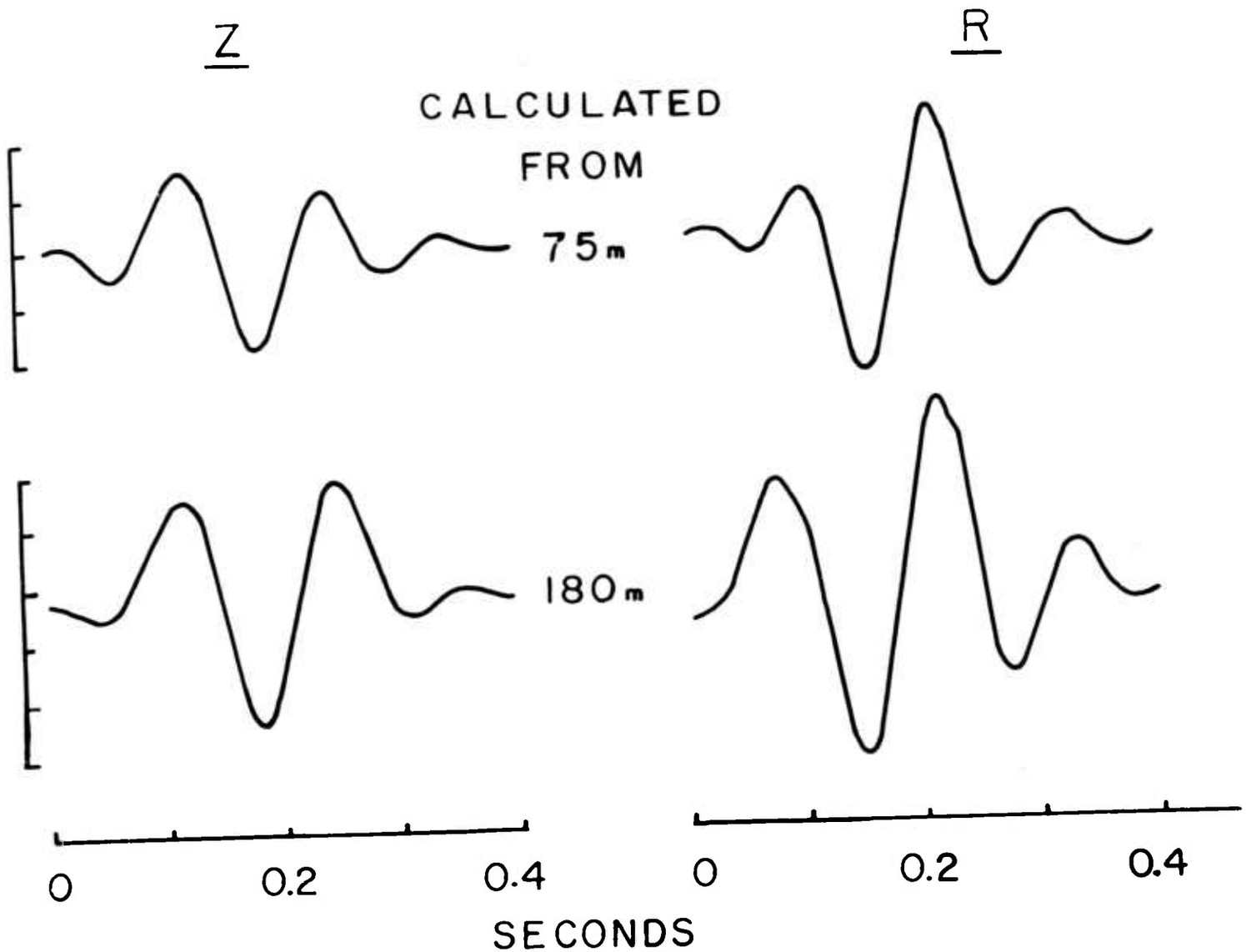

FIGURE 16. SOURCE MOTION, FLORISSANT

180 meters from the source. The agreement of the wave forms on the radial traces is excellent; however, there is a difference in the wave form of the vertical traces. The relative amplitudes of the two peaks on the upward side of the zero line are different. The observed vertical Rayleigh motion at 75 meters, Figure 2, is still distorted by the prograde event which precedes it. The accurate determination of the Fourier phase angles is, therefore, difficult, and distortion of the source function results. These events separate as the distance from the source increases; consequently, the source functions calculated from 180 meters should be considered more reliable.

The source functions at Florissant are oscillatory in nature but much shorter in duration than those at Suffield. The maximum amplitudes occur between 0.175 and 0.220 seconds after origin time. Here also the comparisons shown at distance (Figures 9 and 10) give one confidence that the phase velocity data used in the calculations are reliable. This means that we must look to another source for the delays in the observed maxima.

In the series of tests at Suffield a 500 pound hemispherical charge was detonated on the free surface and recorded between 153 and 366 meters along the same profile as the contained shots. The source functions calculated from the observed motion at 213 meters are shown in Figure 17. The calculated motion of both the radial and vertical components

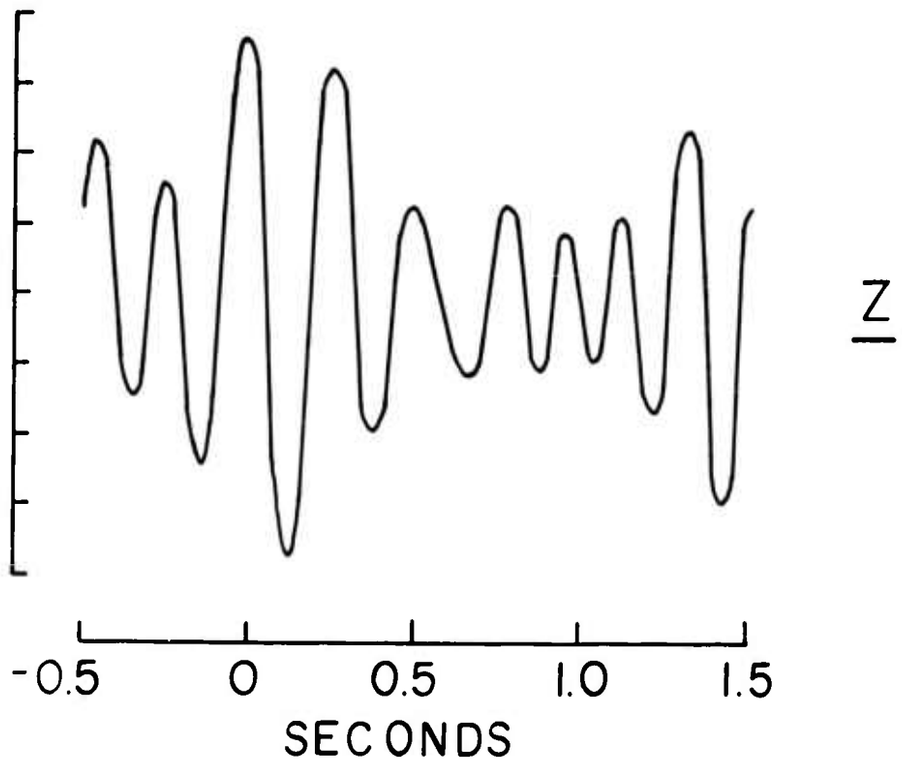

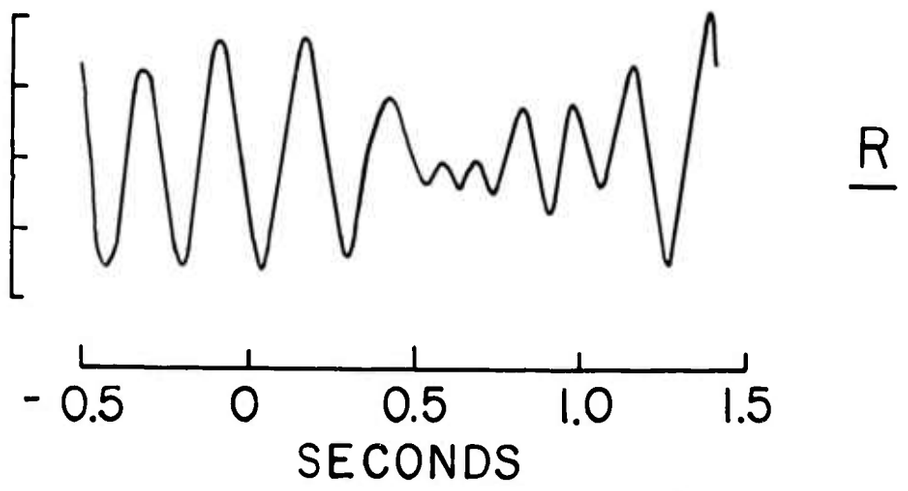

FIGURE 17

SOURCE MOTION, 500 lb. SHOT

-SUFFIELD-

is long and oscillatory just as the motion from the contained shots. However, unlike the contained shots, the maximum amplitudes occur near zero time.

Effects of Asymptotic Approximation in Source Region. Cylindrical spreading was assumed in the calculation of the synthesized motion. The pertinent solution of the wave equation in this case is the Hankel function of the second kind. For distances that are sufficiently large the asymptotic expansion of the Hankel function is used. This gives rise to the $r^{-\frac{1}{2}}$ factor for geometric spreading. It was thought that the use of the asymptotic approximation in the source region might be affecting the calculated results. To check this the exact value of the amplitude and phase of the Hankel function for each frequency was calculated for distances of 18 meters and 30 centimeters. The difference between these computed values and the values from the asymptotic expansion were used to determine a phase and amplitude correction for each frequency. The radial motion at Suffield was synthesized using the corrected values. Comparisons of the synthesized motions at 18 meters and at the source revealed the following: 1) at 18 meters there is no significant change in the motion: amplitudes and frequencies are the same, and 2) at the source there is a reduction of amplitude but the duration of motion and the frequencies are the same. Thus, the use of the asymptotic expansion in the source region seems to be a satisfactory approximation within

the limits of precision of the data and numerical methods employed.

Interpretation of Source Functions. In this discussion, the "source function" is the motion calculated at the surface, over the shot point, which would produce the observed Rayleigh motion at distance when subjected to the given dispersion. For a near-surface burst, for which Rayleigh waves are produced directly, the source function will take the form of the elastic response of the medium to the applied pressure waveform. For a shot buried so deeply that the free surface does not participate in the initial strong motion, the source function represents the response of the medium to a point force applied at the surface, equivalent to the interaction of the body waves from the explosion with the free surface. This response is not the same as the displacement of the boundary of the equivalent cavity in the conventional model of an explosive source.

The accuracy with which the calculated source function represents the actual behavior at the epicenter depends on the extent to which the input spectrum is preserved in the observed motion. The observed spectrum is always band-limited, and the resulting source function must be somewhat oscillatory. A sharply peaked spectrum will yield a highly oscillatory source function.

Aki (1960c) interprets the source function on the assumption that the initial phase, the same for all fre-

quencies, is independent of the layering of the medium. If the distance to the recorder is sufficiently greater than the focal depth, as it is for all of the data used here, then the initial phase of the source function depends only upon the time and spatial history of the applied force at the source. Thus, under the assumption that the effect of dispersion due to the layering and the phase changes introduced by the recording instrument are accurately removed in the process of phase equalization, the polarity and symmetry of the source function, which are determined by the initial phase, can be interpreted in terms of idealized forces acting at the origin.

In his paper Aki compiled idealized source functions for the vertical component associated with an explosive step and an explosive impulse. The waveforms (initial phase) associated with these sources are not unique to them. For example, the response to an explosive step from a point source is the same as that from a horizontal force directed toward the receiver. Figure 18 shows the source functions, vertical and radial components, from an explosive step and an explosive impulse applied at a point in a half-space.

The source functions calculated for Florissant, Figure 16, closely resemble those found by Aki for Rayleigh waves from earthquakes. An examination of Aki's tabulated source functions and the present results indicate that the assignment of these derived waveforms to a particular class

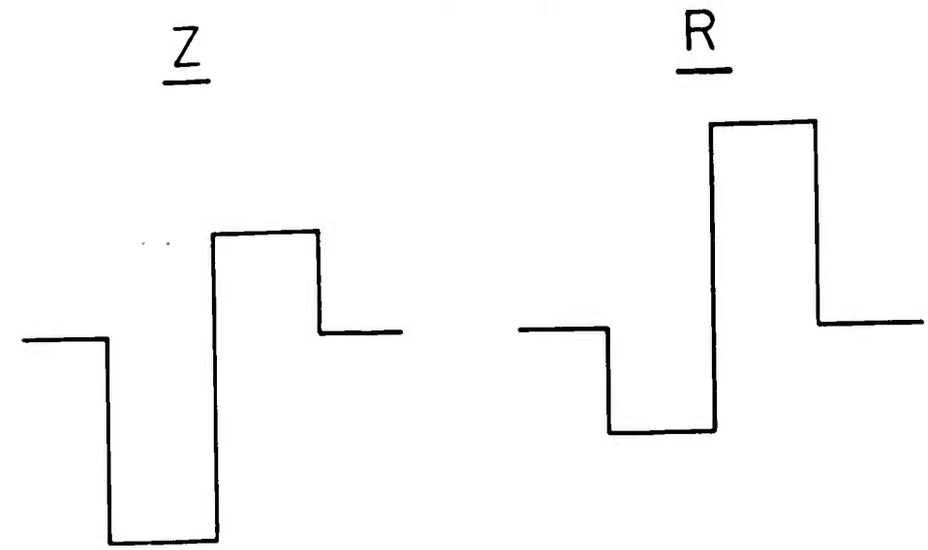

EXPLOSIVE STEP

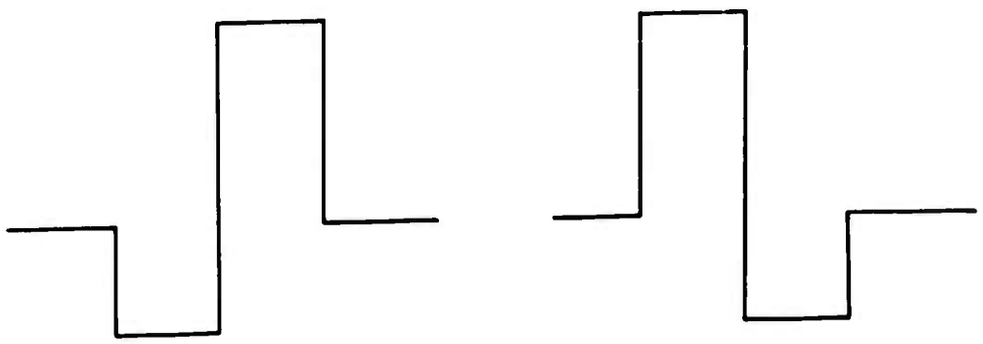

EXPLOSIVE PULSE

FIGURE 18

IDEALIZED SOURCE FUNCTIONS

(even, odd or some combination of these) depends on very small departures from symmetry, and small differences in the amplitudes of displacements adjacent to the maximum motion. A purely even or purely odd function can only result from a two-dimensional source. Since the source in these experiments is known to be a point, the selection of an even or odd function was excluded, even though this requires placing confidence in minor variations in the waveform. If the interpretation is constrained to a three-dimensional solution, then the result, based on the record at 180 meters, for which the second peak on the vertical is greater than the first, but smaller than the trough, while the trough on the radial component is slightly smaller than the following crest, agrees best with an explosive step.

The results for 75 meters indicates a down pulse in force rather than an explosive step. Since it is known that motion other than the fundamental Rayleigh wave is included in the record at this station, little confidence can be placed in the small differences between the two results that require the different interpretations.

It must be recognized that there is no reason to demand that the driving force in the field experiments be either impulsive or a step function, or that the initial phase of all Fourier components be the same. The effect of a driving force that decays monotonically or oscillates would be to destroy the ideal symmetry and extend the source

function in time.

The source functions from the contained shots at Suffield, Figures 14 and 15, are long in duration and of almost constant frequency, a consequence of the narrow frequency spectrum (Figure 6). These source functions cannot be interpreted as those at Florissant, because, as Aki states (1960c, p. 2408): "If the spectrum is peaked, the source function will take an oscillatory form, which is undesirable for the clear identification of its type."

Before considering why the frequency spectrum is so narrow at Suffield let us examine the source functions from the 500 pound surface shot, Figure 17. As in the case of the contained shots, the waveforms of both components oscillate with constant frequency, and the spectrum of the vertical component peaks at 4 cps with the same band width. The fact that the peak of the spectrum does not change with a fifty-fold increase in charge size requires that some factor other than total input energy is controlling the spectrum. The spectrum for a given medium can be affected by crater or cavity size and by the layering present. Since charge size has no appreciable effect here, the near surface layering must dominate the spectrum. The contained shots and the surface shot, two distinctly different sources, produce motion at distance which is identical in the frequency of the waveform but differ in phase by π. This leads to the conclusion that the layering is important in the Rayleigh wave generation process at this site.

It was shown above (Figure 12) that constant frequency motion was observed for longer than one second at a distance approximately one-quarter wave length from the source. These observations suggest that energy is being transmitted from the source region for a period of time much longer than the time duration of the explosion itself. This is typical of a tuned or resonant mechanical oscillator with low damping and leads to the belief that the Rayleigh motion at this site is produced by a resonance phenomenon.

There is additional information to support this viewpoint. In addition to the contained ten-pound shots fired at Suffield, ten pounds was fired on the surface and 3 meters above the free surface. Neither of these shots generated any Rayleigh waves. In August, 1961, a 100-ton surface burst was fired at this test site. In reviewing the seismograms from this test, Kisslinger (1963) pointed out that the Rayleigh wave generated by smaller shots was not present. A review of records from earlier trials at this test site showed Rayleigh waves with the same period and group velocity as those from the smaller charges to be absent from all of the surface shots greater than five tons. Retrograde elliptic motion following the air blast arrival is found on seismograms from these large shots but the arrival times are much too early for this to be the same event as that recorded from the smaller shots. Kisslinger suggested that the 100-ton shot acted as a force downward

on the lower layers and that the longer period Rayleigh motion resulting was controlled by the higher-velocity deeper layers. The size of the crater for the 100-ton shot would tend to support this conclusion. The entire thickness of the low velocity surface layer was involved in the source region.

The evidence presented here leads one to the conclusion that the response of the free surface to the explosive loading that results in the production of the fundamental Rayleigh waves at the two sites is entirely different. At Florissant the source function appears to be independent of the layering whereas at Suffield it appears to be dominated by the near-surface layering. For small charges at Suffield this effect does not depend on whether the charge is at the surface or buried.

It was noted in a previous section that there is a time delay for the maximum amplitude of the source functions from the contained explosions which did not appear in the source functions from the surface shot. This suggests that there is a time delay in the generation process of Rayleigh waves from a contained explosion which does not exist for the surface source. This time delay is longer than P or S wave travel times from the source to the surface. This point merits further study. The data from a small number of tests under nearly similar conditions are not sufficient to allow any definite conclusion.

Source Functions from Higher Modes.

The presence of prograde elliptic motion preceding the fundamental Rayleigh mode at both test sites has already been discussed. Source functions were calculated for these events.

Figure 19 shows the radial- and vertical-component source functions calculated from the observed motion at 180 meters from Florissant. The wave forms are oscillatory and more complex than were the fundamental. Source functions calculated from various distances were not reproducible. This suggests that the phase velocity curve used for the synthesis of the Fourier components is not correct. This is not surprising in view of the interpretation of this prograde motion as a combination of $\overline{F}$ and the M_{21} mode of the Rayleigh wave.

An interpretation of these source functions in terms of a force system cannot be justified in view of the lack of reproducibility observed. If the slope of the phase velocity curve is in error or if the values of the velocity at each frequency are in error by some value, the resulting calculations will be in error. There is good reason to suspect that this is the case.

The motion of the M_{21} branch observed at 183 meters at Suffield was used to calculate the source functions shown in Figure 20. This motion was calculated using a phase

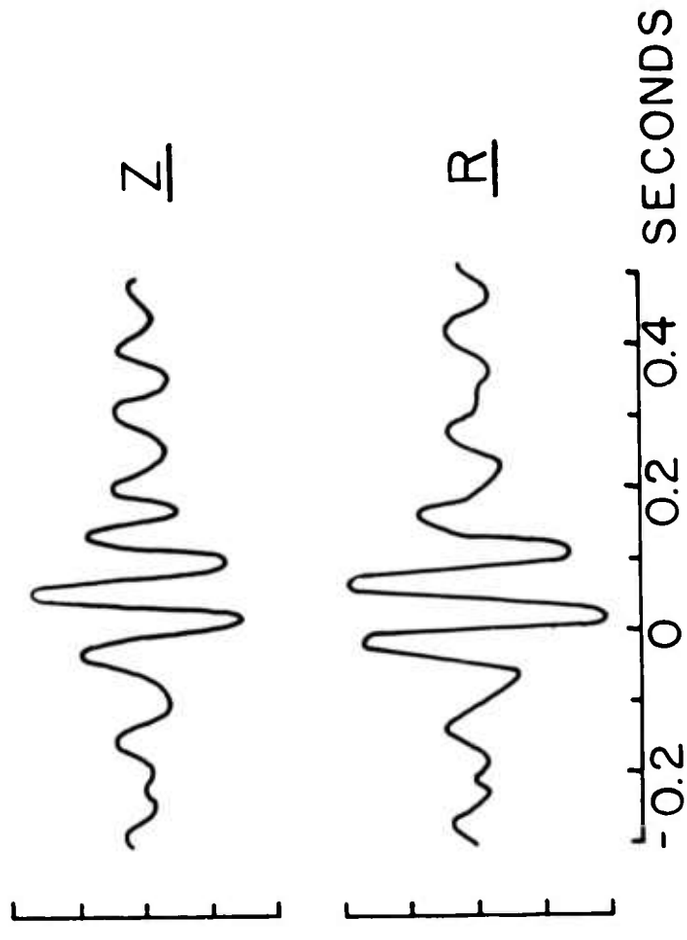

FIGURE 19

SOURCE FUNCTIONS, HIGHER MODE

-FLORISSANT-

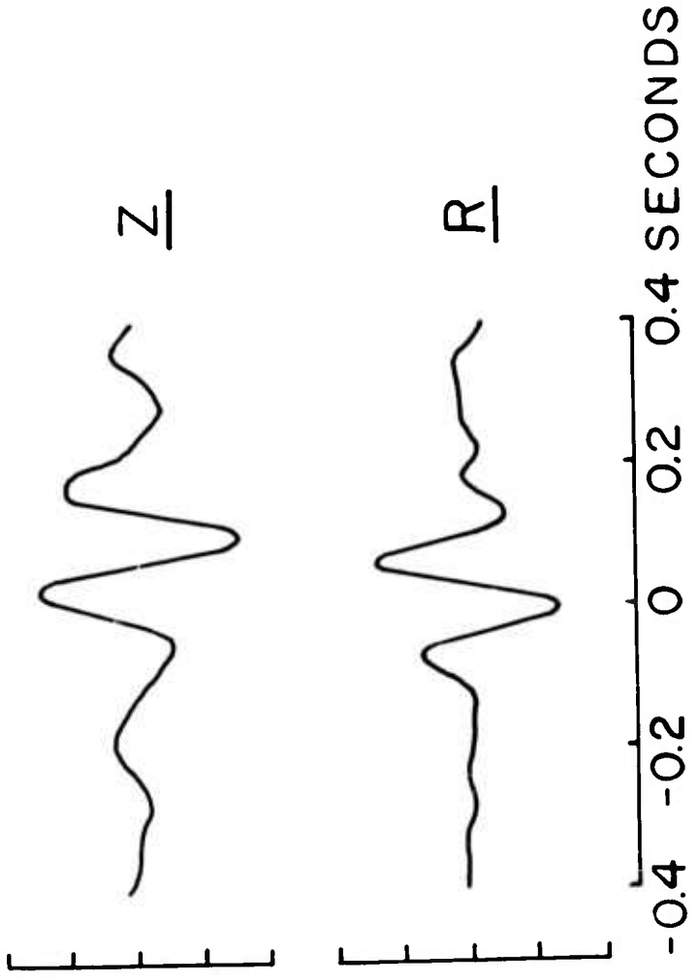

FIGURE 20

SOURCE FUNCTIONS, HIGHER MODE

-SUFFIELD-

velocity curve which was slightly faster than the observed vertical curve in the frequency range from 6 to 11 cps. and slightly lower than the observed radial curve in the same range. This curve was used because tests with the observed curves indicated that both were somewhat in error. The motion synthesized at the source using the observed curves was very similar to that using the average curves but better time agreement between the radial and vertical components was attained with the average curve.

The source function is much simpler than that from the fundamental Rayleigh wave at this site. The spectrum for this event, Figure 6, is broader than that for the fundamental and peaks at a higher frequency. The ground motion for this event, shown in Figure 3, remains pulse-like in nature over the range of recording and does not exhibit strong dispersion.

The difference in the nature of the source function between the M_{21} mode and the fundamental can be interpreted to mean that the generation process is somewhat different for the two events. The source function for the M_{21} mode can be interpreted using Aki's criterion. The waveform of the source function is similar to that associated with a down pulse propagating in three dimensions. This is somewhat surprising in view of the fact that the explosion was contained. This event could not be identified for the 500 pound shot, because its expected time of arrival coincided

with the air blast arrival and the large motion which follows.

The simple nature of this source function strengthens the view that something other than the shot is controlling the generation of the fundamental Rayleigh motion at Suffield.

Synthesis of Love Waves.

The fact that explosions produce prominent horizontal transverse, SH, motion has been discussed in detail for the Florissant test site (Kisslinger, et al, 1961 and Chapter V). The long period motion observed on the transverse trace has been identified as a Love wave. The dispersion curve is shown in Figure 7 and the Fourier amplitude spectrum in Figure 6.

The Love motion from a profile at Florissant was used to calculate the source functions shown in Figure 21. The reproducibility of the wave form from the two distances from which calculations are shown, 150 and 180 meters, is excellent. The waveform is oscillatory but basically fairly simple. The duration and shape are similar to those from the fundamental Rayleigh at this site. The frequency of the waveform is approximately 10 cps which corresponds to the peak of the Fourier spectrum. Clockwise motion (down on the trace) about the source is indicated for this azimuth.

Conclusions.

1. At distances at which the fundamental Rayleigh

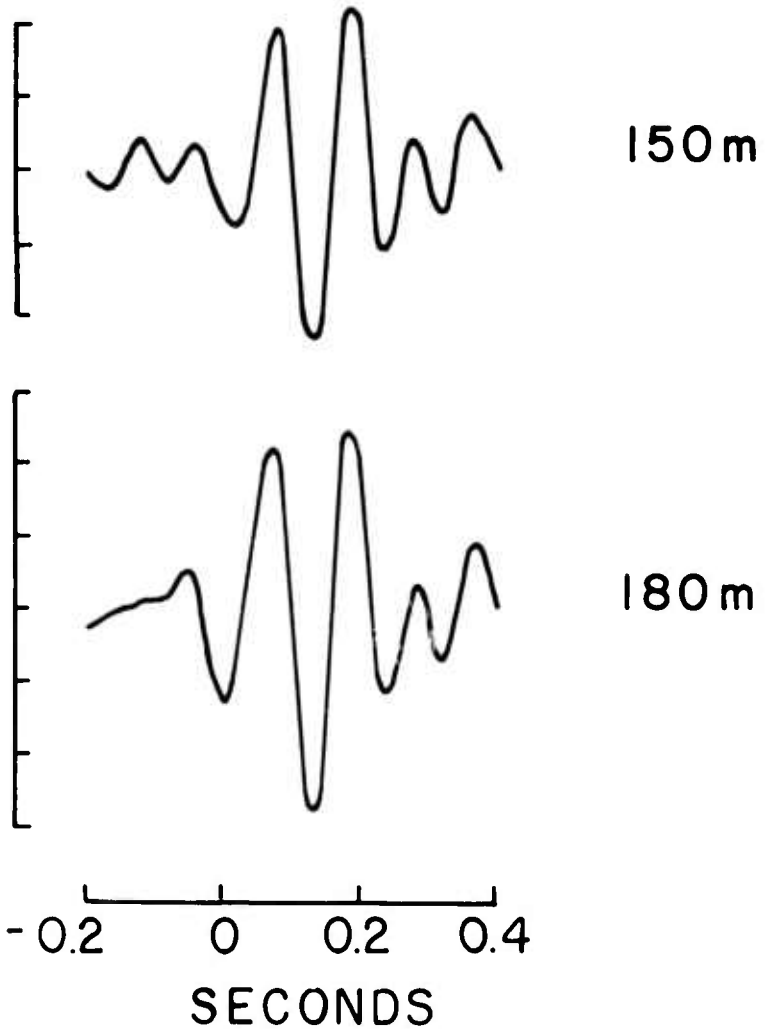

FIGURE 21

SOURCE FUNCTIONS, LOVE WAVES

—FLORISSANT—

motion is separated from the faster events, the synthesized Rayleigh motion matches the observed motion quite closely. This indicates that the method of synthesis of Fourier components is useful, for one can accurately predict the motion at any distance as long as the dispersive properties do not significantly change, and the observed motion does not represent an interference of two or more events.

2. The source functions of the fundamental Rayleigh waves from the two test sites are quite different. Both are oscillatory in nature but the very narrow spectrum at Suffield results in a long duration constant frequency waveform. This has been interpreted to mean that there is a distinctly different response of the near-surface materials to the explosion at the two sites. The evidence at Suffield leads to the conclusion that a resonance phenomenon controlled by the near surface layering strongly affects the character of the Rayleigh wave, whereas at Florissant the layering plays no comparable part in the generation process.

3. The maximum amplitudes of the source functions from contained explosions are delayed as long as 0.3 seconds after the origin time. This is not the case for a surface shot at Suffield. The conclusion is that the delay is due to the generating mechanism for Rayleigh waves from a contained explosion, requiring that energy proceed from the source region for a relatively long time after the detonation.

4. Calculations of source functions for Love waves at Florissant from different distances along one azimuth were very similar.

5. The classification of calculated source functions into particular types in order to interpret the character of the input force is difficult. Confidence must be placed in minor differences in the calculated waveforms, differences that may well be within the accuracy of the data and the analytic procedures.

CHAPTER IV

RADIATION PATTERNS FROM RIPPLE-FIRED SHOTS

Background and References.

For many years quarry and mine operators have been utilizing ripple-fired shots to minimize the damaging effects of their blasting. In practice, the ground amplitude or particle velocity are reduced by a trial and error determination of the optimum spacing and delay times. Willis (1963) studied velocity spectra from instantaneous and .017 sec. delayed multi-hole shots. He found amplitude attenuation from ripple-firing to be considerably more for body waves than surface waves. The effect is dependent on frequency spectrum and wave length of the seismic signal.

Pollack (1963) observed the predicted relationship between the spectrum of a single shot and that of the same signal summed with time delays in a series of controlled ripple-fired quarry blasts. He assumed a smooth, damped oscillatory waveform of approximately .001 sec. rise time and .004 sec. duration (simple body wave arrival) as the unit input signal and compared observed and predicted spectra for 3, 7 and 15 holes delayed, in total, .00166, .00375, and .00664 sec. The effect of any time delays due to spatial distribution on the shots was not considered. These would introduce an azimuthal variation into the resultant signal.

Ripple-firing effects on surface waves are complicated by the addition of a frequency-dependent velocity, so that

the equivalent time delay corresponding to a spatial separation depends also on frequency.

As a part of an overall study of controlled radiation patterns of P, SH, and Rayleigh waves from explosions a series of field experiments in ripple-firing was conducted in the summer of 1962 (shot points 65-72, Table 1). This section of the report presents the results of the experiments.

Data.

Several types of shot point patterns and various time delays were used in the experiments in order to test the effects of the spatial distribution of the individual charges making up the shots, as well as the effects of varying the delay times. Motion was recorded 30 meters from the center of the shot pattern at six equally spaced azimuths with Sprengnether three-component seismographs and the 12 SIE vertical geophones were spaced between the Sprengnethers. The basic separation unit between charges in the shot patterns was 1.5 meters and the unit charge size was 0.25 pound of dynamite. In the subsequent discussion time delays are given in the form of the effective velocity of propagation of the detonation.

In addition to calibration shots (S.P. 69a, b) of 1.25 and 0.25 pound at the center of the detector array, ten multi-hole shots were detonated in the series:

S.P.66: 5 shots simultaneously in a vertical hole 7.6 meters deep

S.P. 65: 5 shots detonated upward at 200 meters/sec. in a vertical hole 7.6 meters deep.

S.P. 67a: 5 shots simultaneously in a horizontal line

S.P. 67b: 5 shots at 210 meters/sec. in a horizontal line

S.P. 68a: 5 shots at 103 meters/sec. in a horizontal line

S.P. 68b: 5 shots at 82 meters/sec. in a horizontal line

S.P. 70: 2 shots at 190 meters/sec. in a horizontal line

S.P. 71: 2 shots at 91 meters/sec. in a horizontal line

S.P. 72a: 8 shots in two horizontal lines (couple) of 4 charges detonated in opposite directions at 185 meters/sec.

S.P. 72b: 8 shots in two horizontal lines (couple) of 4 charges detonated in opposite directions at 91 meters/sec.

All delayed shots were fired with a sequential timer utilizing rotating, staggered cams, capable of firing up to 15 shots. Firing times of the first and last shots were recorded on the SIE timing trace for determining detonation velocities.

Figures 22 through 28 present the reduced seismograms, showing the radiation patterns produced by the various horizontal shot patterns. S.P. 68b is omitted because a malfunction of the timer resulted in an unusually large time lag in the shot sequence. Also, in the case of S.P. 67a, it is doubtful that the total charge detonated. Azimuths are all measured clockwise from the northward end of the pattern.

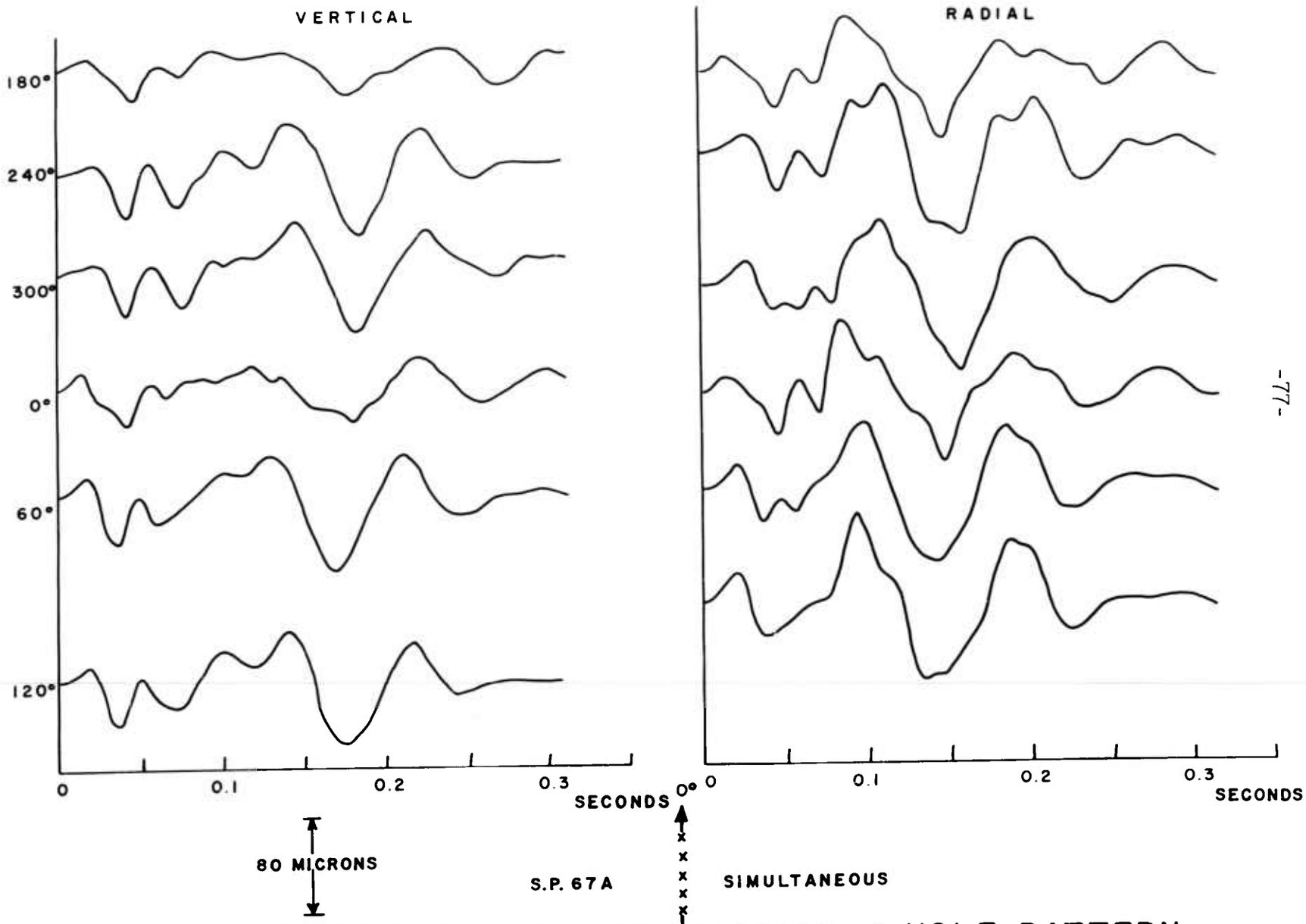

FIGURE 22. GROUND MOTION, 5 HOLE PATTERN

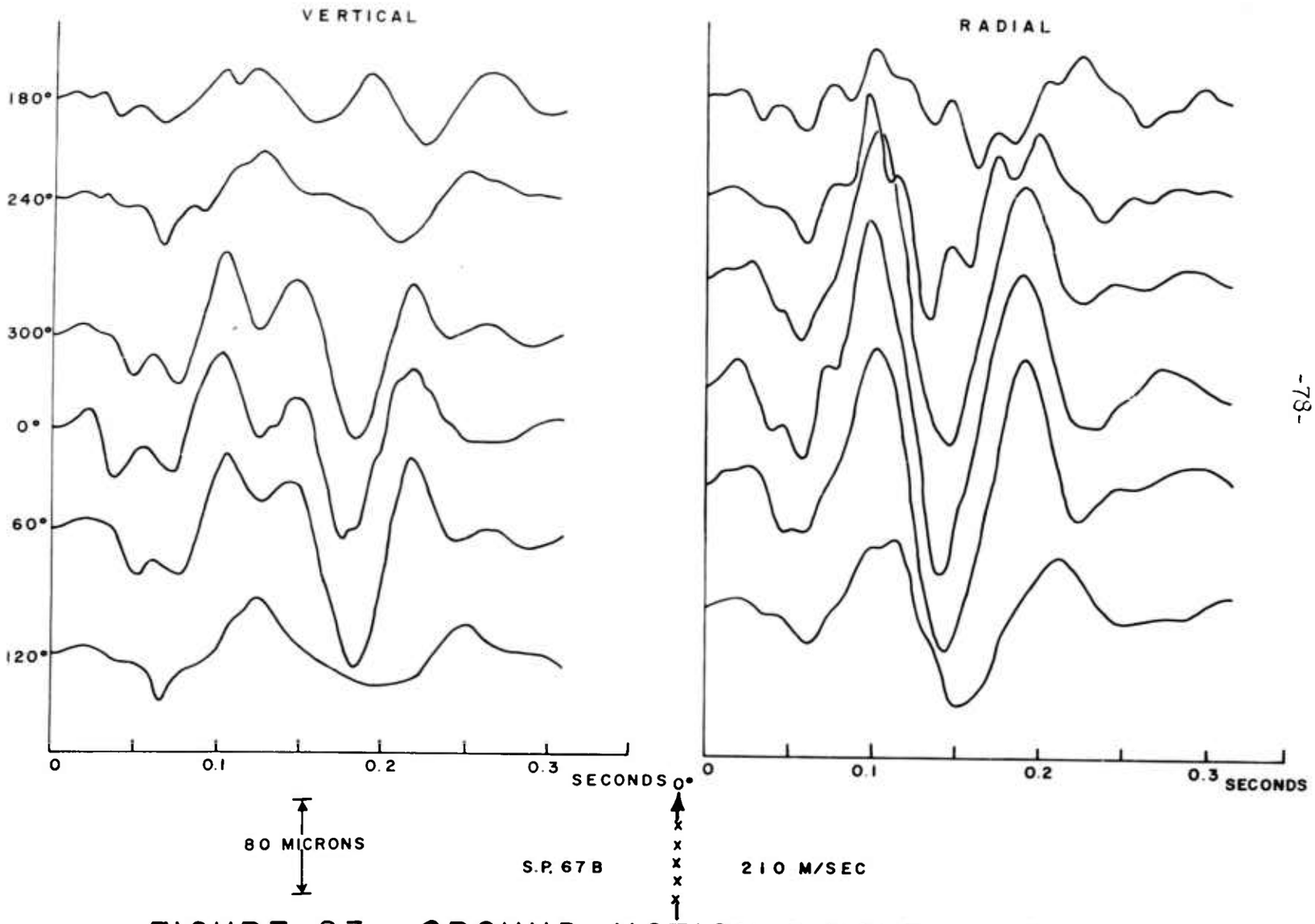

FIGURE 23. GROUND MOTION, 5 HOLE PATTERN

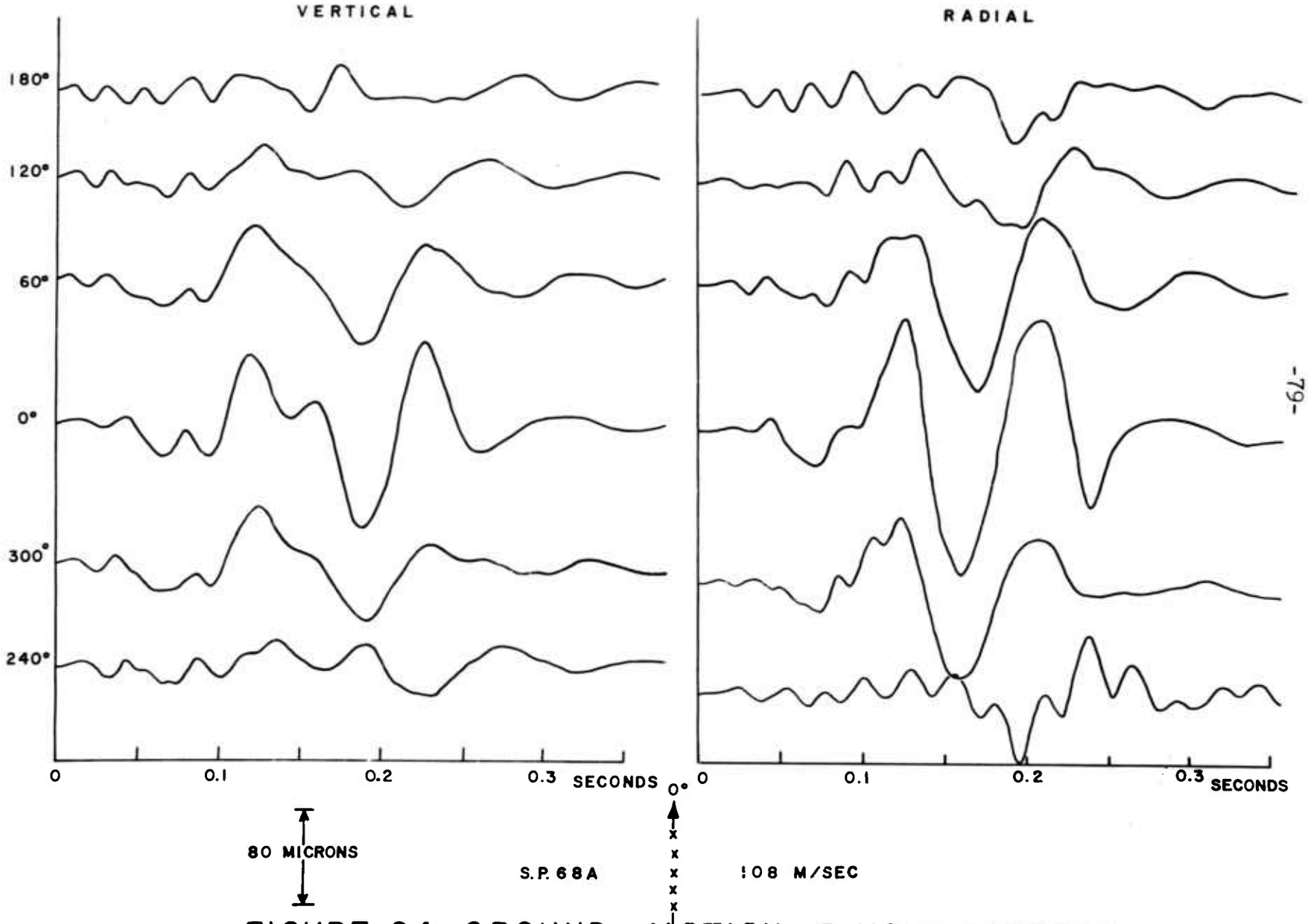

FIGURE 24. GROUND MOTION, 5 HOLE PATTERN

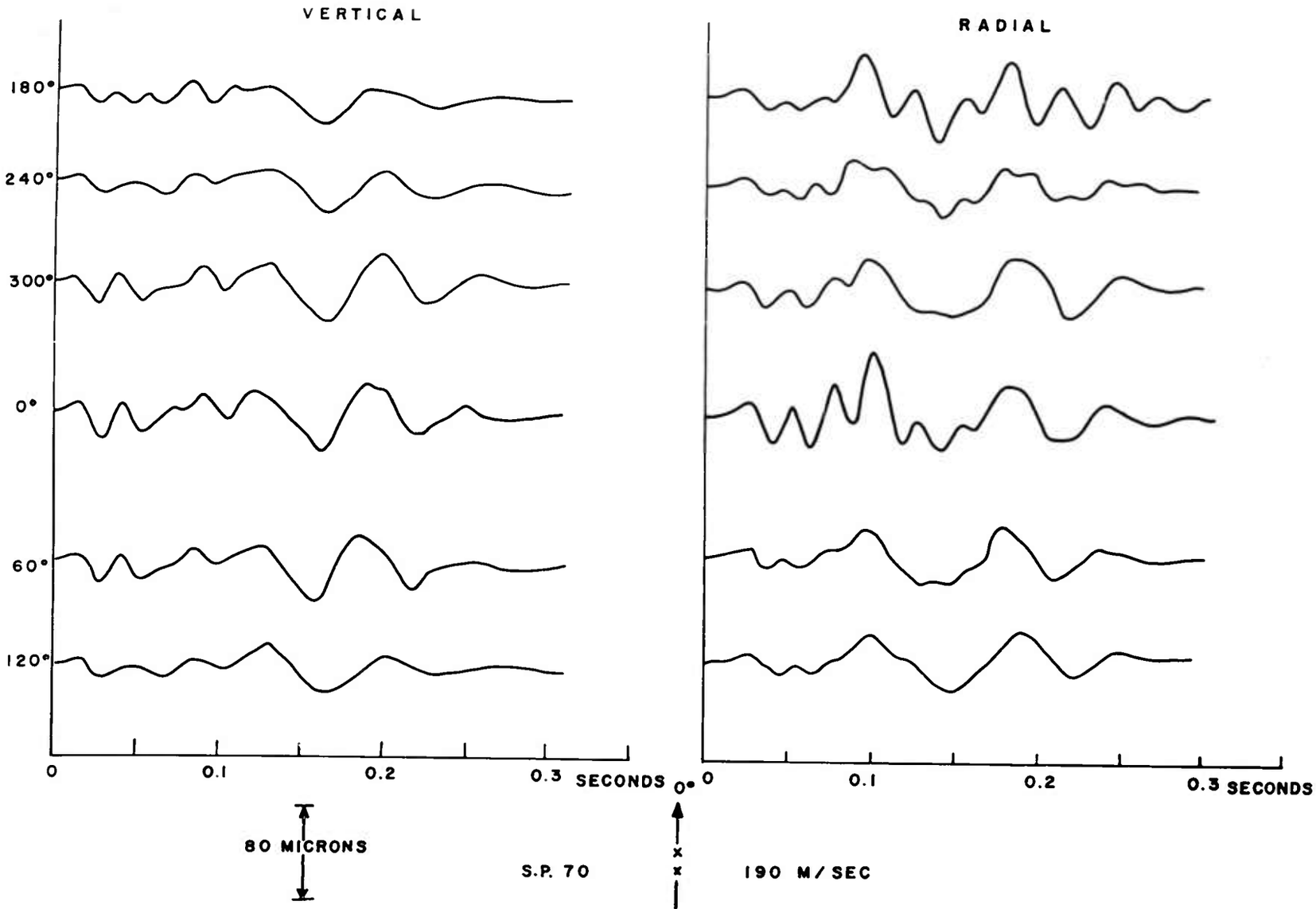

FIGURE 25. GROUND MOTION, 2 HOLE PATTERN

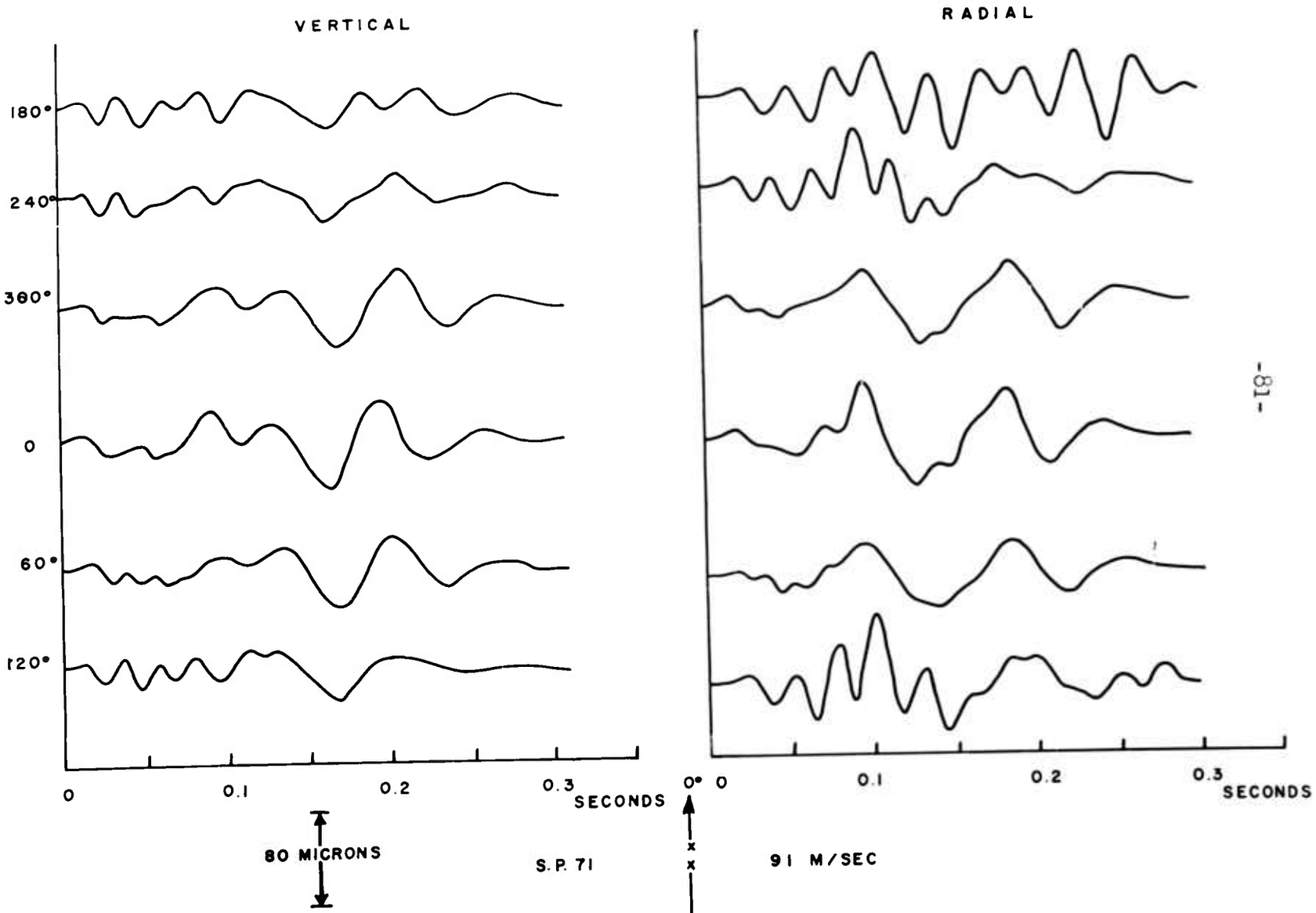

FIGURE 26. GROUND MOTION, 2 HOLE PATTERN

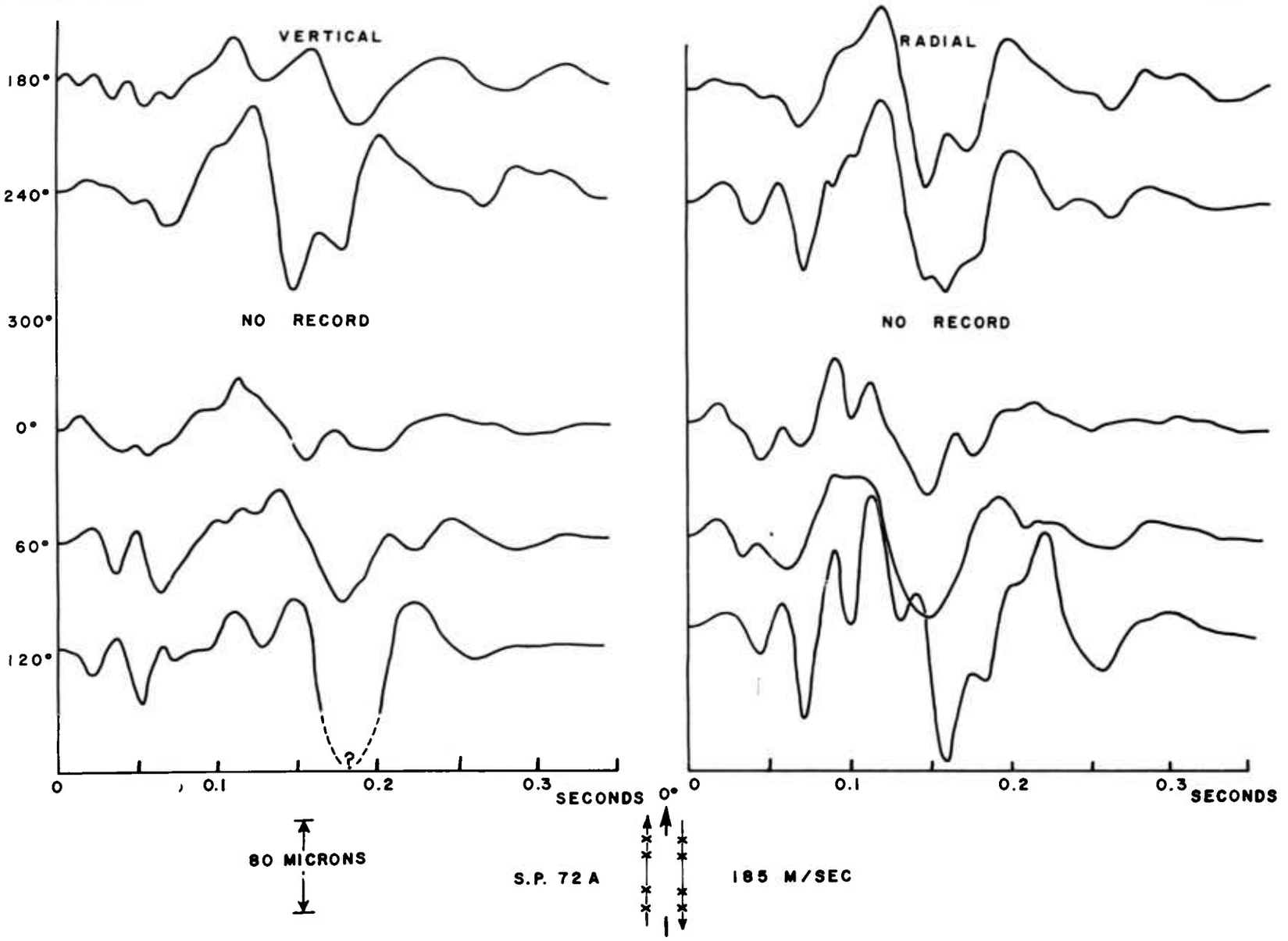

FIGURE 27. GROUND MOTION, COUPLE

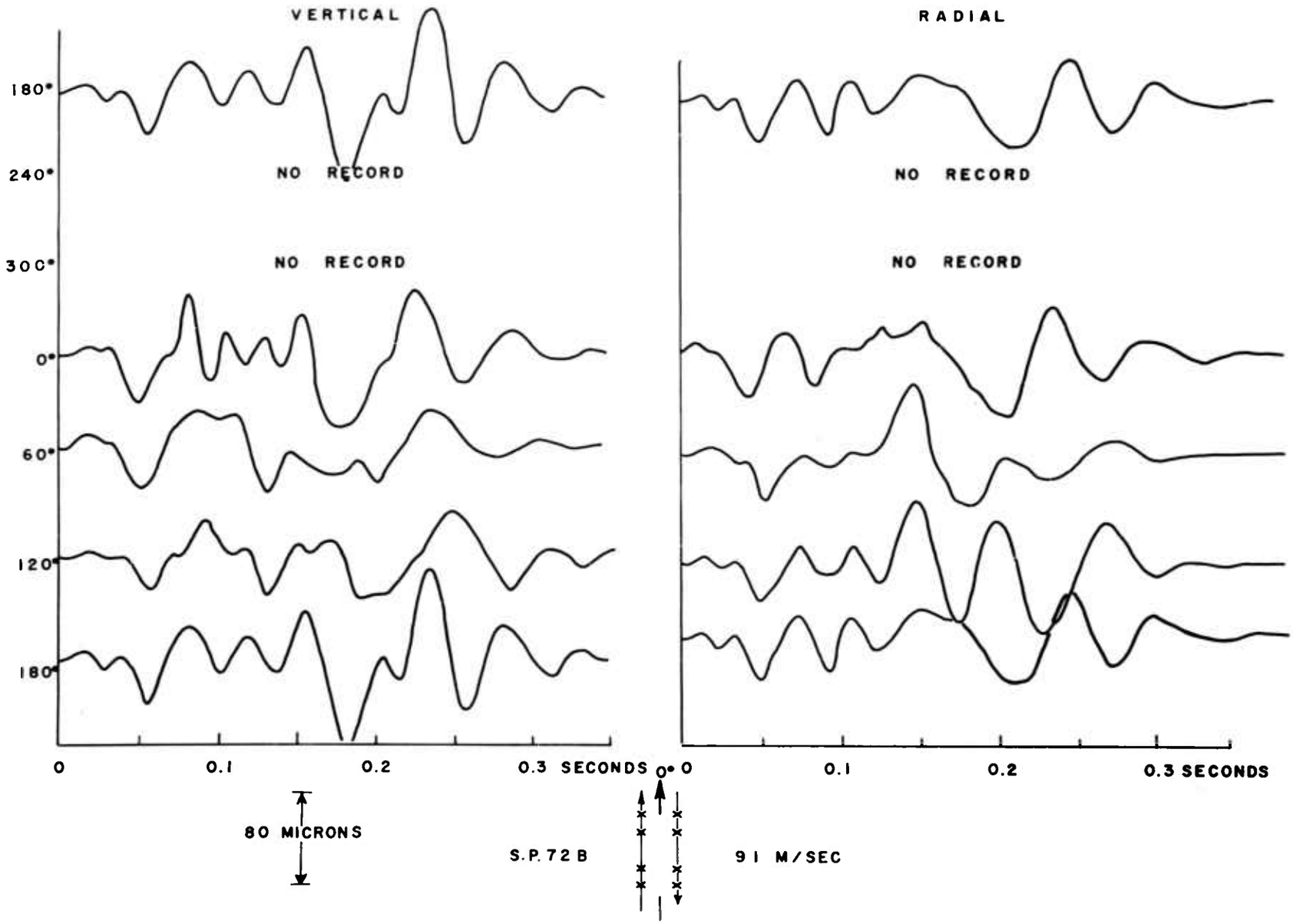

FIGURE 28. GROUND MOTION, COUPLE

Data Analysis.

It is evident from the figures that the temporal and spatial distributions of these shots have severe effects on the radiation patterns. It is also apparent, from the similarity of records at points symmetric with respect to the propagating source, that there are no significant anomalies introduced by differences in path characteristics.

The analysis procedure adopted for these data is an attempt to explain the radiation patterns by simple superposition of the unit seismic signal through Fourier synthesis.

If $f_1(t)$ is the recorded trace from the unit charge from which the delayed system will be constructed, then

$$\sum_{n=1}^{N} f_1(t-\Delta t_n),$$

is the signal from N shots delayed after the first by time Δt_n, where Δt_n is the combined delay due to both temporal and spatial separations, i.e.

$$\Delta t_n = D_n + \frac{\Delta R_n}{V}$$

where:

D_n = firing time delay,
ΔR_n = additional path from n^{th} charge to receiver
V = velocity of propagation of signal, possibly frequency dependent.

In terms of spectra, if

$$F_1(\omega) = \frac{1}{\sqrt{2\pi}} \int_{-\infty}^{\infty} f_1(t) e^{-i\omega t} dt$$

is the "unit" spectrum, then for the composite signal

$$F(\omega) = 1/\sqrt{2\pi} \int_{-\infty}^{\infty} \left[\sum f_1 (t - \Delta t_n) \right] e^{-i\omega t} dt$$
$$= 1/\sqrt{2\pi} \sum e^{-i\omega \Delta t_n} \int_{-\infty}^{\infty} f_1(t) e^{-i\omega t} dt$$
$$= e^{-i\omega \Delta t_n} F_1 (\omega).$$

If the amplitudes, but not waveforms of the individual shots vary, the summation contains an amplitude factor. This is the case for the vertical line of charges, where such a factor was used in the computation. Then the composite spectrum is given by

$$F(\omega) = \sum A_n e^{-i\omega \Delta t_n} F_1 (\omega)$$

where the individual charges give signals

$$f_n (t) = A_n f_1 (t - \Delta t_n).$$

Summarizing, the spectrum of the composite signal is given by the spectrum of the unit signal modified by the multiplicative function:

$\sum A_n e^{-i\omega \Delta t_n}$ for variable amplitudes and delays,

$\sum e^{-i\omega \Delta t_n}$ for variable delays only

$\sum e^{-i\omega n \Delta t}$ for constant delays, Δt, and no spatial effect.

For fixed firing-time delays, the variation in the total delays is introduced by the spatial separation of the individual charges. Without this factor there is no azimuthal effect inherent in time delays.

In the analysis, synthetic seismograms were computed by performing the inverse Fourier transform operation on the computed F (ω). In the most general case of variable delays and charges the synthetic seismogram is

$$f_s(t) = 1/\sqrt{2\pi} \int_{-\infty}^{\infty} \left[\sum A_n e^{-i\omega\Delta t_n}\right] e^{i\omega t} F_1(\omega)\, d\omega.$$

Figure 29 shows the nature of the unit signal used in this procedure. The vertical and radial components and the moduli of the Fourier Transforms are presented. This motion was produced at 30 meters by a calibration shot of 0.25 pound of dynamite. Both the vertical and radial components of motion were found to be very similar in all azimuths and one record was arbitrarily chosen as the standard, $f_1(t)$. Subsequent figures show theoretical seismograms for several of the experimental shot patterns.

Because the predominant energy in the standard signal appears to be the fundamental mode Rayleigh wave, the corresponding frequency-phase velocity relationship was used in calculating the equivalent time delays due to spatial distributions. The dispersion curve is well-known for the experimental area. (see Chapter III).

Figure 30 shows the theoretical seismograms for the vertically stacked shots. In this case there is no azimuthal variation of the signal. Because of the amplitude-depth function used, the upper shot controls the appearance of the seismogram resulting in little apparent change of the waveform. This depth-dependence function was constructed from

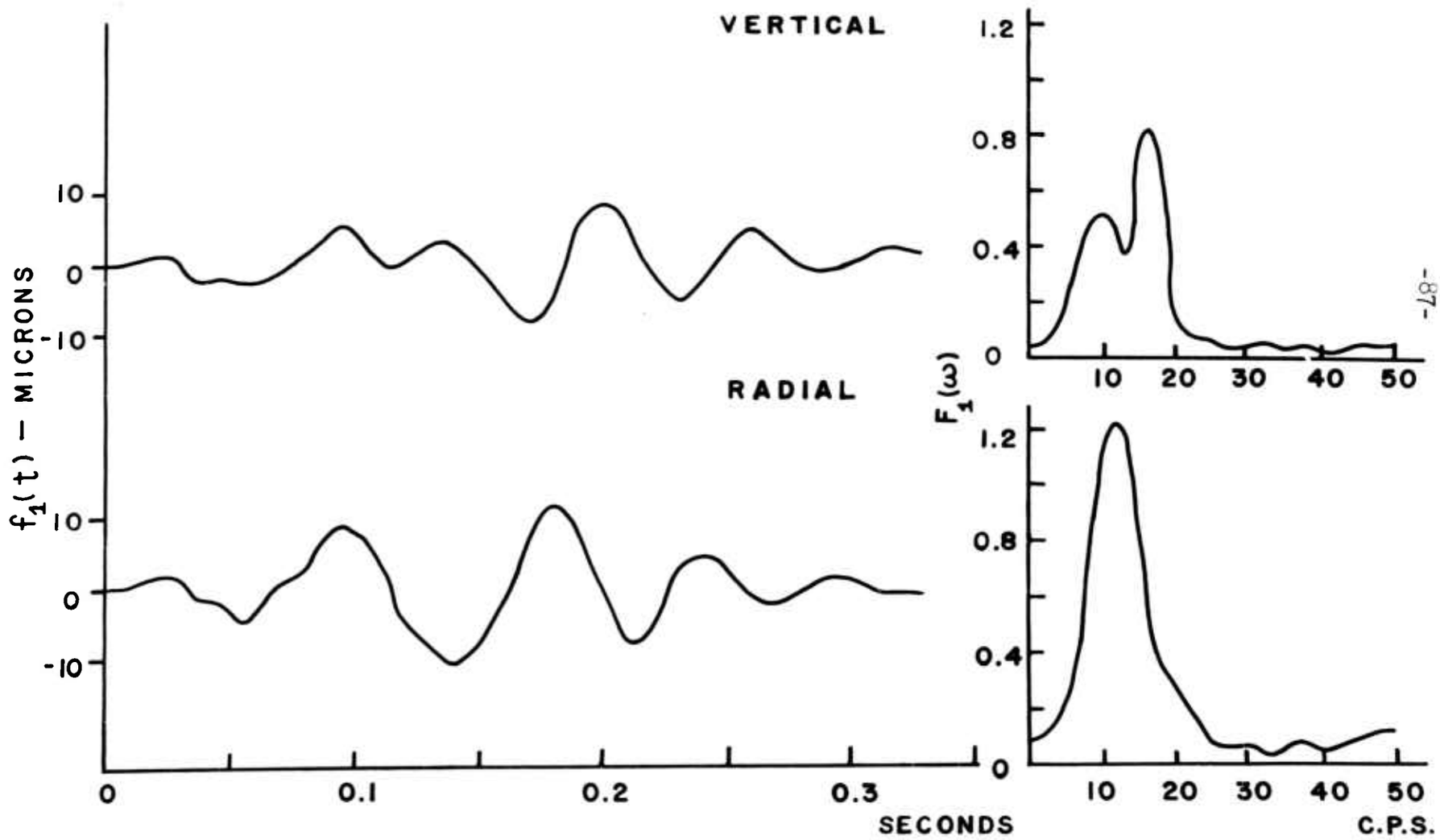

FIGURE 29. UNIT SIGNAL FOR SYNTHESIS OF RIPPLE-FIRED SHOTS

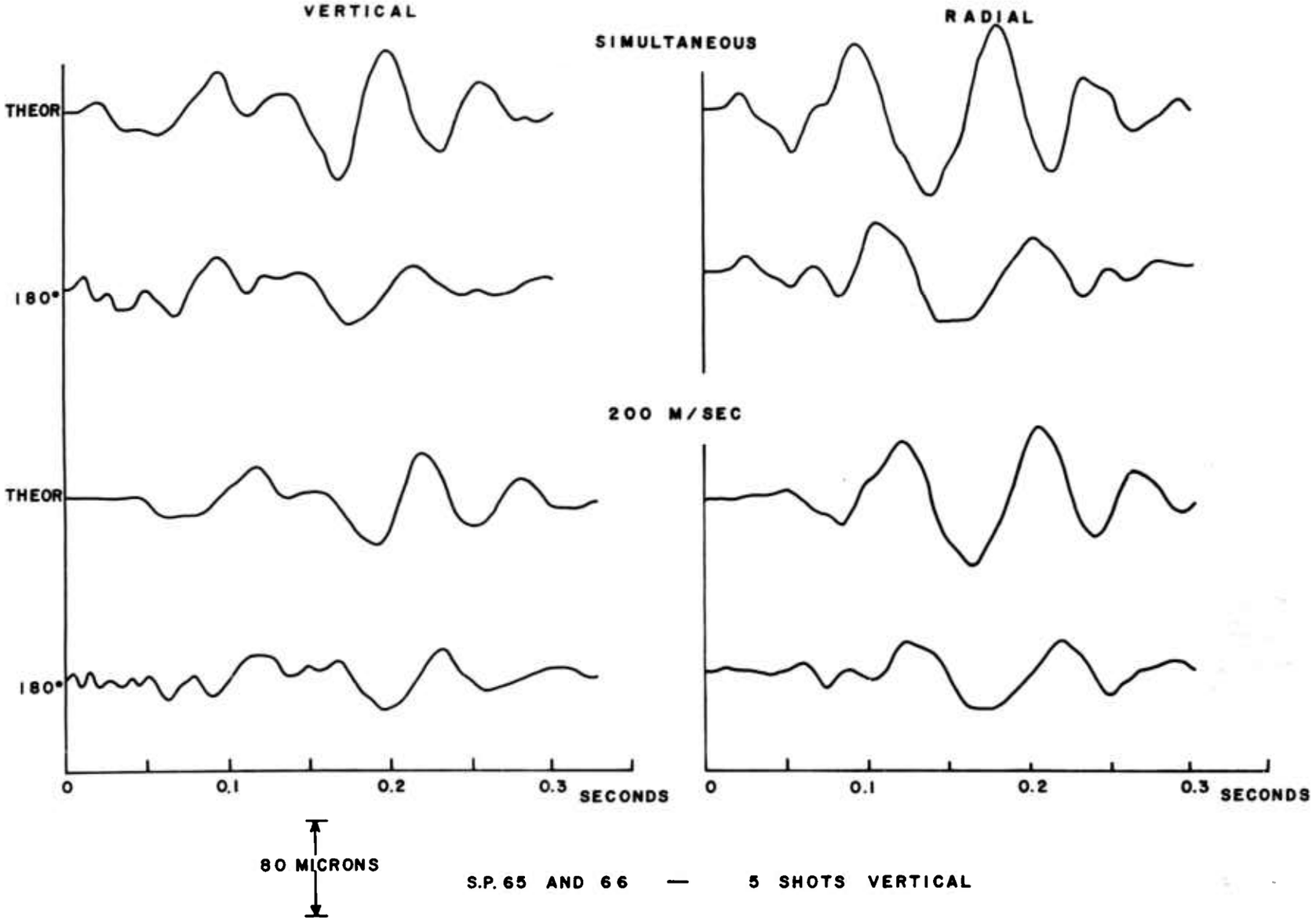

FIGURE 30. OBSERVED AND CALCULATED MOTION, VERTICALLY STACKED CHARGES

observation of amplitude change over the same depth range for other shot points in the field program. Table 3, in which unit amplitude is assigned to the shallowest shot, presents this relationship. Zero time corresponds, in the case of the delayed shot, to the firing time of the top charge. The actual seismograms are those from 180° azimuth. The high frequency (50 to 80 cps) body wave events at the beginning of the record are not present on the theoretical seismograms because of the 50 cps cut-off on the standard spectrum, a result of digitalizing increment. In addition, the amplitude-depth function used does not apply to the body waves, having been determined for the Rayleigh wave.

Table 3

AMPLITUDE - DEPTH RELATIONSHIP FOR VERTICAL PATTERNS

Depth (m)	A
1.5	1.00
3.0	.30
4.5	.15
6.0	.10
7.5	.08

Figures 31 and 32 show theoretical seismograms for the five-shot horizontal line fired simultaneously and at 108 meters/sec.

Figure 33 shows theoretical seismograms for the two-shot horizontal line fired at 91 meters/sec. With the exception of the high frequency components in the records, the agreement is generally good. On the vertical components, traces were mistakenly synthesized at azimuths midway between re-

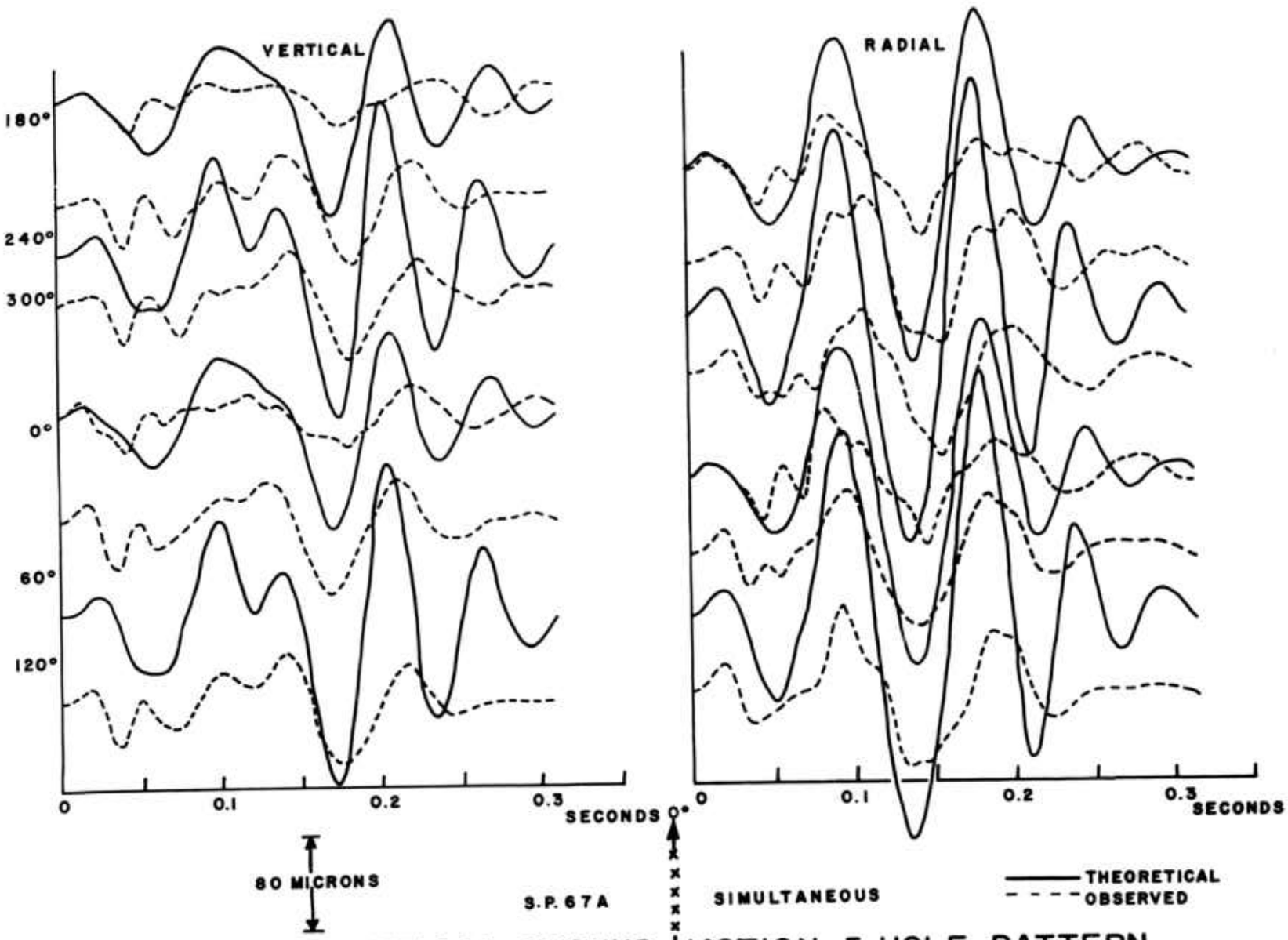

FIGURE 31. THEORETICAL GROUND MOTION, 5 HOLE PATTERN

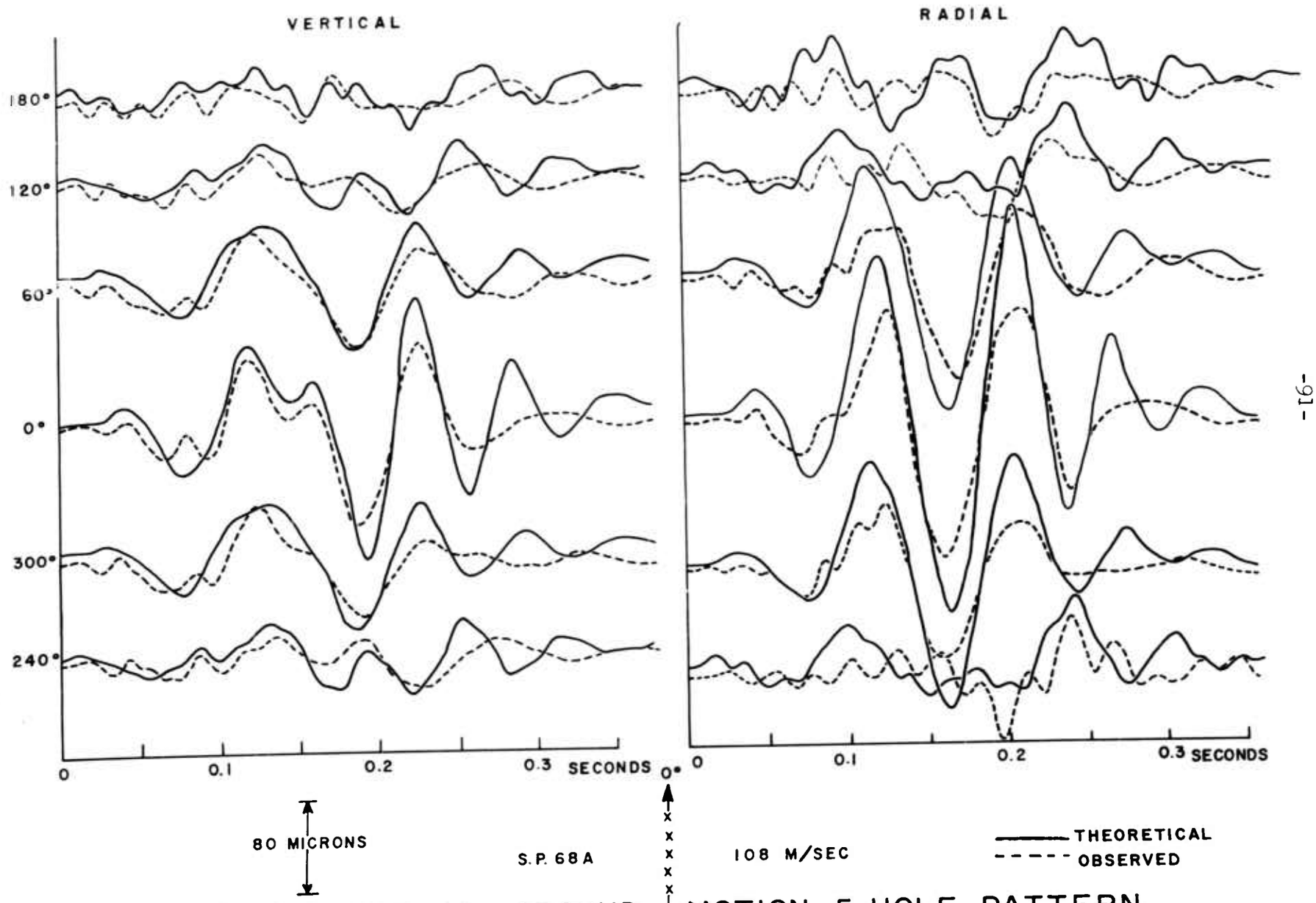

FIGURE 32. THEORETICAL GROUND MOTION, 5 HOLE PATTERN

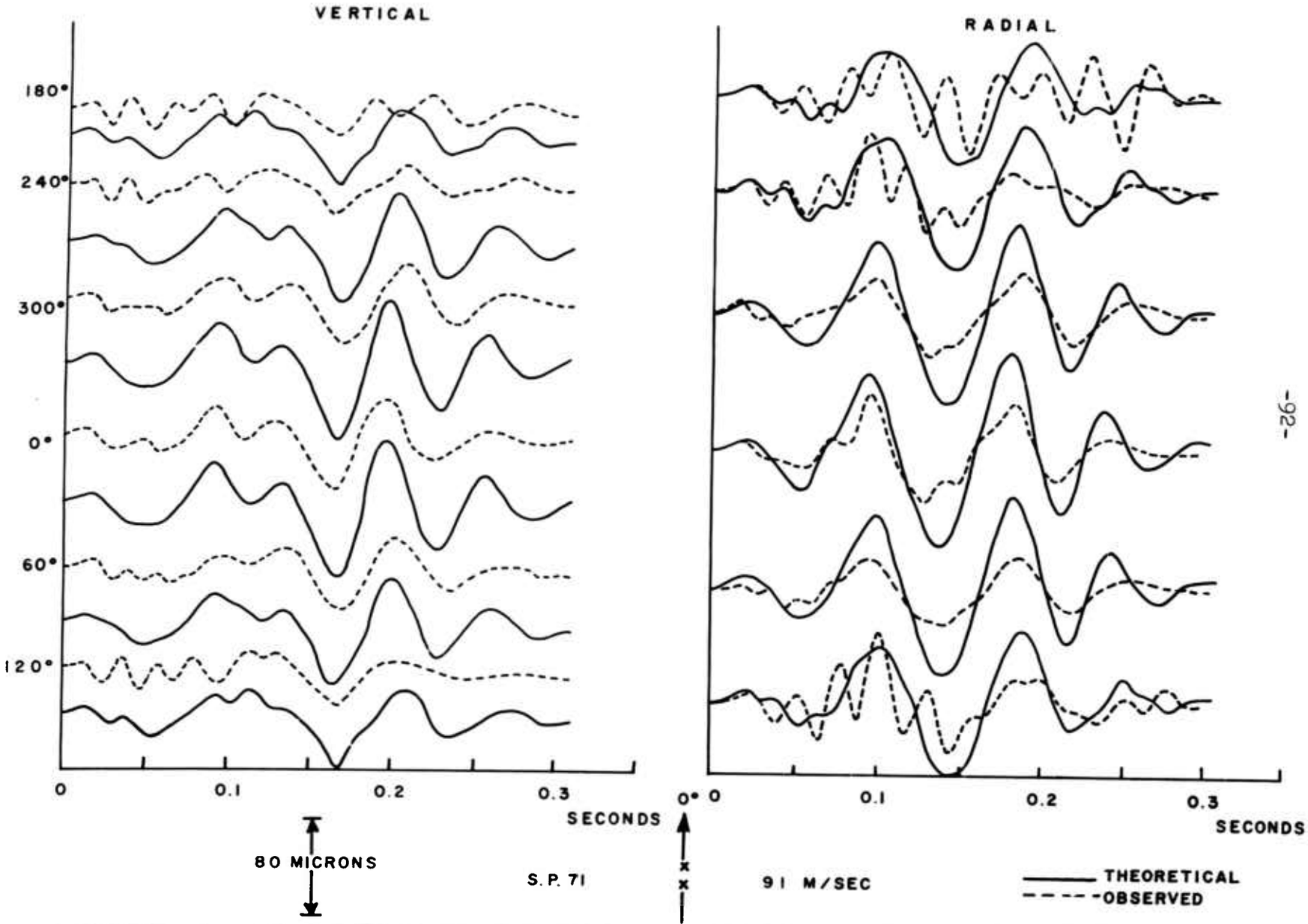

FIGURE 33. THEORETICAL GROUND MOTION, 2 HOLE PATTERN

cording azimuths. However, the change is gradual enough that the comparison can be made. The shot at 190 meters/sec. is similar except that higher speed reduces the severity of azimuthal variations.

Figure 34 is the theoretical pattern for the double horizontal line at 91 meters/sec. No records were obtained at 240° and 300°, which should be equivalent to 60° and 120° by symmetry. The 185 meters/sec. pattern is very similar. In this case agreement is generally good, although there are some significant amplitude differences.

Summary and Conclusions.

While there are discrepancies, probably due to loss of high frequency components, incomplete charge detonations, and errors in assignment of velocities to frequency components, radiation patterns observed from ripple-fired shot arrays can be reasonably well explained theoretically by simple superposition. Fourier theory indicates that a perturbation to the unit spectrum in the form of the sum of a product of amplitude and phase change factors yields the composite spectrum. The total time delay consists of a fixed increment and a spatial time equivalent, depending upon receiver position. The spatial distribution gives rise to the azimuthal radiation pattern. Synthetic seismograms were computed and plotted on an IBM 1620 for all recording azimuths. Comparison with observed motion indicates generally good agreement.

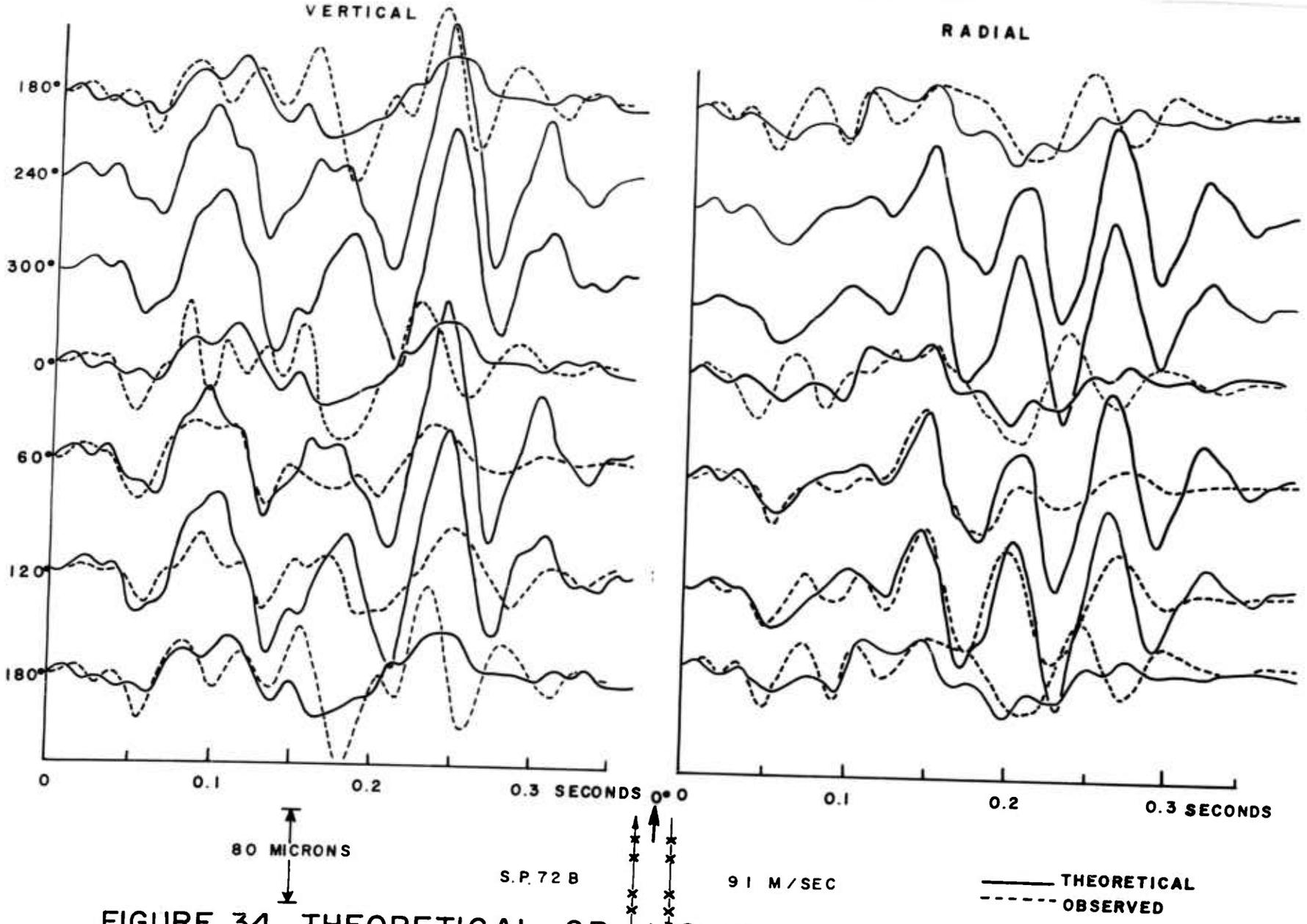

FIGURE 34. THEORETICAL GROUND MOTION, COUPLE

The severity of the azimuthal variations that can be produced suggest that maxima or minima of Rayleigh wave energy from explosions can easily be oriented if ripple-firing is feasible, and if the shot point layout can be arbitrarily selected.

CHAPTER V

HORIZONTALLY POLARIZED SHEAR WAVES

Introduction.

The properties of shear waves generated by underground explosions was the first subject of investigation in this research program. Simple methematical models of an explosion as a source of seismic waves fail to predict the existence of shear waves proceeding directly from the neighborhood of the explosion. The observed presence of shear waves polarized in the plane of incidence (SV waves) is readily explained by the conversion of compressional energy at subsurface interfaces and at the free surface of the earth, and so their occurrence cannot be taken as a significant departure from simple explosion theory. Horizontally polarized shear waves (SH waves) cannot be generated in this manner, and so it was decided that the best way in which to study explosion-generated shear waves was to concentrate on SH waves.*

The existence of SH motion of large amplitude on seismograms from explosions had long been known to seismologists working with three-component records of quarry blasts, but these had never been studied systematically. It was determined very quickly from the first experiments carried out in this program that SH motion is always produced by buried

*It is possible for apparent SH motion to arise by reflection and head wave propagation from subsurface beds that are not parallel to the earth's surface.

shots, and that these waves have some well-defined properties. A paper, hereafter referred to as Paper I, in which these properties are explained and possible generating mechanisms are discussed was published in 1961 (Kisslinger, et al, 1961). The important properties may be summarized as follows.

1) Both body shear waves and Love waves are generated by the explosion. These waves have frequencies in the same band as the compressional and Rayleigh-type waves.
2) Love waves are propagated with a pronounced azimuthal variation in amplitude, marked by a pattern of nodal lines with reversed polarity on either side of the nodes.
3) The observed reversals in polarity are not apparent reversals of the phase associated with the maximum amplitude as a result of non-symmetry of the dispersive properties of the layered system. Reversal of the entire horizontal transverse waveform, down to fine details, has been observed in many cases, and the pattern of radiation has been found to be maintained over a range of distances.
4) In soft materials, such as clay or alluvium, the body shear waves are roughly one-fourth to one-third the amplitude of the compressional waves, and Love waves have average amplitudes about the same fraction of the Rayleigh wave, although they may be almost as big at the maximum of a lobe. In these materials the azimuthal distribution of radial and vertical motion is completely

symmetrical, and the SH motion is undoubtedly independent of these.

5) In brittle materials, such as sandstone and limestone, all types of motion are somewhat asymmetrical, and the shear waves may be as large as the other motion recorded. A nuclear shot in granite has confirmed the large amplitudes of shear waves from shots in competent materials.

6) The shear energy that is directly produced by the shot almost certainly is formed in the transition region of non-linear behavior around the explosion. Processes in this region are only partly understood, but recent work has made significant progress toward clarifying them (Bishop, 1962). The present investigators prefer the growth of radial cracks as an adequate source of shear waves with the observed properties.

Basic Observations.

The decision was made at the beginning of the study to put aside all preconceived notions of what properties explosion-generated shear waves should have, and of how they might be generated. Experiments were carried out that were designed to provide basic data on these questions. Since the first experiments were completed, hundreds of additional seismograms have been collected in connection with other aspects of the research that contain further evidence. All of the information supports the original conclusions as published in Paper I, and, indeed, strengthens the arguments

presented there.

The fundamental point is that for a point source in a site composed of essentially horizontal beds of uniform composition, the amplitude of the SH motion is different in different directions, and most important of all, the polarity of the waveform is completely reversed in some directions compared to others. The importance of this fact lies in the difficulty that would have been encountered in trying to explain the origin of this motion if it had been found to be radiated uniformly in all directions. Since numerous observations confirm that the radial and vertical components of motion are uniform with azimuth under the same conditions, there can be no doubt that the mechanism of generation of the close-in SH motion is quite independent of the other modes of propagation.

A convenient manner in which to portray the amplitude data is by means of polar plots of the amplitude of a selected phase, one which can be correlated at all instruments. If a similar analysis were attempted using dispersed Love waves recorded at different distances and over different paths, it would be necessary first to phase equalize the signals, using appropriate phase velocity curves and one of the techniques of Chapter III, before attempting to determine the proper polarity to assign to each record. However, in these records, in which the layering and distances are identical, it is possible to pick a prominent phase and

correlate it around the circle.

Examples of polar plots for Florissant are given in Paper I, and data for Suffield, Alpha and Augusta are presented in Figures 35, 36, 37, and 38. The data for Suffield are the best obtained during the project because ten seismographs were available. On Figure 35, the transverse ground motion is plotted at its correct azimuth. The presence of two nodes, with reversed polarity of either side, is quite clear. The increase of high frequency energy in the neighborhood of the nodes is typical. A polar plot based on the phase correlated by the dotted circle on Figure 35 is shown on Figure 36. The radiation pattern for the P wave is given on the same figure, and the coincidence of a slight bulge in the amplitude with the nodal lines for SH is further evidence that there is a wave-generating mechanism operative that is superimposed on the basic compression. In all cases, the radiation patterns show either two or four lobes. In the case of four-lobed patterns, two of opposite polarity were usually bigger than the other two.

The Florissant site is the only one in which enough shots were fired to give information on the consistency of orientations of this radiation pattern. A strong tendency was found for the nodal lines to be in a fixed direction over large areas of the site, north-northwest and south-southeast being the most frequently observed orientation. Occasionally a pattern with a totally different arrangement of

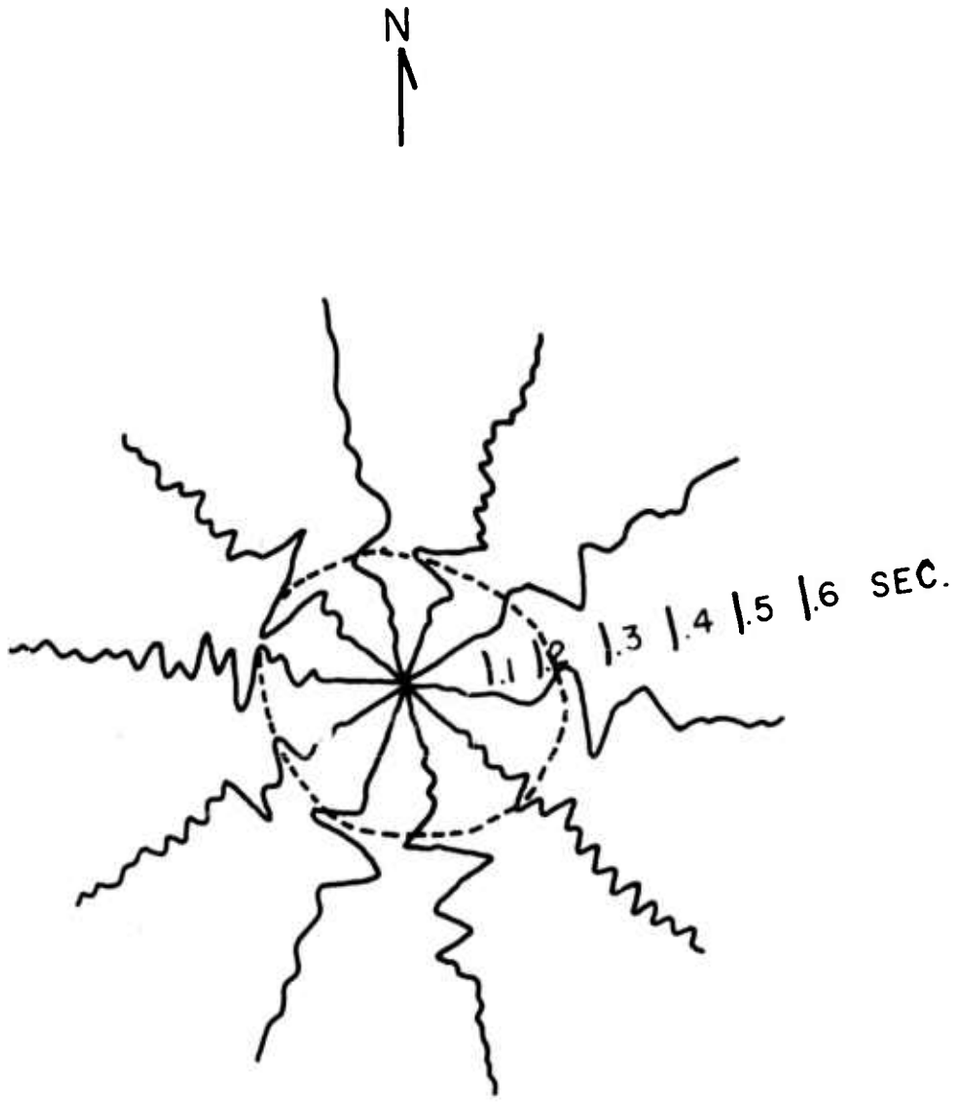

FIGURE 35

SH WAVEFORMS

AS A FUNCTION OF AZIMUTH

-SUFFIELD-

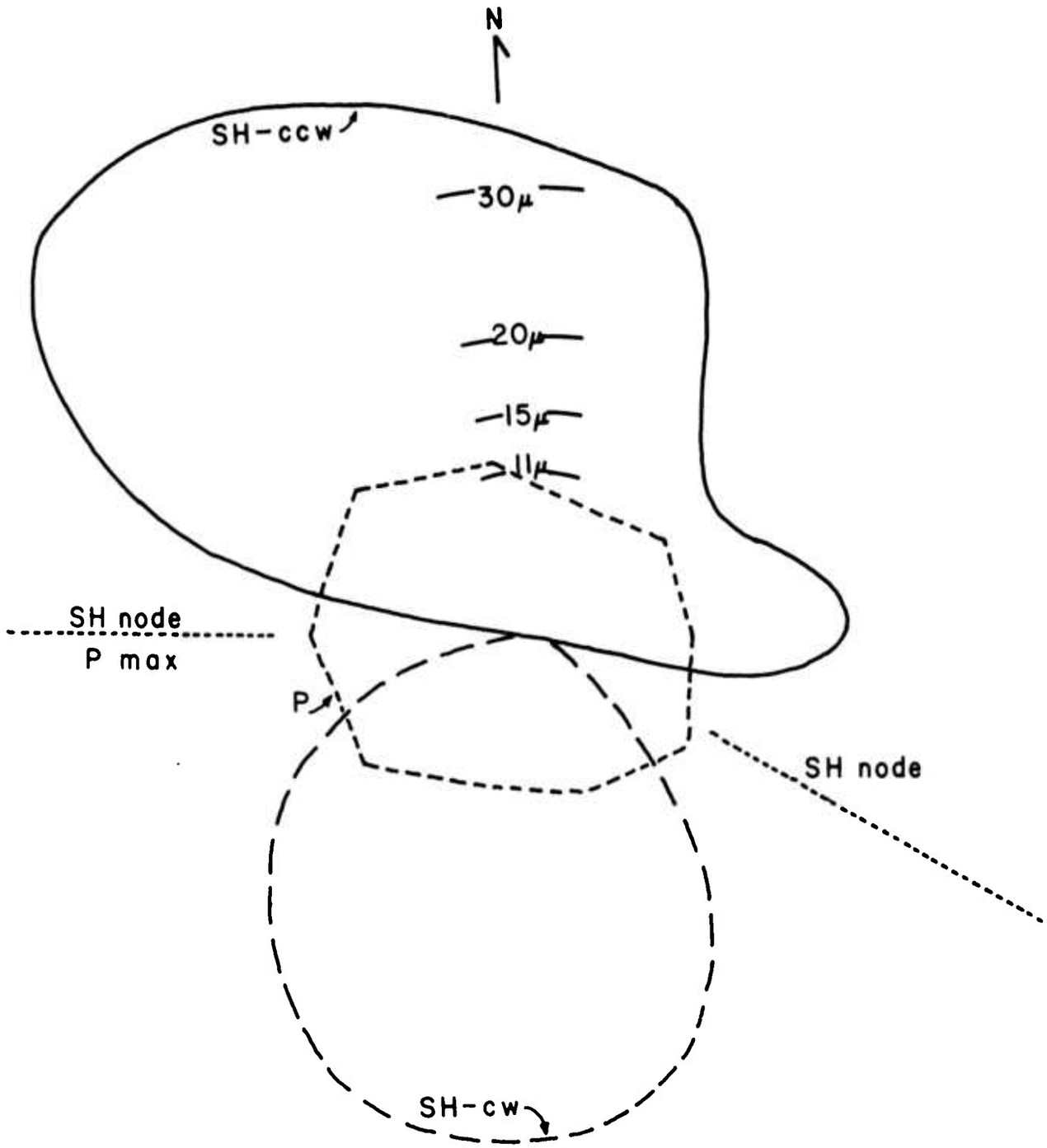

FIGURE 36

RADIATION PATTERNS, P AND SH

-SUFFIELD-

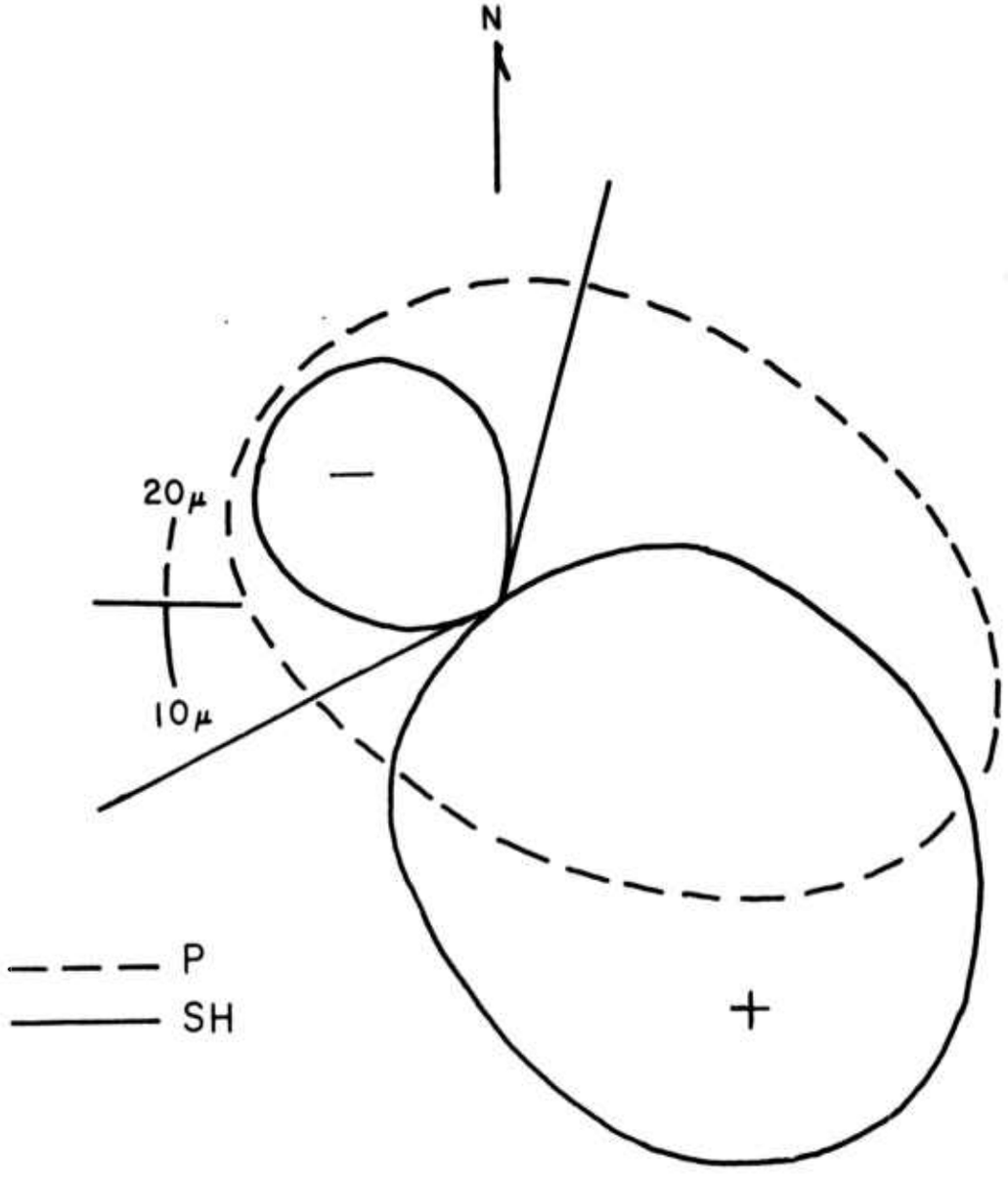

FIGURE 37

RADIATION PATTERNS, P AND SH

-ALPHA-

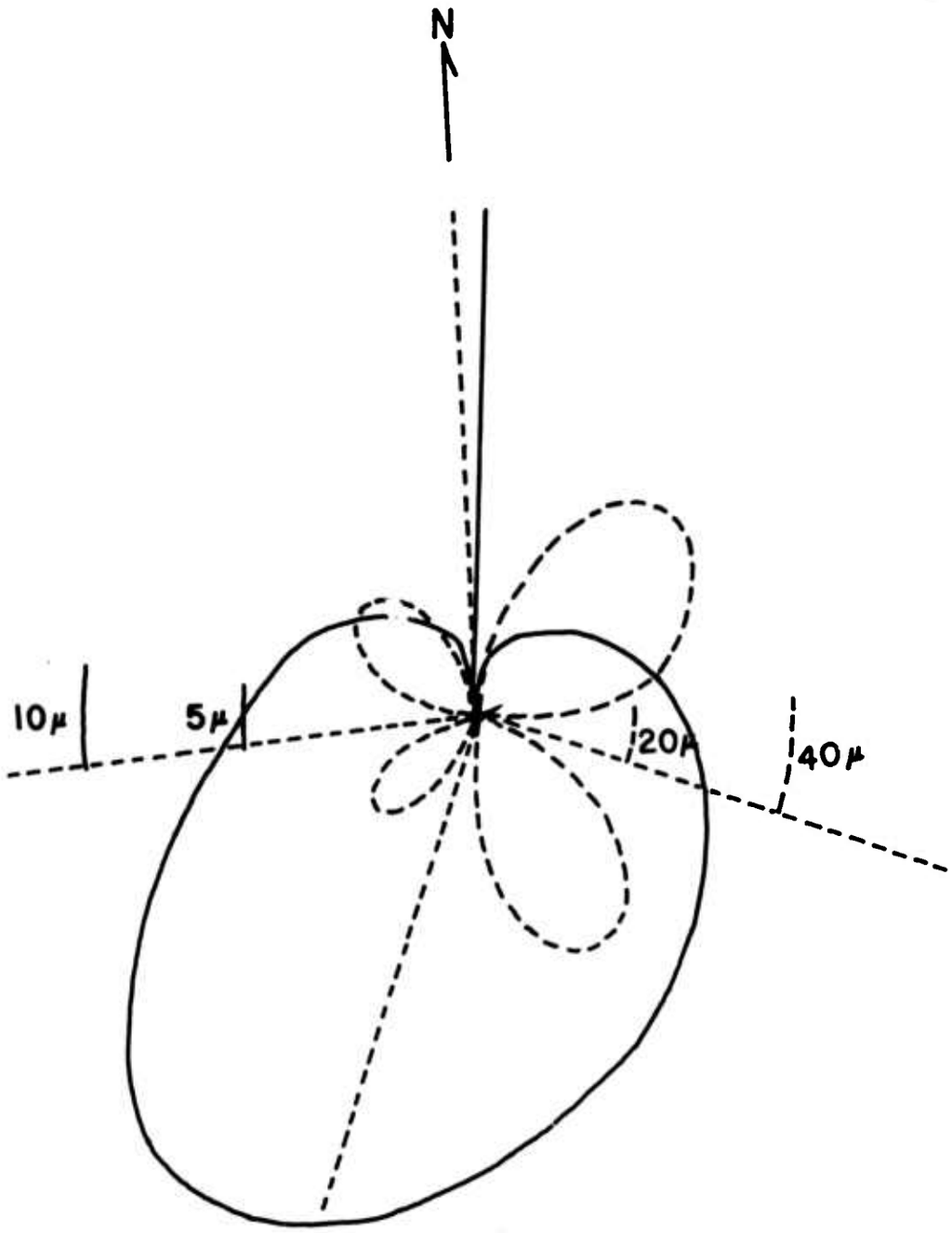

FIGURE 38

RADIATION PATTERN, P AND SH

—AUGUSTA—

nodes and lobes was found. Following the initial discovery of the SH radiation pattern, the investigators expected to find these patterns occurring at random. If one postulates crack formation as a primary source of this motion, then a tendency to a fixed orientation is plausible. While cracking from an explosion might be expected to be a somewhat chaotic and random process, it is likely that in any given test site there are directions of weakness in which the material ruptures most easily. In the case of limestone or granite, these directions might be expected to be related to the joint pattern in the region and to regional tectonic stresses. In the case of soils, these directions would be related to the structure of the soil resulting from the process of deposition.

Radiation Pattern as a Function of Distance.

Two further questions were investigated: Is the radiation pattern observed at one distance maintained at greater distances, and to what extent is it possible to alter the radiation pattern by changing the source? A definitive answer to the first question could have best been obtained by surrounding the shot with at least three rings of instruments at different distances. Such a procedure would have required many more seismographs than were available, so a compromise was found.

First, at the Florissant site instruments were set up at two ranges, covering a quadrant within which a node had been

frequently observed. The distances were 30 and 60 meters (S.P. 51 and 52). Clearly, if the radiation pattern is not maintained when the range is increased by a factor of two, the whole hypothesis collapses, and further investigation is unwarranted. The transverse component of ground motion for S.P. 51b is presented in Figure 39. It is quite clear that the node in the west-northwest direction between instruments 1 and 2, 3 and 4 is expressed at both distances. Results for 52b are similar.

These data provide an opportunity to check the method of computing the position of the nodal lines, viz., linear interpolation between positions of reversed polarity, using the amplitude of a correlated phase at each station. For S.P. 51b, if the large peak on instrument 6 is selected as the phase to be correlated, interpolation between 1 and 2 puts the node at 24.5° north of west, while interpolation between 1 and 6 puts it 20.8° north of west. If the next turning point is selected, that is, the largest trough on instrument 6, the results are: 16.5° using 1 and 2, and 19.3° using 1 and 6.

If now the records at 60 meters are used, the result corresponding to the biggest peak on instrument 5 is 18° north of west using 3 and 4, and 15.4° using 3 and 5. The results for the following turning point are 27.6° using 3 and 4,and exactly the same, 27.6°, using 3 and 5. If all eight of these values are taken as independent measurements of the

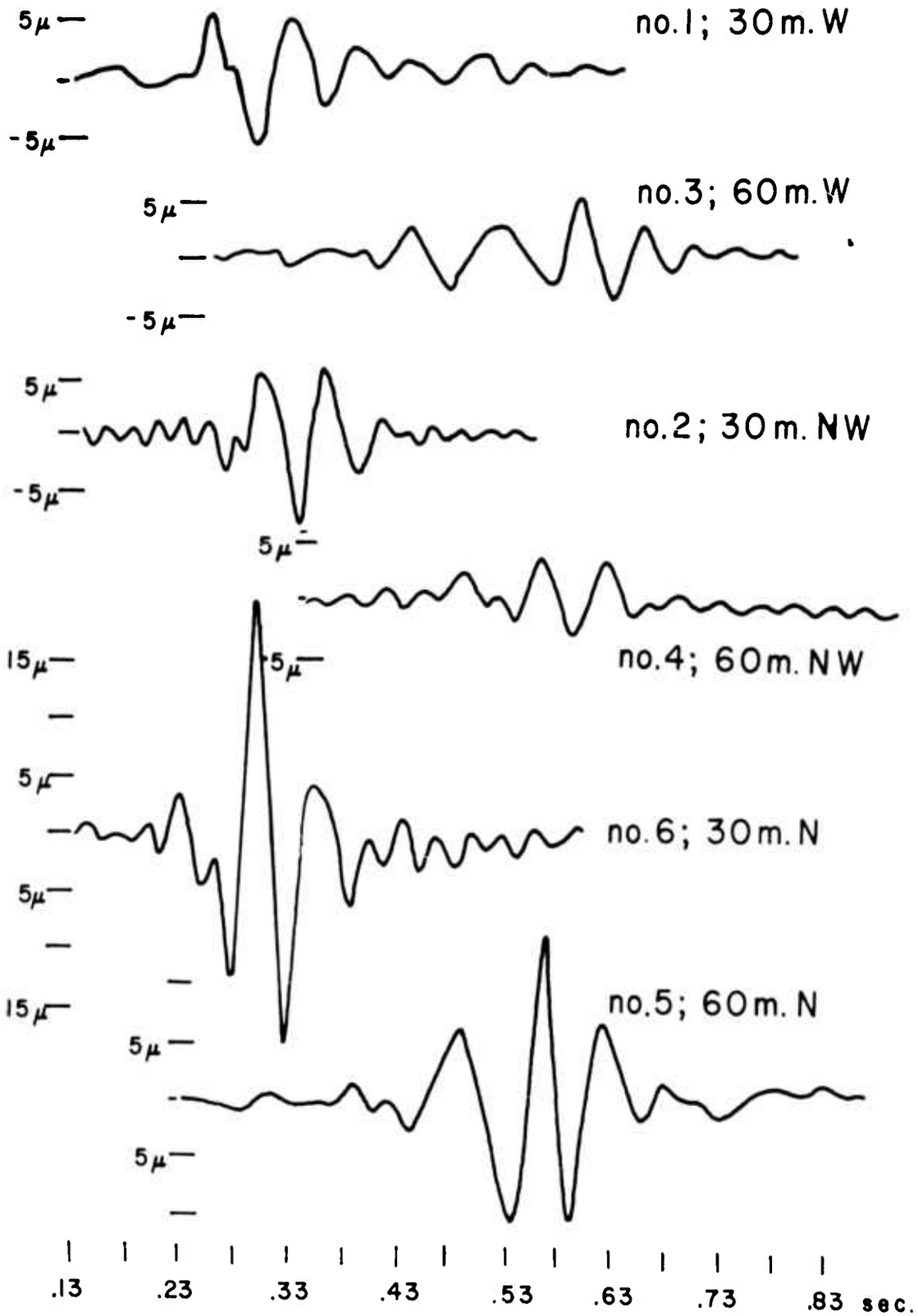

FIGURE 39. SH GROUND MOTION, FLORISSANT, S.P. 51b.

angle, the mean value is 21.2°, with a standard deviation of 4.5°.

It may be concluded that linear interpolation is justified, since for any one phase at one distance, the result for the instruments covering 45° is very close to that for the instruments covering 90°. Most important is the result that the mean position of the node from the data at 30 meters, 20.3° north of west is very close to the position from the data at 60 meters, 22.2°.

With these satisfactory results obtained, further experiments were conducted to determine if the same pattern could be observed as far out as 210 meters. It was not possible to go out this far at the Florissant site without encountering some pronounced topographic features in some directions. Because of the shortage of available instruments, the data from three shots are combined in this part of the study. The three shots were all in the same part of the test site as S.P. 51 and 52, discussed above. Combining the results of separate shots is justified first because the records from 51 and 52 indicated not only that the orientation of the radiation pattern remained fixed, but the SH waveforms were fairly well reproduced. Then, in order to provide additional control, one instrument was always kept in the same position relative to the shot, 30 meters to the north. The five measurements of transverse ground motion at this position are presented in Figure 40. Although there are differ-

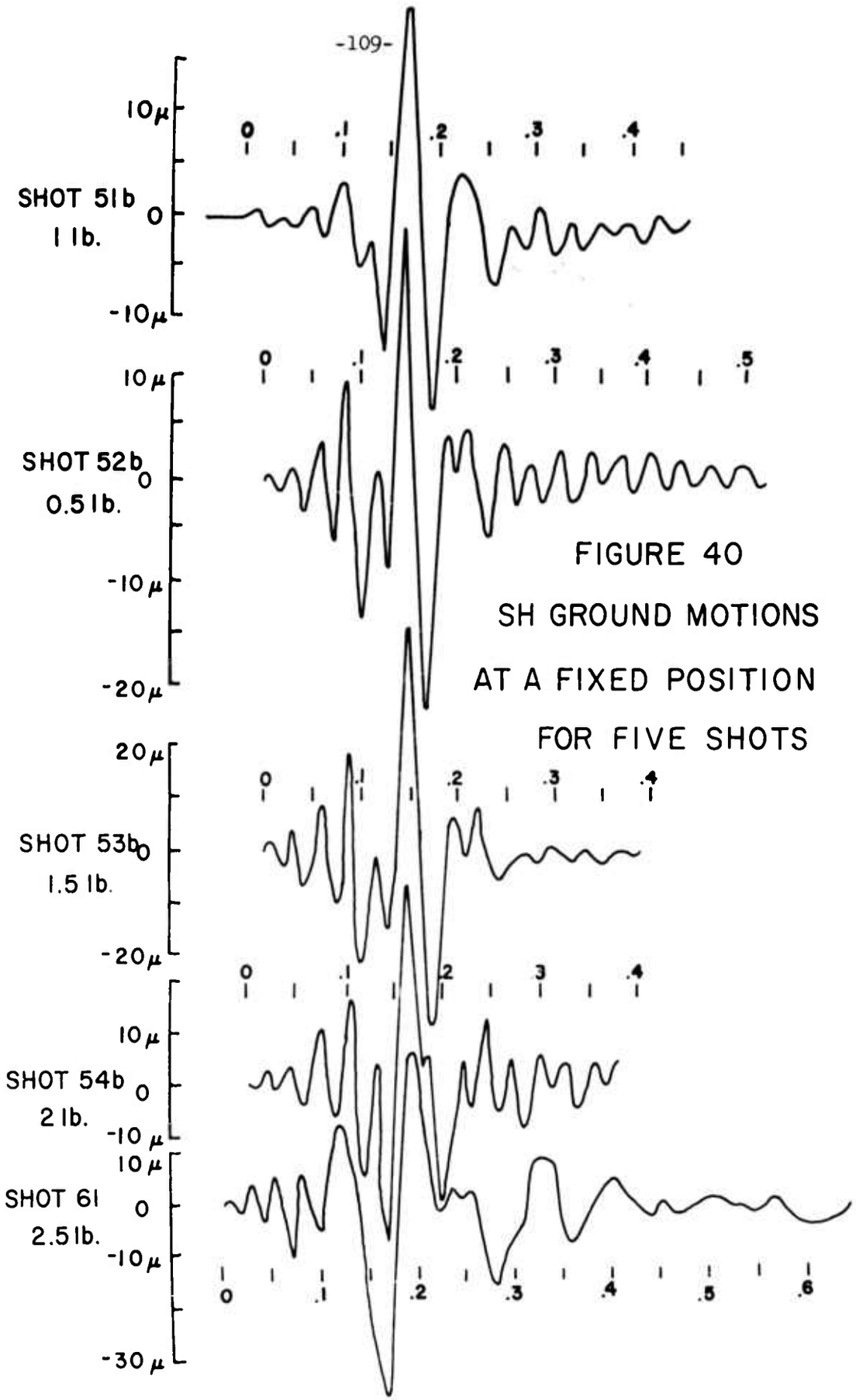

FIGURE 40

SH GROUND MOTIONS

AT A FIXED POSITION

FOR FIVE SHOTS

ences in detail, the major features, especially the character of the long period Love wave, are reproduced.

Five profiles covering a 180° arc from the north through west to south could be derived from the records of S.P. 53b, 54b, and 61. The transverse ground motion along these lines is given on Figures 41 and 42. Instrument 5 was to the north, in line with the fixed instrument at 30 meters. Unfortunately, it was impossible to move out in this direction more than 122 meters. A comparison of the records made by Instrument 5 for S.P. 51b and 53b, and for 54b and 61 provides additional evidence of reproducibility.

Timing control during these experiments was not very good. The zero-time device in two of the instruments was reliable, so that times of selected events could be taken from these records. Then the Rayleigh waves, which, as pointed out before, were very much the same in all azimuths, could be used to fix the time for the other records on which no time break appeared. This only worked, of course, for those instruments that were at the same distance from the source. Therefore, a few of the records for which topography forced the use of distances other than the standard ones could not be timed.

The same radiation pattern was determined from these three shots as from the first two. On some of the records the amplitudes were too small to allow correlations of phases to be made with confidence and these were excluded

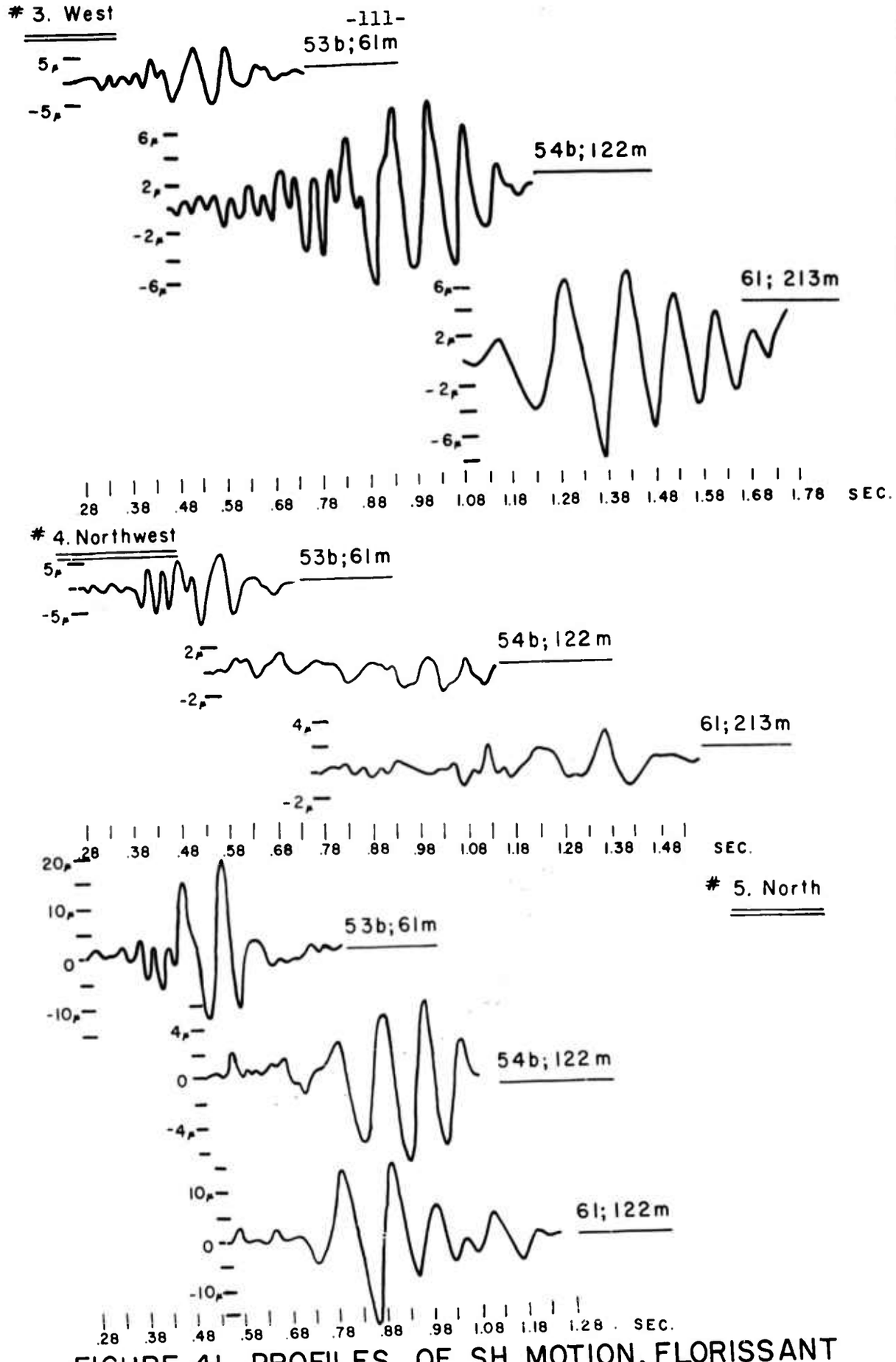

FIGURE 41. PROFILES OF SH MOTION, FLORISSANT

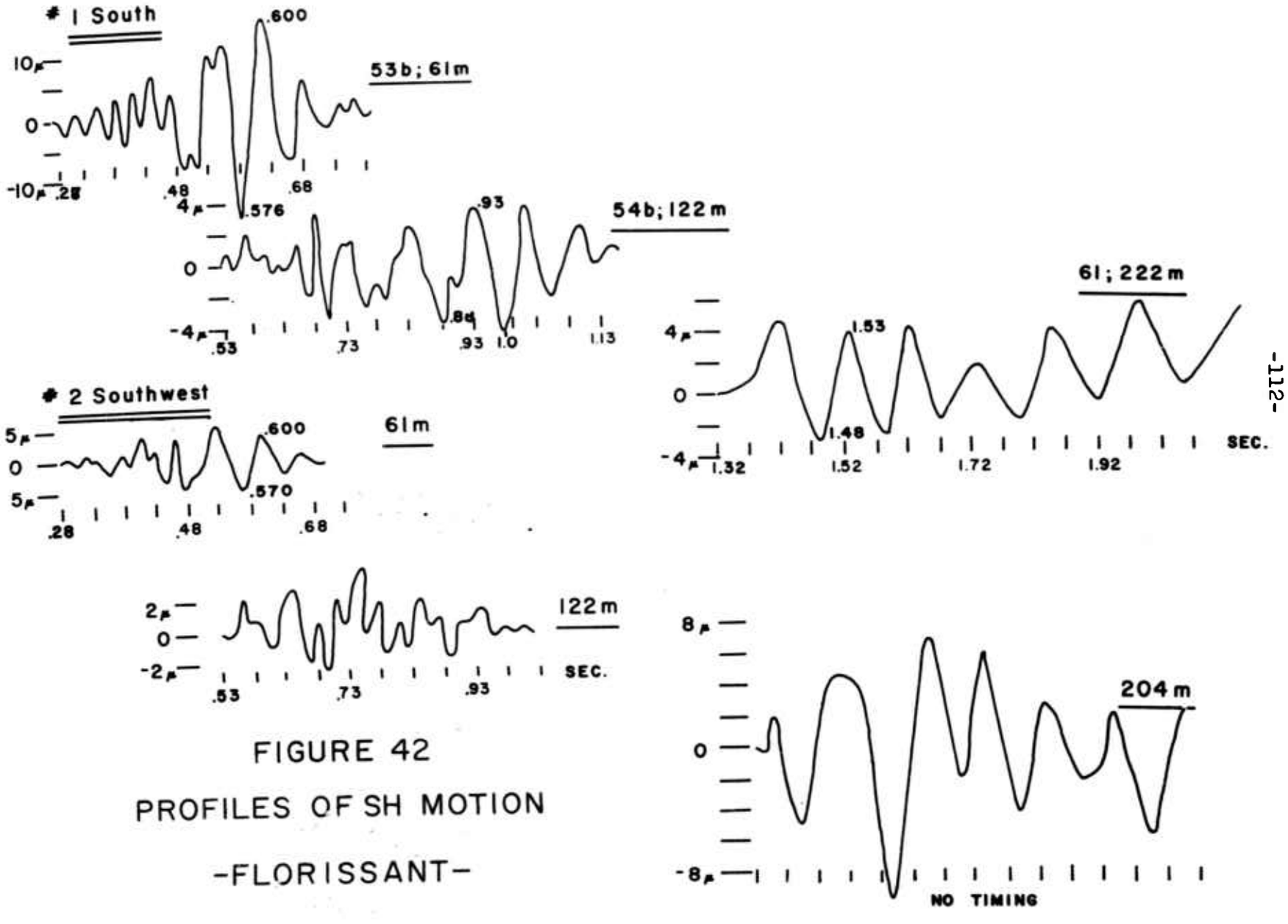

FIGURE 42

PROFILES OF SH MOTION

-FLORISSANT-

from the analysis. In all cases the polarity on the traces to the south, southwest, and west was the same, and reversed from that to the northwest and north. The mean position for the node was found to be: at 61 meters, 24° north of west; at 122 meters, 49° north of west, and at 213 meters, 34.5° north of west. Amplitudes in the southwest quadrant did not vary as smoothly as had been noted previously at smaller distances, as a very low amplitude, but with the proper polarity, was observed on Instrument 2 at 61 and 122 meters. Variations in topography are most likely the explanation as this instrument was separated by a valley and creek from the shot point.

These data lead to the final conclusion that the radiation patterns observed at short range do propagate outward. This provides further evidence that the polarity reversals are real, and not apparent reversals resulting from asymmetrical dispersion, and that the Love waves are truly propagating outward from the source region, and are not formed along the path by conversion of other wave types.

Modification of the Radiation Patterns.

Shots in Water-Filled Pits. Experiments were conducted at Florissant to test the effect on the SH waves of shooting in small pits filled with water. These experiments must be considered to have failed because it was impractical with the facilities available to dig and fill pits of sufficiently great size to provide a real test of the effects. The

original concept was to shoot in a pit large enough that purely normal stresses within the elastic limit of the surrounding earth materials would be applied to the walls of the pit. For the small pits used, a great deal of water was lifted vertically, and fell back, so that the input was more like a vertically applied pulse, and the records are indeed very similar to those from shallow buried shots.

One series of experiments will be described, those at S.P. 56. Shot 56d was 0.5 pound charge, buried flush with the surface. The crater produced by this shot was dug out to form a hemispherical pit with a radius of 0.8 meter. This pit was filled with water, and another 0.5 pound shot fired at the surface of the water. The pit was then reshaped to form an ellipsoid, with the major axis trending north-south, and twice as long as the minor axis, refilled, and another surface shot fired. The final test was a shot in the bottom of the water-filled ellipsoidal pit.

The analysis of the data is summarized in Figures 43 to 46. The effect on all components of shooting in the water was minor. The shot at the bottom of the pit produced records very similar to the original tamped shot, but with greatly increased amplitudes on all components. In particular, the SH motion from this shot was very much like the original shot, so that repeated loading of the same source region results in reproducible motion. This fact must be reconciled with the hypothesis that crack formation is

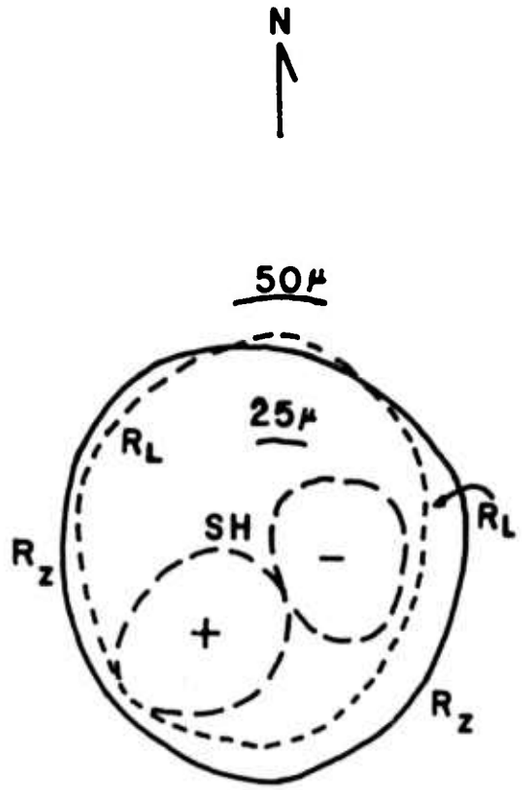

FIGURE 43

RADIATION OF SURFACE WAVES

S.P. 56 d

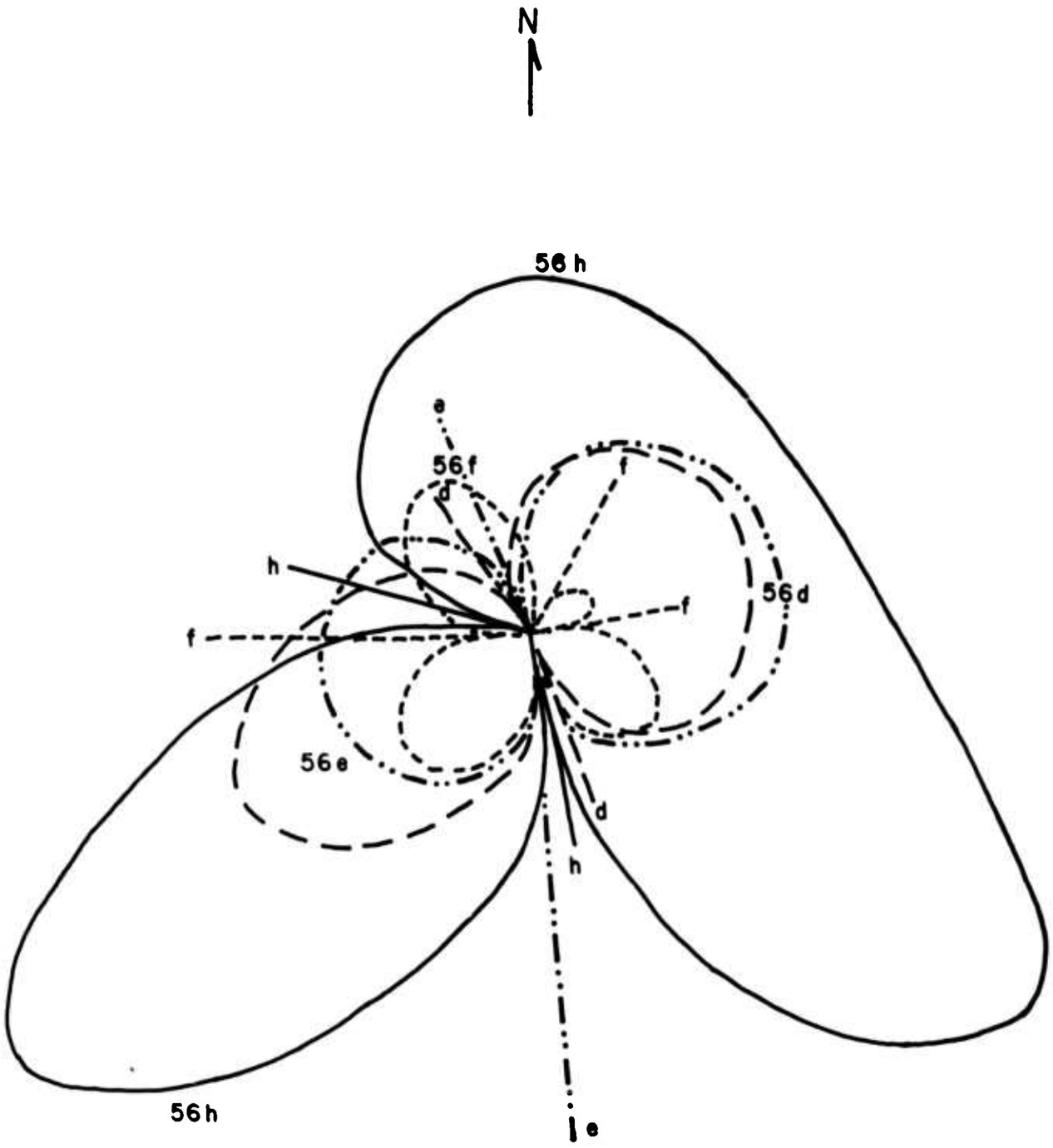

FIGURE 44

SH RADIATION PATTERNS

S.P. 56 d, e, f, h

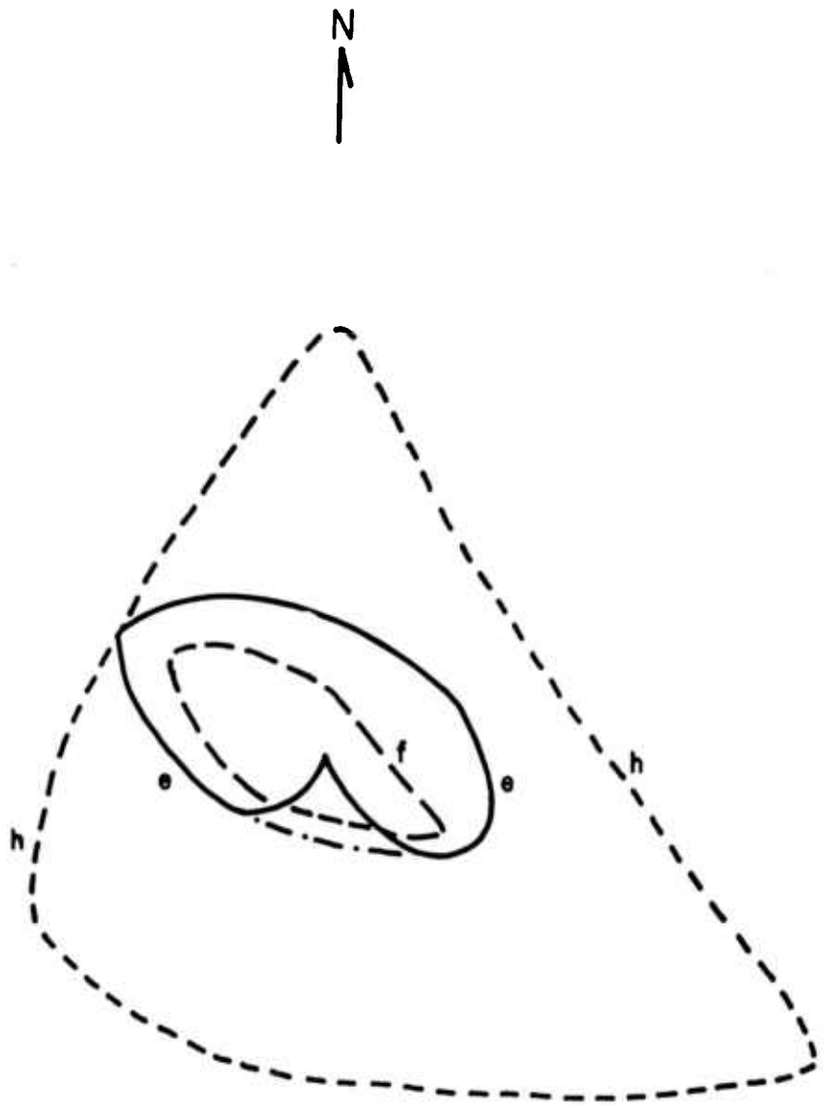

FIGURE 45

ALTERATION OF SH

BY SHOOTING IN THE PITS

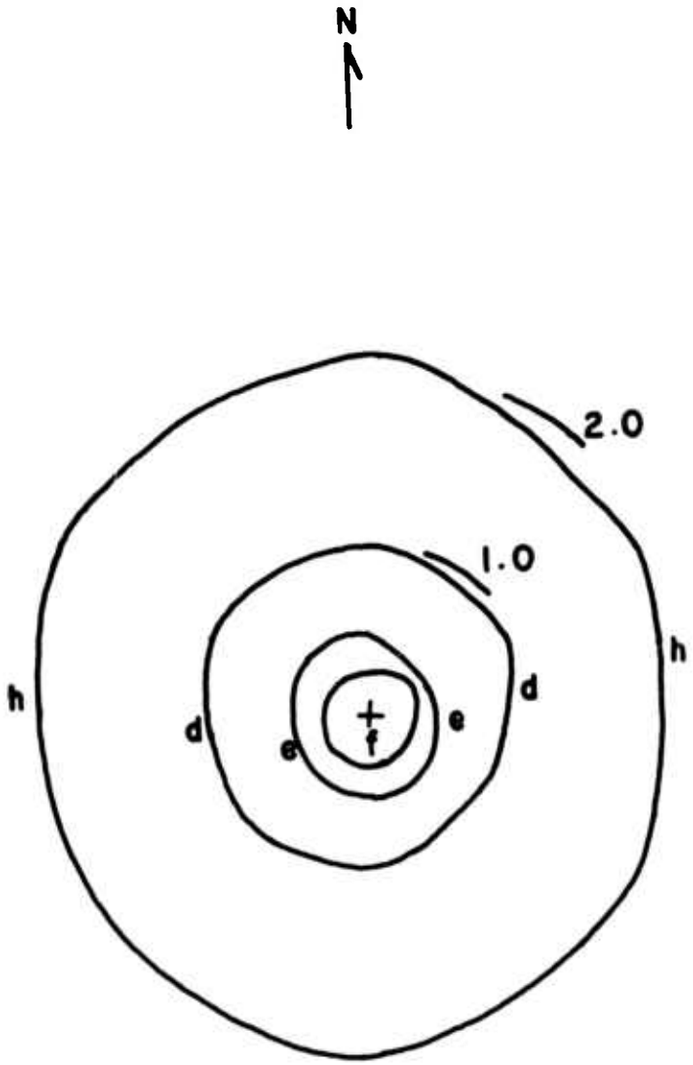

FIGURE 46

RAYLEIGH WAVE RADIATION

S.P. 56 d, e, f, h

responsible for the SH motion. Apparently once an underground crack pattern has been established, repeated loading results in further motion along the same cracks. The fluid in the pit fills the cracks, and the pressure from the shot is transmitted through the fluid to produce further motion of the crack walls, as well as further extension of the crack.

Shooting at the top of the water-filled pit reduces the amplitude of all events in the same manner as a poorly tamped surface shot in soil. The SH motion is altered in some directions, and the effect on SH is greater than on the Rayleigh wave, though, it must be emphasized, the observed effects are minor. Even the minor effects are difficult to interpret, since possibly effects of hole fatigue are included. The Rayleigh wave is used as a basis of comparison because its waveform is so well known at this site, it is symmetric in its distribution, and it is reproducible from shot to shot. Shot 56d was used as the calibration shot. A phase in the vertical component of the Rayleigh wave (R_Z), the longitudinal component of the Rayleigh wave (R_L), and in the Love wave (SH) that could be correlated on all of the seismograms was selected and its amplitude read. The radiation of these three phases for the calibration shot is shown in Figure 43. The two-lobed SH pattern, with the typical northwest-southeast orientation of the nodes, and

the almost circular pattern for the two Rayleigh components is seen.

The pattern for 56e, the top center of the circular pit, now shown here, was very similar. The minimum in R_L to the southwest is more pronounced. The shot in the top of the elliptical pit, 56f, produced a poorly defined four-lobed SH pattern. In particular, the reading on the northeast instrument on which the interpretation as a four-lobed, rather than two-lobed, pattern depends is very doubtful because of a small amplitude and great difficulty in correlating the selected phase. When the shot was placed at the bottom of this same pit, a distorted two-lobed pattern was obtained. The SH amplitude on the north instrument (Number 1) in shot 56d was taken as the unit amplitude, and the patterns for all four shots, referred to this unit, are shown in Figure 44.

The alteration of the correlated phase relative to the original shot was measured by dividing the amplitude on each instrument by the value on the same instrument for 56d. If there were no effect at all, the result would be a circle of unit radius, and if the radiation were unchanged but the amplitudes were altered, the plot would be a circle with appropriate radius. As seen in Figure 45, the actual result for 56e is a slight increase in amplitudes in the northwest direction and a decrease to the northeast and southwest. The bottom shot, 56h, produced SH motion roughly twice as

large as the original shot, but the signal to the southeast was three times the original, while that to the northwest was only about one and one-half times the original, and had the opposite sign. The reversal in sign at a station near a node is not surprising, and is also observed on 56f.

The three shots taken together indicate a tendency for a relative strengthening of the signal in the northwest-southeast direction, but this tendency has no obvious connection with the pit, which was either circular, or elongated north and south. It is recommended that further work in which the shots are fired in bodies of water big enough that any directly produced shear motion is decoupled from the earth be carried out.

The amplitude of the Rayleigh waves were altered in roughly the same manner as the Love waves, that is, those shots that produced smaller Love waves also produced smaller Rayleigh waves, though, of course, the Rayleigh wave radiation remained quite symmetric. The Rayleigh wave radiation normalized to the north instrument 56d, is shown in Figure 46, in which it is seen that the bottom shot produced Rayleigh waves with twice the amplitude of the original buried shot, while the shots at the top of the pits produced appreciably smaller motion. No evidence of any effect of the shape of the pit on the radiation pattern can be seen.

A final comparison that can be made is the enhancement of SH motion relative to the enhancement of the Ray-

leigh wave. To measure this the ratio of SH for the pit shots divided by the values at the same instruments for the calibration shot (the values on Figure 44) were divided by the corresponding ratios for the Rayleigh wave (not plotted here). The values are scattered somewhat, but on the average, the value for the top of the circular pit was 1.91, for the top of the elliptical pit 2.03, and for the bottom of the elliptical pit, 0.95. Therefore, rather than reducing the production of SH motion, as had been anticipated, the shots in the water actually doubled it relative to the Rayleigh wave, while the shot in the bottom of the water yielded the same proportions of Rayleigh and SH motion.

SH Motion from Ripple-Fired Shots. The Rayleigh wave motion produced by the ripple-fired, multi-hole shots was discussed in Chapter IV. The SH motion generated by the horizontal patterns will be described here. The experiments were outlined in the previous chapter. The method that has been used to study SH radiation does not work as well for these seismograms because the superposition of the signals from the component parts of the charge produces waveforms that cannot be readily correlated around the circle of instruments. As explained in the discussion of Rayleigh waves, since the signal from a single shot is almost identical in all azimuths, the superposition of this waveform with proper time shifts will explain the recorded motion. Because, as has been seen above, the SH radiation from a single shot is

fundamentally complicated and largely unpredictable, analytical superposition is impractical, even though this is undoubtedly the way to explain the observed motion.

The calibration shots for the ripple-fired series, S.P. 69a and b, produced a four-lobed pattern (Figure 47) almost identical to that predicted by a formula given by Knopoff and Gilbert for the first motion due to a crack growing from S70°W to N 70° E at twice the shear velocity (see Figure 12 in Paper I). The two-hole shot fired with the shorter time delay (equivalent to propagation velocity of 190 meters/sec., S.P.70) produced smaller SH motion on all components. The character of the motion in the direction away from which the shot was propagating was completely altered, and no correlation with previous records or the other records for this shot could be made. The phase that had been correlated in analyzing S.P. 69 could be picked out on the records toward which the shot propagated, with the same polarity. On the shot fired with slow velocity of 91 meters/sec. (S.P.71), the character was much the same as for the shorter delays, but it was possible to carry a correlation through. The resulting pattern of radiation (Figure 47) consisted of only two lobes, a small one which covered the two smaller lobes from 69a, and a large one covering roughly the two larger lobes from that calibration shot. Nodal lines to the north and to the southeast were preserved.

Tracings of the original seismograms from three five-hole

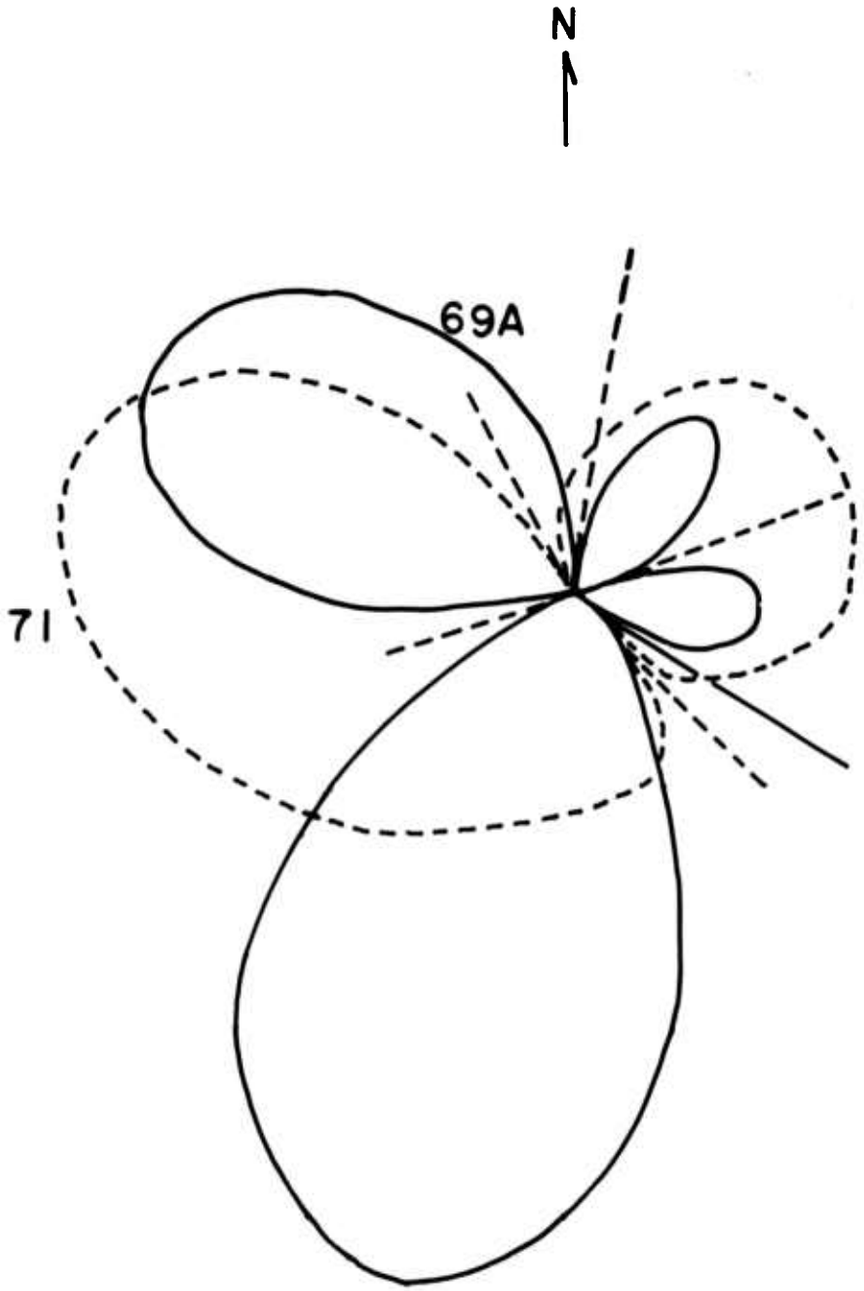

FIGURE 47

SH RADIATION, S.P. 56 d, e, f, h

shots, and from the two eight-hole, two-line pattern are shown in Figure 48. For all shots the instruments were placed in a circle with Number 1 to the north (roughly), and 60° spacing, with 2 to the northwest, 3 southwest, 4 south, etc. For the five-hole patterns, the charges, spaced at five foot intervals, were aligned north to south, and detonated from south to north (from instrument 4 to instrument 1). Geometrically, 2 and 6 were symmetrically placed with respect to the line, as were 3 and 5. For the "simple couple" type shots (S.P. 72a and b), the eight shots placed on two parallel lines, five feet apart, extending north to south. Detonation was initiated simultaneously at the south end of the west line and the north end of the east line. In examining the seismograms in Figure 48, it must be recalled that the static magnification of instruments 3, 4 and 5 is about 1.8 times that of the other three.

The shot in which all the charges were fired simultaneously (67a) gives the basic pattern for the five-hole shots. It may be seen that the motion recorded in line with the pattern (at 1 and 4) is a minimum. The Love wave pulse can be correlated on all records except 1. The records at the symmetric points 2 and 6 are very much the same, though 6 has larger amplitudes, and the other symmetric pair, 3 and 5, have easily correlated phases of similar amplitudes but with reversed polarity. When the same line of shots is fired at an effective propagation velocity of 290 meters/sec.

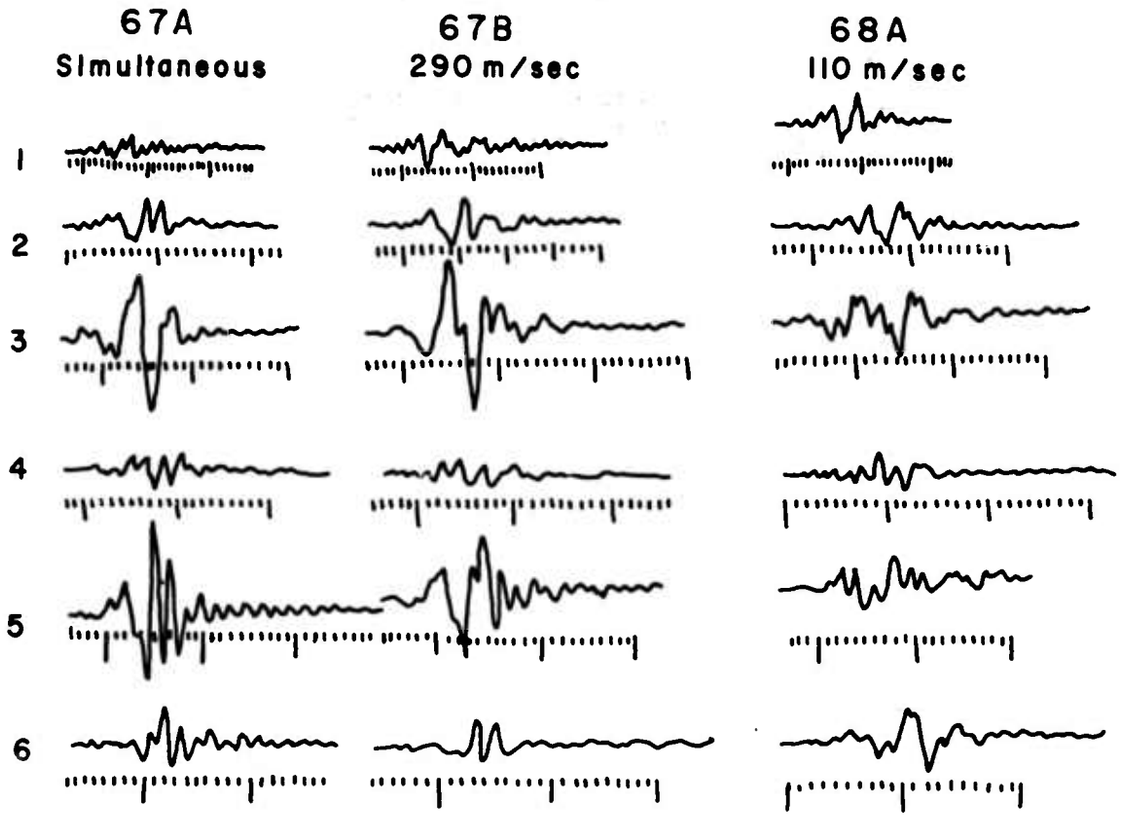

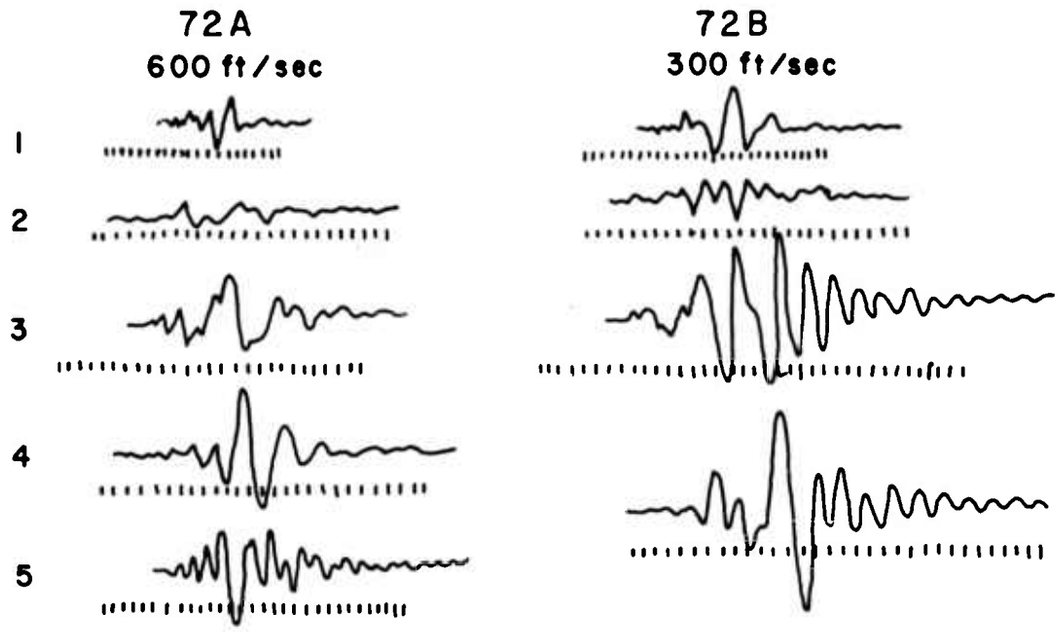

FIGURE 48

SH MOTION FROM HORIZONTAL PATTERNS

(67b) the same waveforms are observed, only a bit more extended in time as a result of the duration of the input. No significant change in radiation is noted. The slower speed, 110 meters/sec. (68a), resulted in marked reduction of the large amplitudes at instruments 3 and 5, and proportionally greater motion on the other instruments; in other words, more uniform radiation.

Because of instrument difficulties, the simple couple experiments were incompletely recorded. The most remarkable effect observed is the increase in amplitude in-line with the pattern. In particular, the seismogram at the south end, Number 4, is very large. When it is recalled that this was the direction of minimum motion for the single line pattern, the enhancement must be regarded as an effect of the pattern. However, if the pattern truly simulated a couple, this should be the direction of a node of SH motion. This result is unexplained. The extended duration of the motion is also to be noted.

CHAPTER VI

THE EFFECT OF SOURCE DEPTH AND SHOT POINT MEDIUM ON THE SEISMIC SIGNAL

Knowledge of the properties of explosion-generated seismic waves is largely empirical based on the analysis of countless seismograms produced by explosions covering a tremendous range of yields and fired under a wide variety of conditions. Attempts to understand this large body of data have led to theoretical developments concerning the processes of wave formation and wave propagation that are the foundation of this branch of seismology. Many aspects of this theory are well-developed, but because of the complex nature of the materials of which the earth is composed and the complex structure of the medium through which the waves must propagate to the seismograph, the interpretation of particular observations is often difficult. In particular, the seismologist is called upon to isolate the effects of a number of variable parameters that are part of the circumstances surrounding any test explosion.

Data concerning the effects of several of these variables, depth of source, medium in which the source is located, and charge size, were gathered during this project. The results on the effect of charge size are of doubtful value for two reasons: the range of yields available was not sufficiently great to adequately define significant trends; and during some of the tests that were specifically

designed to give data on this question the experimenters were unfortunate in getting some bad dynamite, which did not completely detonate. Some references to the effect of charge size are included in the other sections of this report, but no systematic evaluation is possible. The conclusions concerning the other two parameters will be discussed in this chapter. For a summary of the present state of knowledge of the factors affecting the close-in properties of the seismic signal, see Kisslinger (1963).

Effect of Source Depth on the Seismic Signal.

The depth of the charge below the surface will affect both body and surface waves. Surface waves depend for their existence on the presence of a free surface, and, in general, their amplitude decreases as the source depth increases. The effect of increased source depth is not as simple for body waves. If the shot point medium is homogeneous, the effect of increased shot depth is to reduce the amplitude of the direct P-wave. This results from increased ambient stresses at the shot which make the cavity size smaller. This decrease in cavity size also causes an increase in the frequency of the direct P-wave. In a real experimental situation, the properties of the medium at the shot will change with depth, and this will override the effect of increased stress. That is, for a limited range of depths, P-wave amplitude and frequency will depend more on the medium than on the depth.

Effect on P-Waves. The predominant frequency in the P-wave has been found to be affected markedly by the medium at the depth of the charge. The analysis of a step function in pressure applied to the walls of a spherical cavity in an infinite medium indicates that at distances beyond two or three cavity radii, the P-wave should be damped sinusoid with angular frequency given by

$$\omega = \frac{(q + q^2)^{\frac{1}{2}}}{(1 + 2q)} \frac{V}{a}$$

where: V is the P-wave velocity; a is the cavity radius; $q = \mu/\lambda$, the ratio of shear modulus to Lame's constant (Sharpe, 1942; Blake, 1952, Kisslinger, 1963a). The damping is given by

$$\zeta^2 = \frac{q}{1 + 2q}$$

where ζ is the fraction of critical damping. For large values of Poisson's ratio (small q) low frequencies and small damping are to be expected. The radius, a, of the equivalent cavity is usually not known for a given medium and yield.

At Florissant a series of shots in two holes, one 14.6 meters deep and the other 38.1 meters deep, were fired to gather data for P- and S-wave velocities and the study of the generation of Rayleigh waves. These shots also yielded data useful for checking the theory of the waveform of the direct P-wave.

At this test site the velocity of the P-wave in the clay-loess overlying the Mississippian limestone changes at the water table whereas the S-wave velocity does not show a marked change at this boundary. This results in the high values of Poisson's ratio presented in Chapter III. Above the water table the P-wave velocity has an average value of 460 meters per second. For this part of the section $\lambda = 3.3\mu$, consequently the frequency of the P-wave is $f = \omega/2\pi = 57.5/a$ cps, where a is in meters, ζ is 0.43, and the damping ratio (peak to trough) is 4.53. Below the water table the P-wave velocity is 1800 meters per second, $\lambda = 42.5\mu$, $f = 84.9/a$ cps, ζ is 0.15, and the damping ratio is 1.61. These predicted values may be compared with those observed, presented in Table 4. These data were taken from records at a range of 2.5 meters from 1.5 pound shots in a single hole at depths from 38 to 7.5 meters. For the shots deeper than 14 meters both frequencies and damping ratios are close to those predicted for a cavity radius of one meter. It is assumed that the damping associated with the medium at the source is preserved in the signal observed at the surface. The same radius gives good agreement for frequencies, but not for the damping ratios for the shallower shots. The velocities used for the calculations are averages for the layer, and there may be unknown variations in the velocities in thin layers at any level.

Table 4

FREQUENCY AND DAMPING OF P-WAVE
FLORISSANT SITE, RECORDED AT 2.5 METERS

Depth (meters)	Frequency (cps)	Damping Ratio (First Peak to Trough)
38	77-80	1.30
32	91	1.61
26	77	1.43
20	59	
14	77	0.96
8	59	1.50

The observed P-wave motion over the shot point from a series of 0.5 pound charges at various depths in the 14.6 meter hole showed considerable variation in waveform. The damping ratio was much less than that predicted for most of the shots. This was thought to be due to the interference of the direct wave and the primary reflections from the known boundaries in the clay section. To check this, theoretical seismograms of the P-motion were made. The waveforms used as input for these theoretical seismograms were constant-frequency damped sinusoids with the first peak equal to unity. The theoretical frequency and damping given above were used. The geologic model used for the calculations, given in the table below, was made from observed uphole times from the deep holes.

Thickness (meters)	P-Velocity (meters/sec.)
6.1	305
9.2	518
30.5	1830
∞	3100

In calculating the theoretical seismograms, transmission and reflection coefficients at each interface were calculated, assuming normal incidence. All primary reflections from boundaries below the shot were added to the directly transmitted wave at the proper time delay.

The comparison of the observed and calculated motions from three of the shots in the third layer are shown in Figure 49. The general agreement is good. The theoretical motion for the source at 26 meters shows stronger motion after the arrival time of the reflection from the top of the Misssissippian limestone than is seen on the field record.

Theoretical P motion for shots in the upper layers were calculated using a waveform with a damping ratio of 4.53. The theoretical motion did not resemble the observed motion because the damping was much too large. Another set was calculated using a waveform with the theoretical frequency of 57.5 cps, but the damping ratio equal to 1.61. Figure 50 shows the comparison of the observed and calculated for shots in the middle layer. The agreement for the shots at 14.6 and 11.6 meters is good. There is a zero shift on the observed traces resulting from the strong motion hitting the seismometer. There is fair agreement for the shot at 9.1 meters but the agreement is very poor for the shot at 7.6 meters. Peaks and troughs are observed at approximately the correct times, but the relative amplitudes are much reduced. It is evident that the expected reflections are

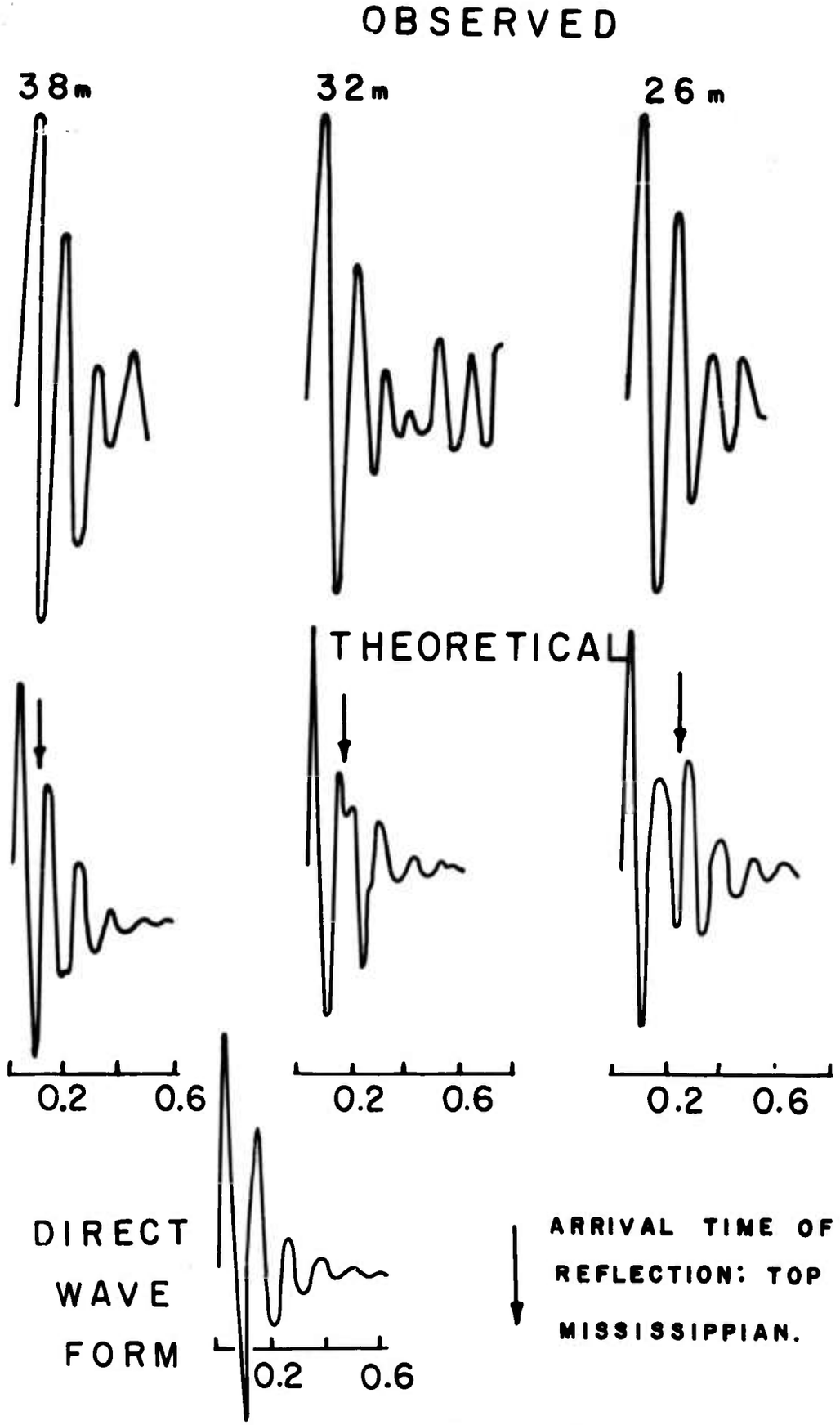

FIGURE 49. P MOTION OVER THE SOURCE, FLORISSANT

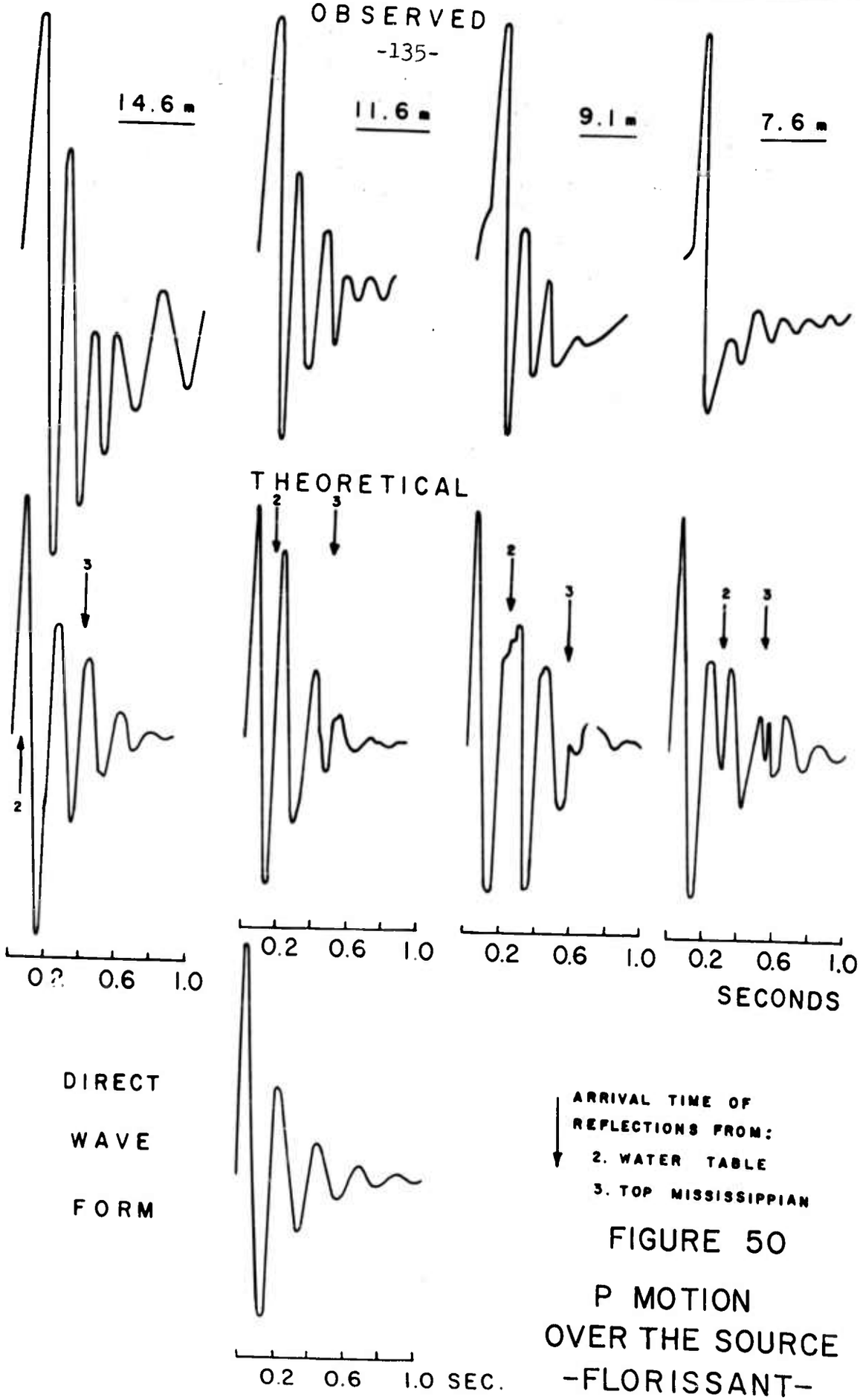

FIGURE 50

P MOTION
OVER THE SOURCE
-FLORISSANT-

not well developed for the shallow shot. Whether this absence of strong down-going energy from the shot is due to losses in the shallow zone or scattering from the cavities left by the prior deeper shots is not known. The agreement indicates that the damping used in the calculations is more nearly correct than the value predicted from theory. The combined effect of decreased damping and consideration of the primary reflected events along with the direct wave give a reasonable explanation for the oscillatory nature of the P-motion at these intermediate depths.

The comparison of the theoretical seismograms and the observed motions for shots in the upper layer are shown in Figure 51. The agreement is not as good as at the greater depths. The most striking difference is the apparent absence of a reflection from the boundary at a depth of 15.3 meters (water table) on the observed trace. This reflection is strong on the calculated traces. The observed frequencies are lower than those in the calculated motion.

The general agreement of the theoretical seismograms and the observed traces from shots in the two lower layers can be interpreted to mean that the P-wave from these contained explosions has the waveform of a damped sinusoid with a frequency predicted by the theory discussed at the beginning of this section. However, as the source moved closer to the surface, lower values of damping than that given by the theory were required to get reasonable agreement. The pro-

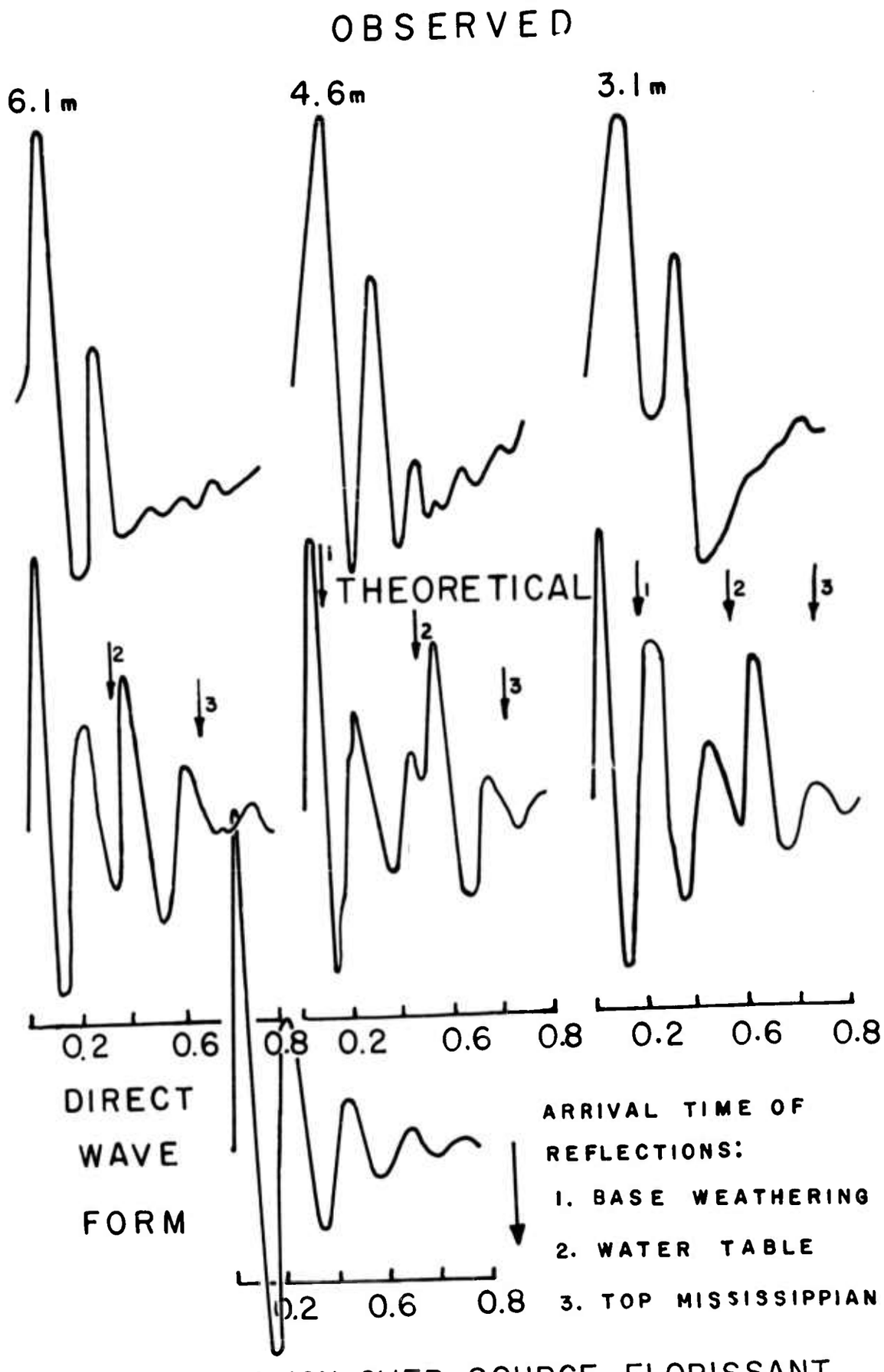

FIGURE 51. P MOTION OVER SOURCE, FLORISSANT

longed oscillatory nature of the P-motion observed from shots at certain depths is adequately explained by the combined effect of the primary reflections from the near surface boundaries and the oscillatory nature of the initial waveform.

At the very end of the research program, a series of larger charges (4.5 pounds) was fired under conditions similar to the deep shots discussed above. The vertical component of ground motion over the shot point from 4.5 pounds at 38, 32.2 and 19.9 meters is shown in Figure 52. The arrival time of the reflection from the top of the limestone is also shown. The waveforms are not oscillatory as in the previous examples, but appear as highly damped pulses. The damping of the waveform should depend only upon the elastic properties of the medium and not upon the size of the charge. The observed decrease in frequency is expected with the increase in cavity size, but the decrease to 8 cps from 85 cps for a charge increase of three times is too great to be explained on any such simple basis. These data are completely anomalous for the test site. Admittedly it proved discouraging, after the excellent results for the first series discussed, to encounter a set of data that did not fit the same simple theory. It is evident that a further study of the possible effects of yield on damping as well as frequency of the primary signal is required.

The P-wave amplitudes were studied from one sequence

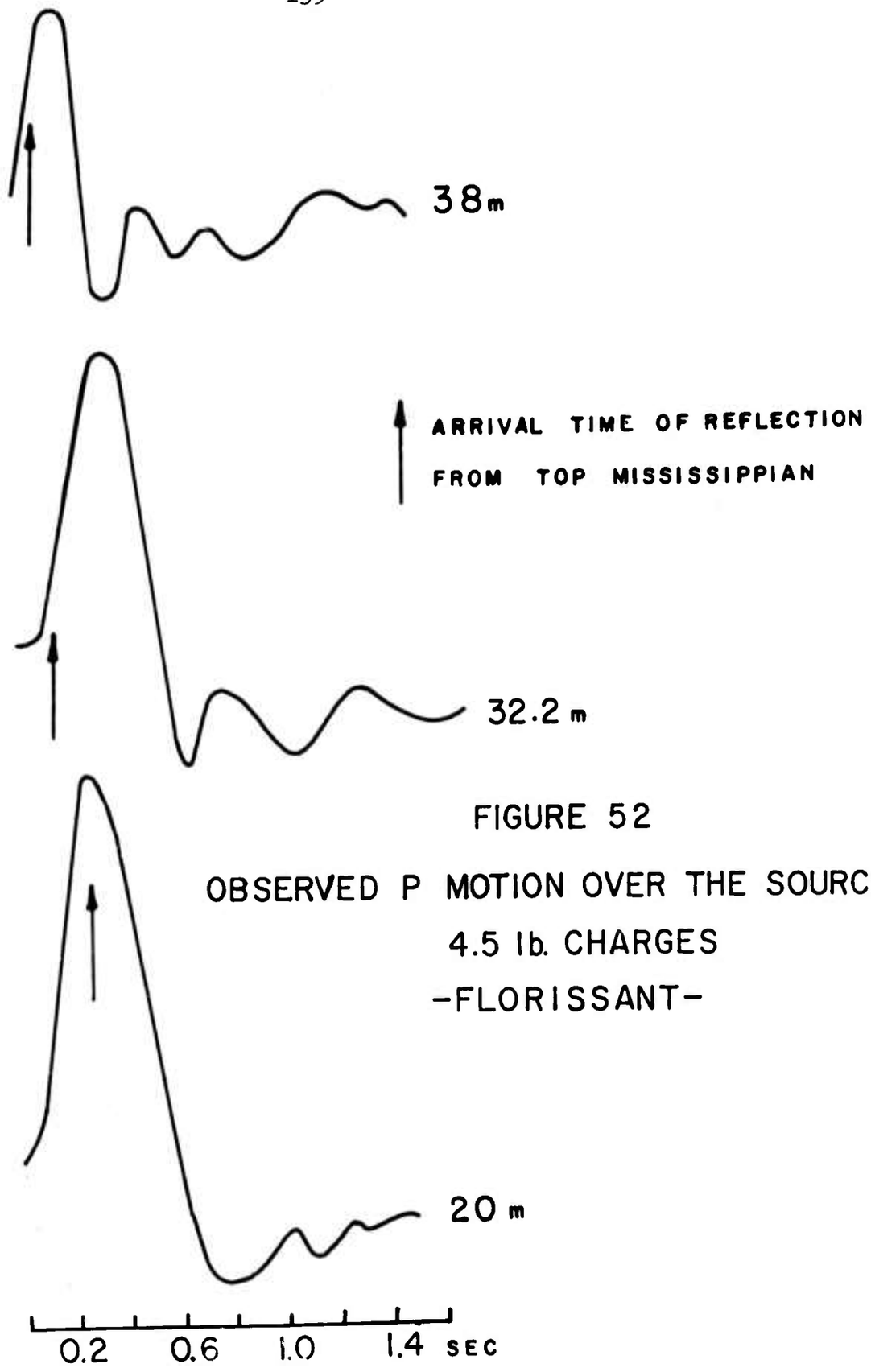

FIGURE 52

OBSERVED P MOTION OVER THE SOURCE

4.5 lb. CHARGES

-FLORISSANT-

of charges. The amplitudes measured (vertical component) directly above a sequence of 0.5 pound shots fired at depth of 14.5 to 1.2 meters closely fit a decay law of $d^{-1.5}$. The effect of distance is combined with depth, and undoubtedly is predominant. This is somewhat more rapid attenuation than ordinary spherical wave propagation implies, but a more rapid rate than r^{-1} for the peak displacement is expected even for perfectly elastic behavior in the region near the source, as shown by J. Vanek (1959). Thus the effects of viscous losses, transitional propagation, and depth are combined, masking the effect of any one of these.

Effect on Rayleigh Waves. The effect of depth on Rayleigh waves is well illustrated in a sequence of three shots at depths of 0.82, 2.72 and 5.3 meters recorded at 25 meters at Florissant (S.P. 12). This motion, shown in Figure 53, shows the decrease in amplitude with increasing shot depth even though the charge size of the deepest shot is twice that of the shallow shot. Another interesting feature of these shots is the emergence, as the depth increases, of an event preceding the Rayleigh motion. This event is most probably a higher mode, and the deepest shot may have been located near an antinode for this mode. The presence of the M_{21} mode at this site is discussed in Chapter III.

In an effort to gain a clearer understanding of the generation of Rayleigh waves from a contained explosion, several sequences of shots in deep holes were fired at the

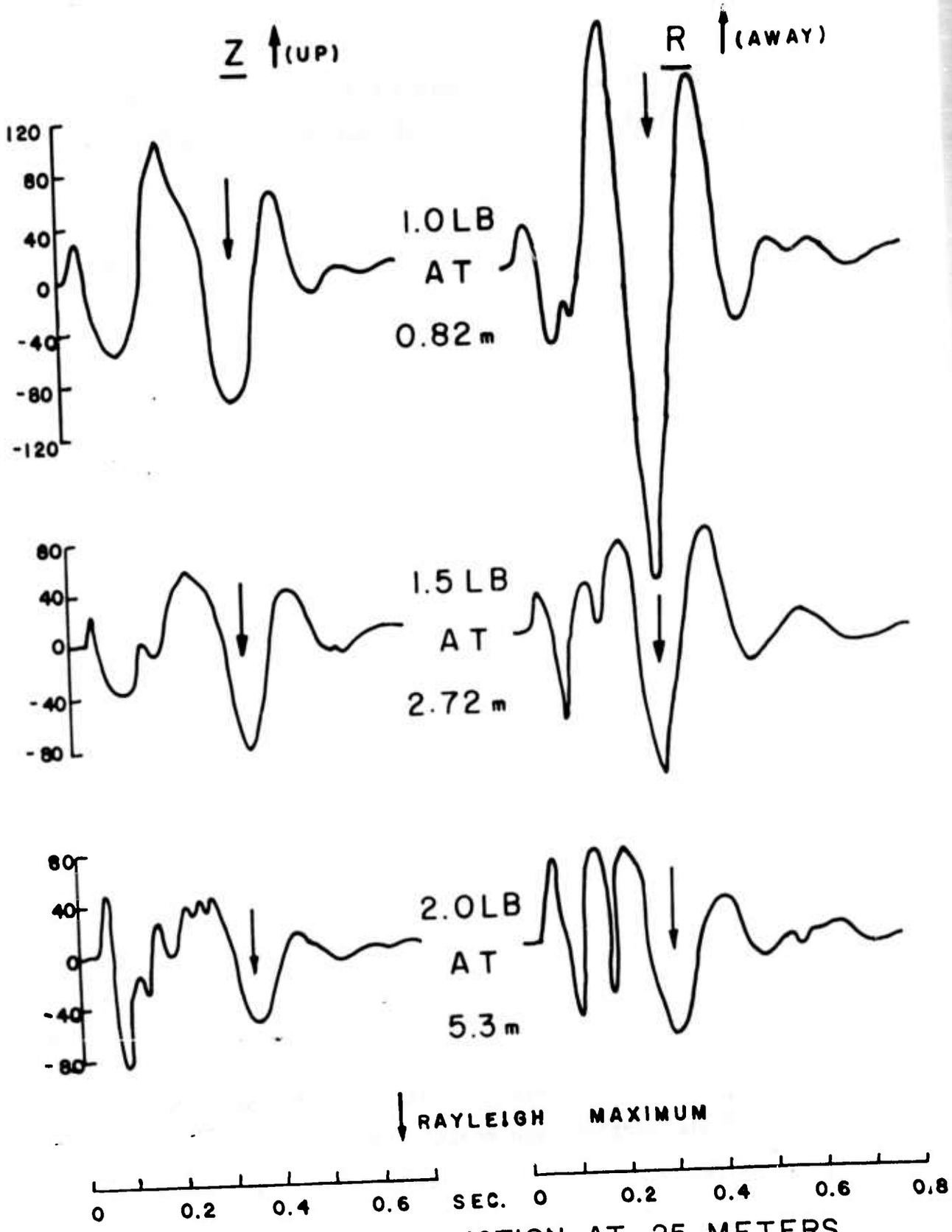

FIGURE 53. GROUND MOTION AT 25 METERS, VARIOUS SOURCE DEPTHS

Florissant test site. One sequence of 0.5 pound charges, at various depths between 1.0 and 14.6 meters, was instrumented with three-component Sprengnether seismographs aligned along a profile at 0, 2.5, 5, 7.5, 10, 15 and 25 meters. This was supplemented with the SIE refraction equipment. Two vertical geophones were placed beside each Sprengnether between 0 and 15 meters. The output of one geophone at each distance was passed through a 0 to 13 cps filter and the other through 14-100 cps. This was done in an effort to record on the high gain equipment any long period motion that might be present in the source region.

The vertical and radial components of ground motion at 2.5 meters are shown in Figure 54, and the motion at 15 meters in Figure 55. At 2.5 meters the motion from the 3 meter shot is dominated by the Rayleigh wave but this event rapidly disappears as the shot depth increases. At 15 meters the motion from the shallow shot is largely Rayleigh wave. The vertical component shows the rapid decay of amplitude of this event which appears to be totally absent at this distance from the shots deeper than 7.6 meters.

The motion from these shots was Fourier analyzed to obtain the spectrum at one distance for all depths and at all distances for one depth. The result of these analyses are shown in Figures 56 and 57. Figure 56 contains the spectra of the vertical and radial components for various distances from 0.5 pounds at 3 meters. The peak between

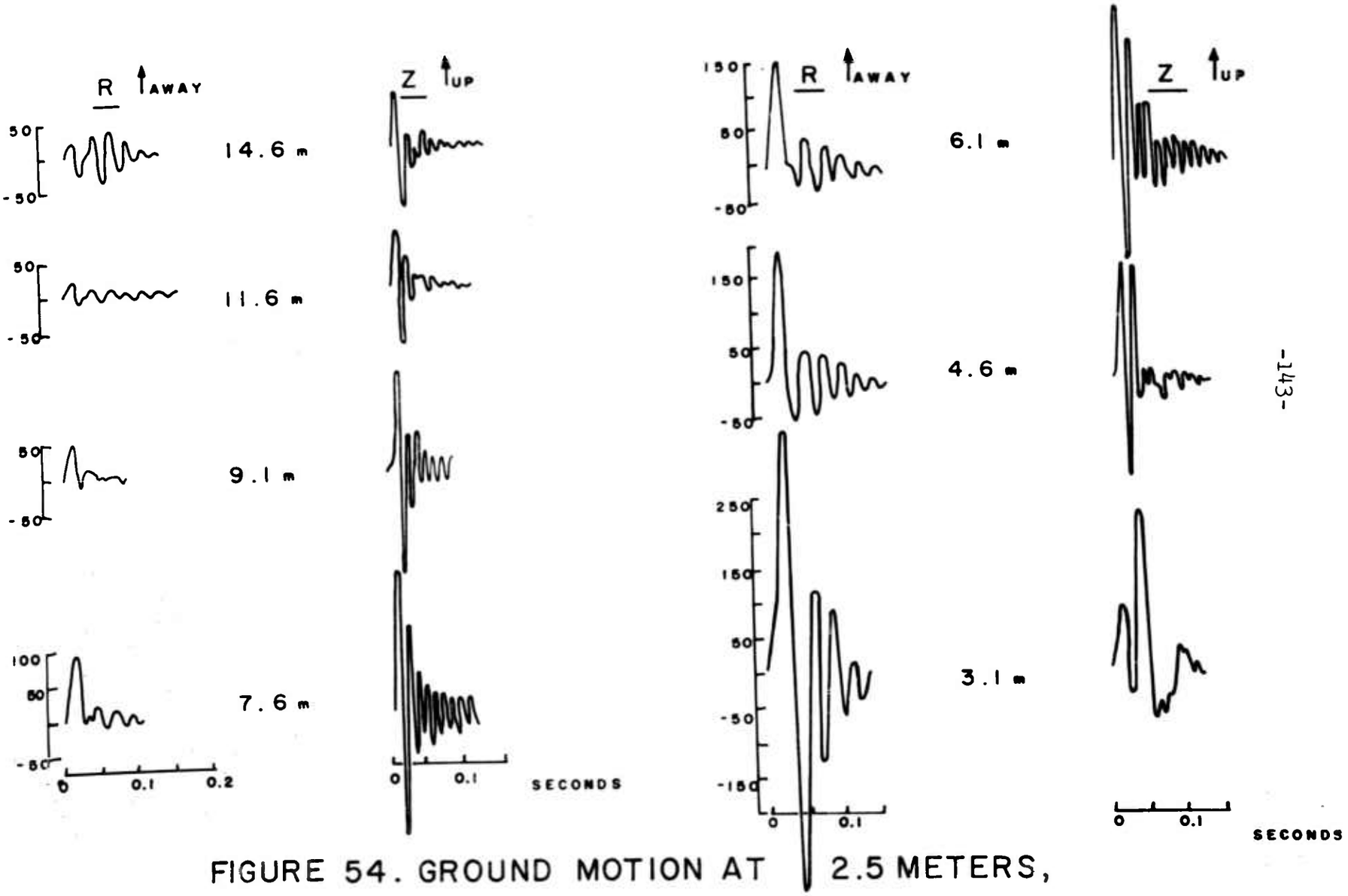

FIGURE 54. GROUND MOTION AT 2.5 METERS, VARIOUS SOURCES DEPTHS

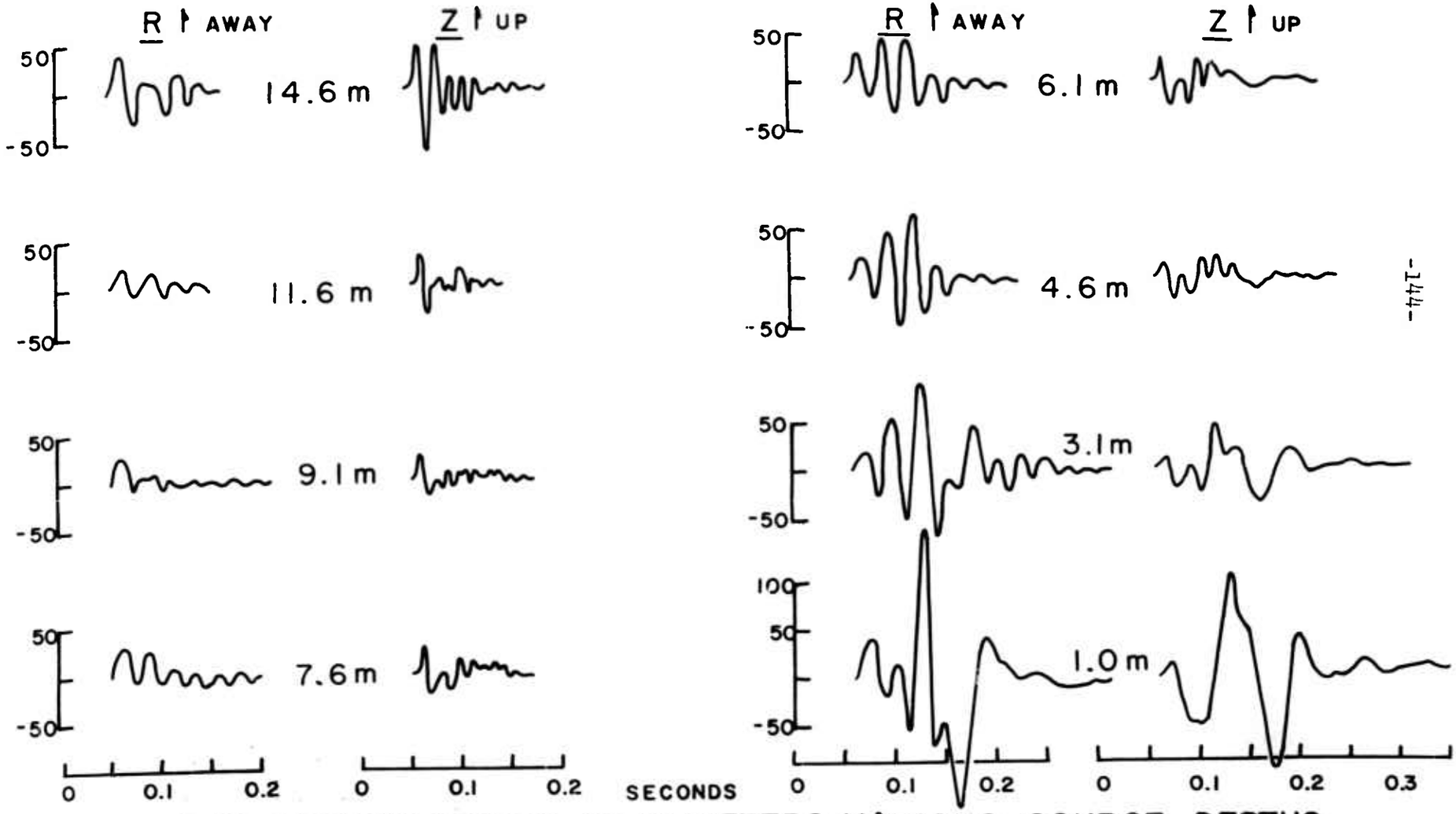

FIGURE 55. GROUND MOTION AT 15 METERS, VARIOUS SOURCE DEPTHS

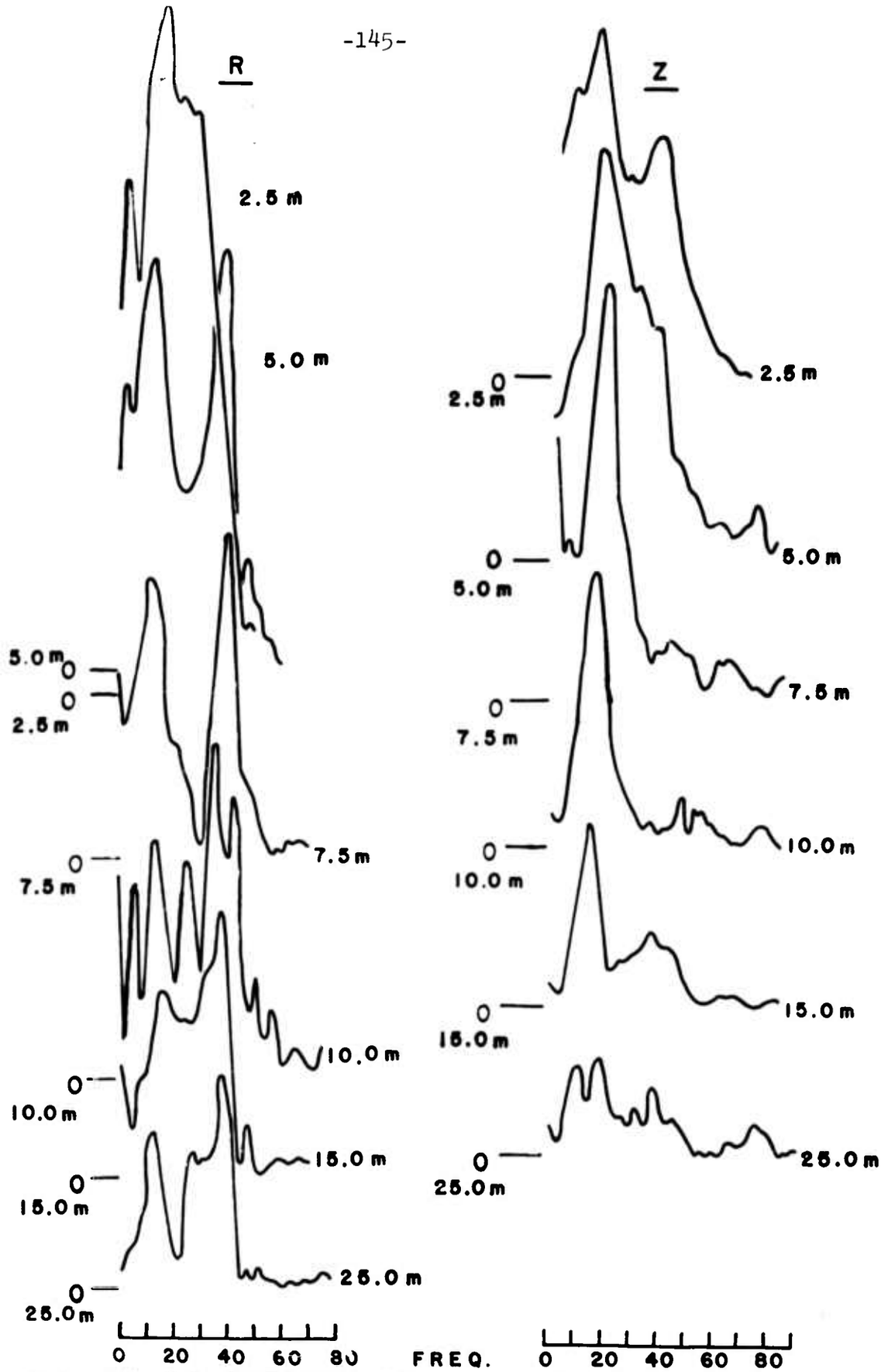

FIGURE 56. SPECTRA AT VARIOUS DISTANCES, ONE SOURCE DEPTH

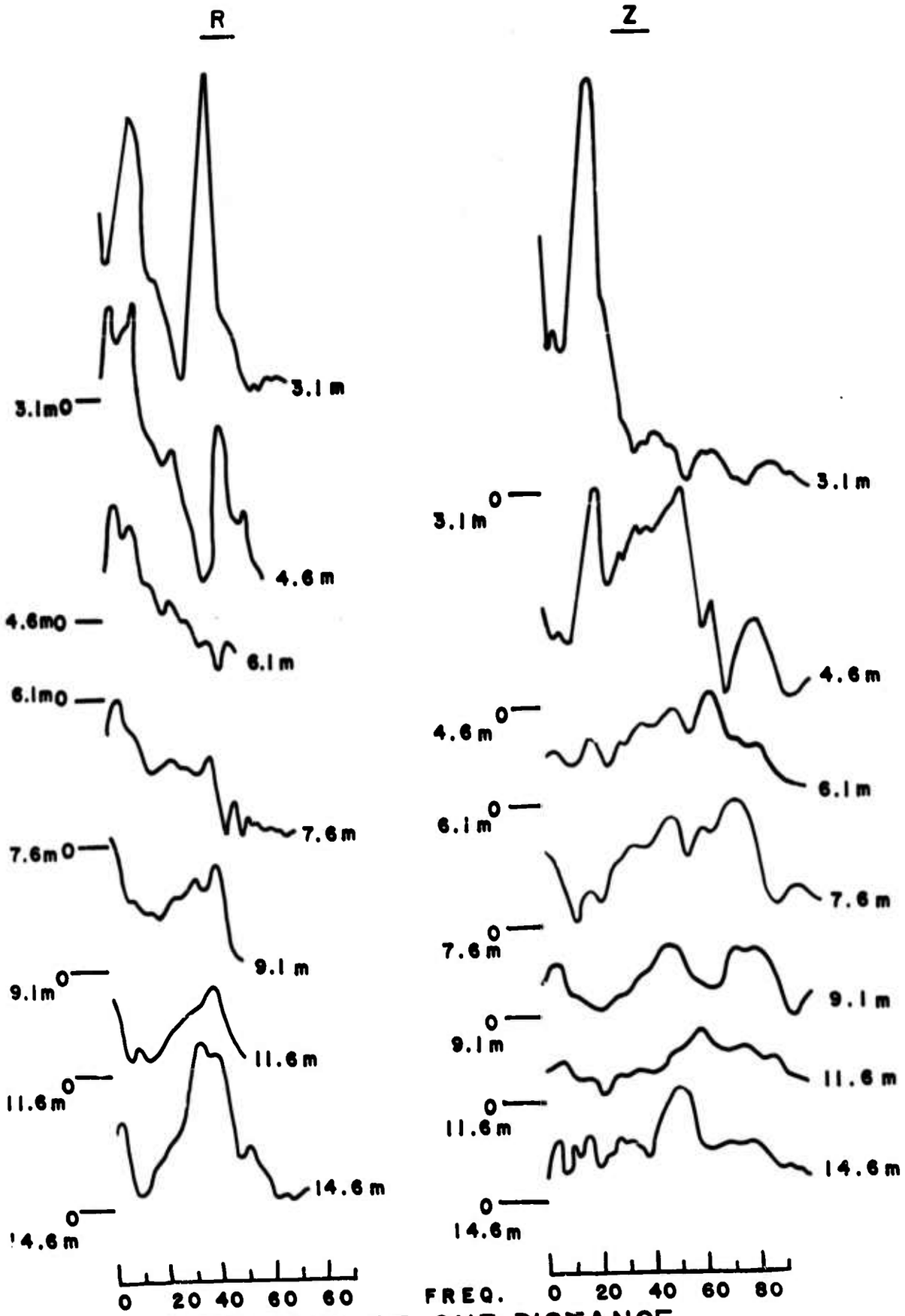

FIGURE 57. SPECTRA AT ONE DISTANCE, VARIOUS SOURCE DEPTHS

10 and 20 cps corresponds to the Rayleigh wave. The peak at 37 cps on the vertical component at 2.5 meters from the shot point is from the P-wave. As distance increases the Rayleigh energy dominates the spectrum of the vertical components. The sharp peak at approximately 40 cps on the radial component may be associated with a higher mode of the Rayleigh wave. This peak is prominent on the radial component, Figure 57, at 7.5 meters for the shot at 4.6 meters but is absent from the shot at 6.1 meters and begins to reappear on the deeper shots. This would mean that the shots at 3 and 4.6 meters are near an antinode and the shot at 6.1 meters is near a node. This figure displays strikingly the change in the energy in the Rayleigh wave as depth increases. The Rayleigh peak diminishes to the point that for shots at 7.6 meters and deeper the spectral amplitude is in the noise level in the range of 10 to 20 cps.

These data support the result derived by Nakano (1925), that there is a zone on the free surface, the radius of which depends upon the depth of the source and the velocities of the medium, within which the Rayleigh wave does not exist. This distance is given by (Ewing, Jardetzky and Press, 1957)

$$x \quad \frac{c_r h}{\left[\alpha^2 - c_r^2\right]^{\frac{1}{2}}}$$

where: h is the depth of the shot,
c_r is the Rayleigh wave velocity, and
α is the P-wave velocity.

Under the assumption that the Rayleigh wave velocity is approximately equal to the shear velocity of the upper layer, a good approximation for 12 cps (see Florissant phase velocity curve, Figure 7), the critical distances for the shots in this sequence are:

Depth (meters)	Distance (meters)
3.05	1.47
4.60	2.22
6.10	2.95
7.60	3.67
9.10	4.40
11.60	5.60
14.60	7.05

It has been shown that the Rayleigh energy is very much reduced on the records at 7.5 meters from the shots deeper than 6.1 meters, yet the table shows that this distance is near the critical distance for the 14.6 meter shot but well beyond the critical value for all others. Pekeris and Lifson (1957) calculated curves of vertical and horizontal displacement at the free surface as a function of the ratio of radial distance to depth of source for a point source. These curves showed that the Rayleigh wave was not identifiable for distances less than or equal to depth of source divided by the square root of two and was barely visible on the vertical component at five times the depth. Thus for a shot 7.6 meters deep, the vertical component of the Rayleigh wave would be poorly developed at 38 meters from the source and probably would not be recorded on the low

magnification Sprengnethers used in this experiment.

However, the filtered high gain records obtained with the SIE refraction equipment contained long-period motion, approximately 12 cps, even over the source for all depths of shots betwen 1 and 14.6 meters. This is shown for the 3 meter shot in Figure 58. This long period motion is seen to step out across the spread. The possibility that this long period motion was actually the response of the filters and amplifiers to an impulsive input was considered and rejected for the following reasons:

1) the same motion is seen on the low sensitivity traces produced by the completely mechanical Sprengnether portable seismographs; 2) the impulse response of the recording system is known (shown in the figure), and while there is a fairly long transient, for filter setting 0-13, it is not oscillatory and does not resemble the recorded motion. These records indicate that even inside the zone in which the Rayleigh wave should not exist, there is oscillatory motion of long duration. Presumably this will be true as long as the charge is buried deeply enough that no cratering takes place.

If it is true that oscillatory motion of the free surface does exist at very short range, the characteristics of this motion need to be explained. Whereas the oscillatory nature of the P-wave is predicted by simple theory, and the frequency of this wave is known in terms of the properties of

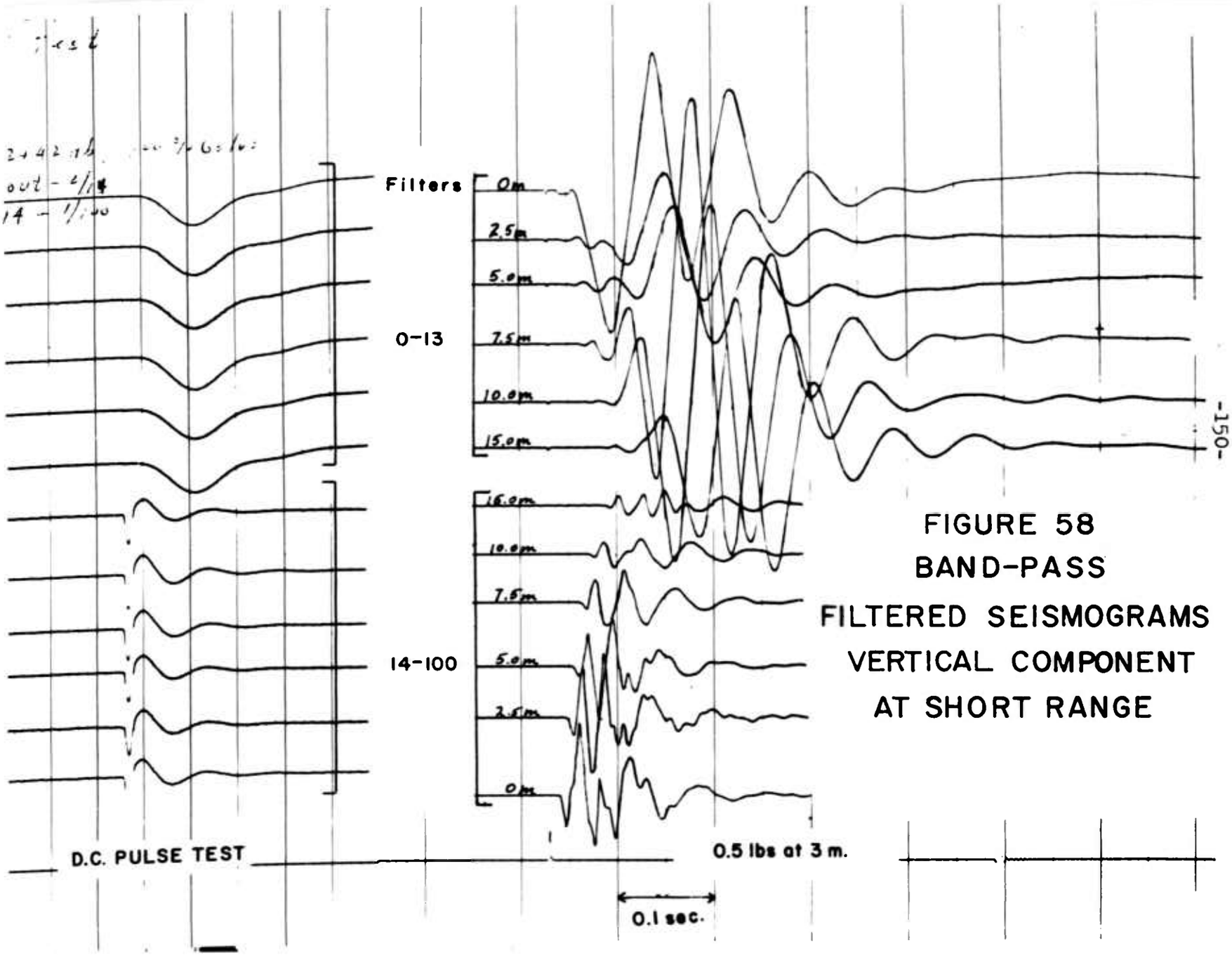

FIGURE 58
BAND-PASS
FILTERED SEISMOGRAMS
VERTICAL COMPONENT
AT SHORT RANGE

the medium, no similar theory for the Rayleigh wave at very short range is known.

Dix (1955) discussed a possible mechanism for the generation of "long waves" from explosions. His hypothesis is as follows: a) the spreading spherical pulses from a buried compressional source are converted into non-spherical secondary disturbances on striking the free surface (essentially a diffraction phenomenon); b) because of the non-spherical character, the propagation is no longer simply in the outward direction but is generally in every available direction, therefore an appreciable amount of energy goes back toward the source or toward a vertical axis through the source; c) thus, energy is held near the source and near the free surface for a long time compared with the time it takes for energy of the signal to be transmitted away from the source neighborhood; and d) this long held energy spreads outward in every available mode, one of which is the surface Rayleigh wave. Kobayashi and Takeuchi (1957) considered surface motion from a buried compressional line source. They calculated profiles of surface displacements at certain fixed times from an impulsive source. They found that the characteristic surface profile, one which persists as the basic waveform for all time, is formed between a time equal to twice the depth divided by the P-wave velocity and five times the same ratio. They related the surface motion before and after this time to the

mechanism proposed by Dix. The presence of the long period motion observed even over the shot point on the high gain refraction equipment might be considered to give support to a hypothesis of this nature for the generation of Rayleigh waves.

A deep hole drilled to 38.1 meters for velocity information was also used to gather information on Rayleigh wave generation. One and one-half pound shots were fired at 38.1 meters and at 6.1 meter intervals up the hole to a depth of 7.6 meters. These shots were recorded with the three component Sprengnethers at 2.5, 7.5, 12.5, 25, 37.5, 50 meters from the hole. The P-wave from the shots has been discussed previously.

The radial component, even at 2.5 meters, shows a pronounced arrival shortly after the P arrival on the vertical, too early to be an S-wave. This event is seen on Figure 59. Its frequency (30 cps) is lower than that of the P-wave (59 cps). At longer ranges, at which P has a radial component, this event is combined with the P-wave. There is also motion on the transverse traces at this time. The nature of this motion is not known at this time.

A second event, present on both the vertical and radial components but dominantly radial is also observed. Correlation of phases indicates that this is the motion which corresponds to the Rayleigh wave at larger distances. A computer program to calculate the travel times of all

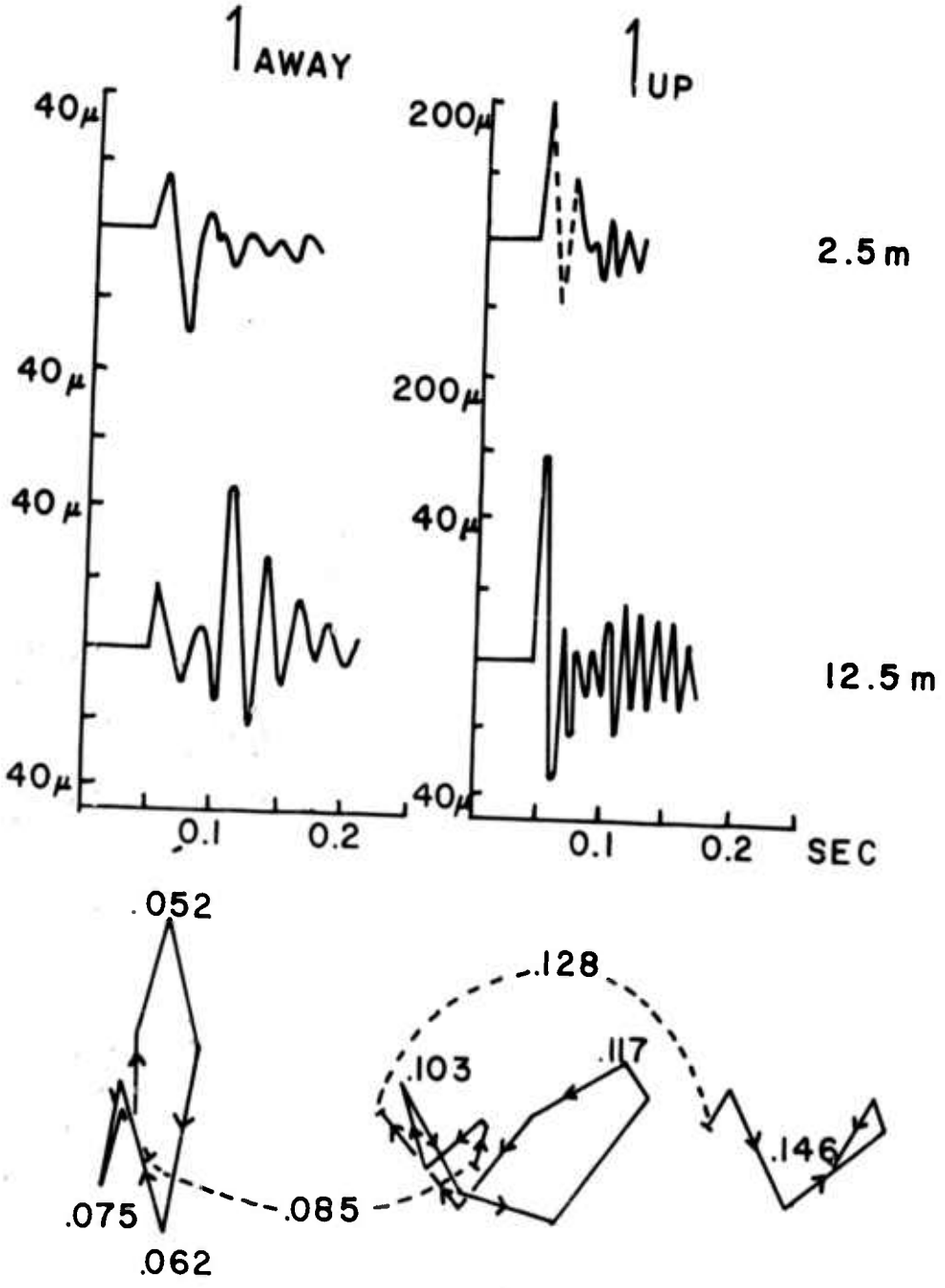

FIGURE 59
CLOSE-IN GROUND MOTION
SOURCE AT 19.8 METERS

direct, reflected, and refracted events for two layers over a half space was developed to get accurate arrival times. These calculations indicate that this event has the arrival time of a direct S-wave. The identification of this as a direct S-wave is quite important because it indicates that these contained explosions do generate sizeable SV motion, a wave type that had not been identified previously at this site, although they have been observed at Alpha and Augusta. The maximum amplitude of this event at 12.5 meters shown in the figure, is almost as large as the maximum P amplitude.

Figure 60 shows the radial and transverse components of ground motion over the hole from 0.5 pounds at 3 meters. The arrival time on both components is that for an S-wave. The motion is oscillatory in nature as it was on the deeper shots, and the rectilinear character of the particle motion may be seen.

Even though this motion converges to the Rayleigh motion it cannot be implied that it gives rise to the Rayleigh wave. The fact that the Rayleigh velocity at the frequencies generated is approximately that of the S-wave in the upper layers at this site would explain this correlation without making the assumption that the S-wave actually gives rise to the Rayleigh wave.

At the Suffield test site, only two shots of varying depth were recorded on a profile. The Rayleigh wave from the

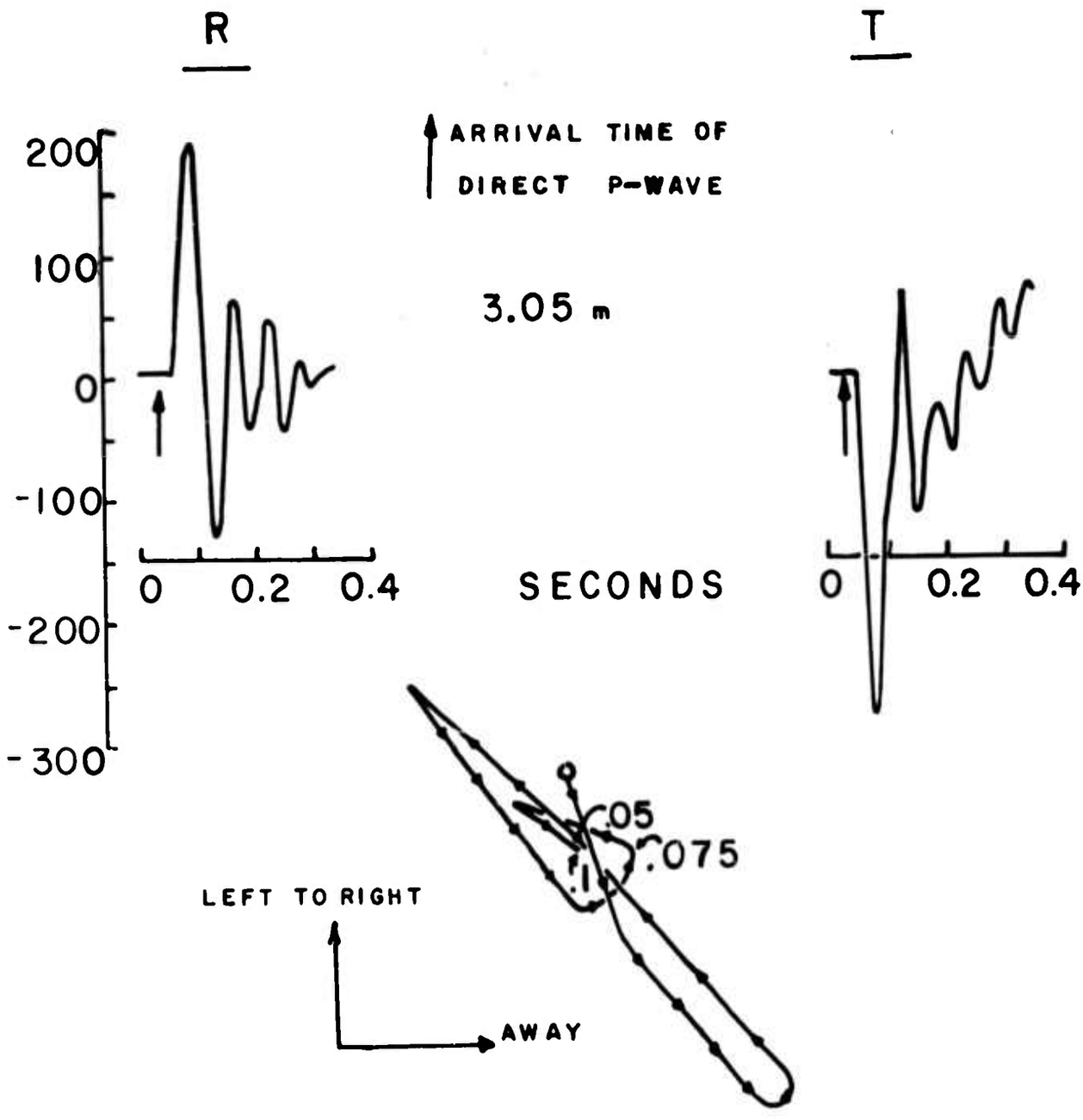

FIGURE 60

HORIZONTAL GROUND MOTION OVER THE SOURCE

SOURCE AT 3 METERS

shallower shot had less amplitude than from the deeper shot. The P-wave showed a similar effect. This is probably the result of a more efficient transfer of energy from the deeper shot even though the two shots were of equal size.

It is known that the Rayleigh wave from a surface shot should exhibit a reversal of polarity with respect to that from a deeply buried explosion. This was found to be the case at Suffield. However, at Florissant the Rayleigh motion from near-surface cratering shots and shots in water-filled pits had the same polarity as that from the buried contained explosions. The reason for the persistence of the Rayleigh wave polarity with depth of the source is not known at this time.

The reversal of polarity has been clearly observed in two-dimensional model studies of explosion-generated waves under Contract AF 19(628)-1689. In those experiments, the reversal seems to occur at a depth nearly equal to the radius of the zone of rupture produced by the explosion.

Effect of Shot Point Medium on the Seismic Signal.

The medium surrounding an explosion plays a dominant role in determining the fraction of the energy released by the explosion that appears in the form of elastic waves, and the characteristics of these waves. The manner in which the medium controls the form of the compressional waves has been discussed in the previous section. In that discussion, changes produced by relatively small variations

in material properties associated with different depths at a single test site were considered. In this section the properties of the signal produced by shallow shots in distinctly different media will be examined.

In view of the fact that the exploration seismologist has long known that the shot point material greatly affects the seismic signal, it is surprising that so little research on this subject has been published. Adams and Swift (1961) have examined the relative output of TNT charges tamped in tuff and salt, but their observation that the signal in tuff is greater than that in salt must be interpreted in the light of the work of Nicholls (1962) (Kisslinger, 1963c). Since the transmission of energy from a chemical explosion is by means of the interaction of a shock wave through the explosive material with the boundary of the hole in which the charge is placed, the ratio of impedances in the two substances is very important in determining how much energy is coupled into the earth. Results obtained for one chemical explosive in several media cannot be extended to other explosives of greatly different properties in the same media. This point is well covered in a recent work by Anderson, et al (1963). Work with nuclear explosions, which act as true point sources in that there is no detonation wave and the initial energy density is very great, indicates that the compressional wave amplitudes are in the ratio of 1: 0.25: 1.11: 1.61

for tuff: alluvium: granite: salt (Werth and Herbst, 1962).

Assuming that the theory developed by Sharpe (1942)and used in the previous section adequately describes the properties of the P-wave in terms of the inner radius of elastic response and the elastic properties of the medium, one must consider the prior question of what properties of the medium determine the size of this equivalent cavity and the amplitude of the stress at its boundary for a given yield. This leads to consideration of the very complex processes occurring in the highly stressed region around the shot.

In view of the lack of very much published data pertinent to this question, it was judged worthwhile to organize the observations that were collected during this research, and to present these as observations, with no attempt at a quantitative interpretation.

The best starting point is a comparison of records under similar circumstances in the four media in which experiments were carried out. Tracings of the field records,not reduced to true ground motion, are shown in Figure 61. The static magnification for each trace is given in parentheses following the designation of the component. Except for the sandstone record, the distances are the same. The depths are very similar, and the charge weights range from 0.5 to 2 pounds. In general, the two shots in unconsolidated material are similar to each other in frequency content and total duration of motion. The records in rock are charac-

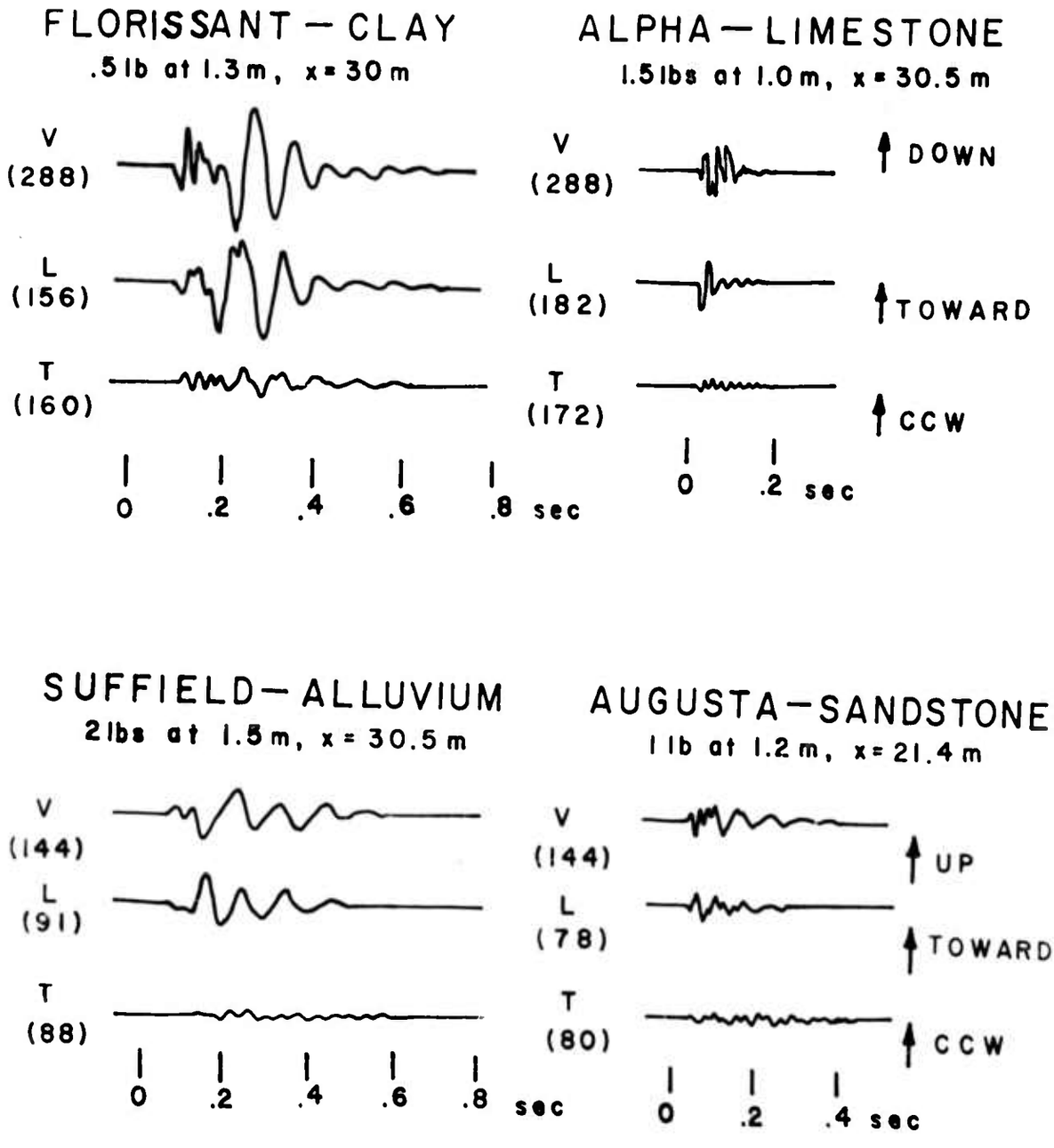

FIGURE 61
SEISMOGRAMS AT THE FOUR TEST SITES

terized by higher frequencies and shorter duration. Even at these short ranges, the records in soil are dominated by the surface wave motion, which is less well-developed for the sandstone, and smaller yet in limestone. At distances of the order of 100 meters, the body waves from these small explosions are too small to be detected with this low-gain instrumentation. The Rayleigh waves discussed in Chapter III are recorded well in both soil media, with dispersion as described previously. The Rayleigh waves in rock materials are barely detectable. In the limestone the Rayleigh wave appears as the typical non-dispersed pulses expected for a point source near the surface of a half-space.

The properties of the signals in clay, sandstone, and limestone have been compared in some detail. From the observed velocities and densities, the moduli in these media are in the ratio of 1:20:350. In the following comparisons of response, rigidity is called upon as the significant parameter, but other properties such as yield stress or viscoelasticity may actually be of equal importance.

The characteristics of body and surface waves observed at Florissant, Augusta, and Alpha are tabulated in Tables 5, 6 and 7. In this simplified analysis of the data, no attempt was made to separate geometric attenuation from absorption losses (this was done for the Rayleigh waves at Florissant and Suffield, Chapter III). Amplitudes were assumed to follow a law

$$u = u_o x^{-n}$$

and the approximate value of n for each wave type determined. This value is listed under "Attenuation Exponent" in the Tables. In general, the body waves exhibit an exponent between 2 and 3, while the value for surface waves is 1.3.

The nature of the waves at Florissant and Suffield have been discussed in the preceding chapters, as has the SH motion at all of the sites. Only a few comments need to be added to the information given in the Tables. At Alpha there is no evidence of layering at depths shallow enough to affect the recorded signals. The direct P, with primarily radial motion, and direct S wave are the only body waves identified. The S-wave exhibits both SV and SH components, in phase. The values of compressional and shear velocity give a value of 0.27 for Poisson's ratio. The velocity of the non-dispersed Rayleigh pulse is concordant with the body wave velocities.

Although the sandstone section was thought to be uniform in composition to a considerable depth, a refracted P-wave was recorded from a boundary at a depth of 15 meters. The dispersion of the indistinct Rayleigh pulse confirms the presence of some layering. A direct S-wave was identified at this site, and a refracted S-wave arrival was also picked. The SH motion on the record selected for reproduction in Figure 61 is quite small, but at other azi-

muths, motion on this component with amplitudes as large as the vertical or radial motion was recorded.

The following conclusions are drawn from all of the data examined. They pertain to small charges of dynamite in the particular media.

1) In a dense, brittle, rigid medium, the maximum ground motion is smaller than in an unconsolidated material;
2) The frequency of all events is higher in the rigid material;
3) No difference in the attenuation of surface waves was found, while the direct P wave is attenuated less in the rigid material;
4) The ratio of P to Rayleigh wave amplitudes is greater in the more rigid material;
5) Shear waves (body waves and Love waves) are bigger relative to P waves and Rayleigh waves in the rigid material. However, there are nodal lines along which the shear motion is very small;
6) The radiation of P and Rayleigh waves departs much farther from symmetry in brittle materials than it does in soft, compressible soil.

Table 5

OBSERVED EVENTS AND MEASURABLE CHARACTERISTICS IN CLAY

Event	Velocity (Meters/sec.)	Frequency (cps)	Amplitude (Microns)	Attenuation Exponent
Direct P	300	25	50-70	3
Refracted P		--	1	--
Direct & Refracted SH	--	50	--	--
	Phase Velocities			
Rayleigh	180-210	6-10	350(25m-1.5 lb) 60(100m-1.5 lb)	1.3
Prograde Rayleigh	350	10-12	30(100m-1.5 lb)	--
Love	205-260	5-10	20(100m-1.5 lb)	--

Table 6

OBSERVED EVENTS AND MEASURABLE CHARACTERISTICS IN SANDSTONE

Event	Velocity (Meters/sec.)	Frequency (cps)	Amplitude (Microns)	Attenuation Exponent
Direct P	1200	30	10-20 (20m-1.5 lb)	3
Refracted P	2500	40	4	2.2
Direct S (SH & SV)	800	40	10-15 (20m-1.5 lb)	--
Refracted S	1700	--	2	--
	Phase Velocities			
Rayleigh	900-1300	12-20	80(20m)-2(200m)	--
Prograde Rayleigh	1400	20	1(200m)	--
Love	1100-1600	15±	60(20m)	--

Table 7

OBSERVED EVENTS AND MEASURABLE CHARACTERISTICS IN LIMESTONE

Event	Velocity (Meters/sec.)	Frequency (cps)	Amplitude (Microns)	Attenuation Exponent
Direct P	4300	50	70-150 (20m-1.5 lb)	2.4
Direct S (SH & SV)	2400	80-100	40 (20m-2 lb)	--
Rayleigh	2100 (Not dispersed)	25 cps	75-1 (20-200m-1.5 lb)	1.3

APPENDIX

LARGE YIELD EXPLOSIONS RECORDED DURING THE PROJECT

Two large yield explosions were recorded during the program, neither of which met completely the requirements to provide data compatible with the seismograms from the numerous small shots. A shot of 100 tons of TNT in the form of a hemisphere was detonated by the Canadian Defense Research Board on the Watching Hill Test Site at the Suffield Experimental Station on August 3, 1961. The experiment was conducted in an expert manner by the Suffield staff and excellent seismograms were obtained, but because the charge was detonated on the free surface it proved to be a poor source for the type of studies that were included in this research.

The results of this work were reported to the Defense Atomic Support Agency and the principal conclusions were given in the Semi-Annual Technical Report No. 2 (Kisslinger, 1962). The entire set of seismograms has been published as Trial Record No. 435 by the Suffield Experimental Station (Jones, et al, 1961). This shot did not produce any unexpected seismological results. Several refracted P waves were identified that agreed in general with the results of an independent conventional refraction survey. Refracted SH waves from the same horizons were recorded, adding to the evidence that such events are a normal effect of an ex-

plosion that strongly deforms the earth materials around it. Analysis of surface waves was difficult because of the overwhelming effect of the air blast arrival and the ground motion coupled to it.

The second large shot recorded was made up of 19,000 pounds of Tovex, buried in a pattern of nine holes, 30 meters apart. The shot point was about 26 km east of Poplar Bluff, Mo., near the epicenter of an earthquake of March 3, 1963. The motion was measured on the three-component instruments at 0.9 km, and at six positions about 3 km from the source. This shot was set up and fired by the U. S. Geological Survey on June 28, 1963 in order to provide travel-time data for a portion of the mid-continent. There was no time before the expiration of the contract to analyze these seismograms, but they are of excellent quality and will be worked on in the future. The pattern of charges was set up to diminish the close-in surface waves, so that it was obviously not an ideal experiment from the viewpoint of this study.

A well-developed Rayleigh wave was recorded at all stations, as well as a very late prominent Love wave. The seismogram at the station 3.2 km to the north is of a different character than all the others, even the one at 0.9 km to the north, in that it contains short period Rayleigh-type waves (probably higher mode events) that are absent on the other instruments. A conventional refraction

record along a north-south profile that included the station at 0.9 km, and extended almost to the 3.2 km station, shows strong evidence of a shallow, buried fault, upthrown to the north, with a throw of about 100 meters, between the source and this north station (but north of the 0.9 km station). If this fault really exists, it would undoubtedly have a strong effect on the short period surface waves.

Practically nothing is known about the tectonics in this entire region of southeast Missouri, a region which is the source of many earthquakes. It is intended to follow up this lead by further geophysical investigation, employing the magnetometer and gravity meter, as well as further seismic work.

BIBLIOGRAPHY

Adams, W. M. and L. M. Swift, 1961, The Effect of Shotpoint Medium on Seismic Coupling, Geophysics, 26: 765-771.

Aki, K., 1960a, The Use of Love Waves for the Study of Earthquake Mechanism, Jour. Geophys. Res. 65: 323-332.

Aki, K. 1960b, Study of Earthquake Mechanism by a Method of Phase Equalization Applied to Rayleigh and Love Waves, Jour. Geophys. Res. 65: 729-740.

Aki, K., 1960c, Interpretation of Source Functions of Circum-Pacific Earthquakes Obtained from Long-Period Rayleigh Waves, Jour. Geophys. Res., 65: 2405-2418.

Anderson, D.C., R.D. Fisher, E. L. McDowell, A. H. Weidermann, 1963, Close-in Effects from Nuclear Explosions, TDR-63-53, Air Force Special Welfare Center, Kirtland AFB, New Mexico.

Blake, F. G., Jr., 1952, Spherical Wave Propagation in Solid Media, Jour. Accoust. Soc. Amer. 24: 211-215.

Crockford, M. B. B., 1949, Oldman and Foremost Formation of Southern Alberta, Bull. Am. Assoc. Petr. Geol. 33: 500-510.

Dix, C. H., 1955, The Mechanism of Generation of Long Waves from Explosions, Geophysics, 20: 87-103.

Ewing, M., W. Jardetsky, and F. Press, 1957, Elastic Waves in Layered Media, McGraw-Hill.

Gilbert, F., S. J. Laster, M. M. Backus, and R. Schell, 1962, Observation of Pulses on an Interface, Bull. Seis. Soc. Am., 52: 847-868.

Jones, G.H.S., C. Kisslinger, and S. A. Cyganik, 1961,Seismograms Obtained Near the 1961 Surface Burst of 200,000 lb. TNT, Trial Record No. 435, Suffield Seismic Studies No. 5, DRB Project No. D89-16-01-05, Suffield Experimental Station, Ralston, Alberta.

Jones, H. J. and J. A. Morrison, 1954, Cross-Correlation Filtering, Geophysics, 19: 660-683.

Kisslinger, C., 1953, The Effect of Variations in Chemical Composition on the Velocity of Seismic Waves in Carbonate Rocks, Geophysics, 18: 104-115.

Kisslinger, C., 1959, Observations of the Development of Rayleigh-Type Waves in the Vicinity of Small Explosions, Jour. Geophys. Res. 64: 429-436.

Kisslinger, C., 1960, Motion at an Explosive Source as Deduced from Surface Waves, Earthquake Notes, 31: 5-17.

Kisslinger, C., 1962, Seismic Waves Generated by Chemical Explosions, Semi-Annual Technical Report No. 2, Contract AF 19(604-7402).

Kisslinger, C. 1963a, The Generation of the Primary Seismic Signal by a Contained Explosion, VESIAC State-of-the-Art Report, Institute of Science and Technology, The University of Michigan.

Kisslinger, C., 1963b, Ground Motion Studies, Project U.S. 14, 1961 Canadian One-Hundred Ton High Explosive Test, Prepared for Defense Atomic Support Agency.

Kisslinger, C., 1963c, on "The Effect of Shotpoint Medium on Seismic Coupling," by W. M. Adams and L. M. Swift, Discussion, Geophysics, 28:111.

Kisslinger, C., E. J. Mateker and T. V. McEvilly, 1961, "SH Motion from Explosions in Soil," Jour. Geophys. Res., 66: 3487-3496.

Kobayshi, N. and H. Takeuchi, 1957, Wave Generations from Line Sources within the Ground. Jour. of Physics of the Earth, 5: 25-32.

Nakano, H., 1925, On Rayleigh Waves, Japan J. Astron. Geophys., 2: 233-326.

Nicholls, H. R., 1962, Coupling Explosive Energy to Rock, Geophysics, 27: 305-316.

Pekeris, C. L., and H. Lifson, 1957, Motion of the Surface of a Uniform Elastic Half-Space Produced by a Buried Pulse, Jour. Accous. Soc. Am. 29: 1233-1238.

Pollack, H. N., 1963, "Effect of Delay Time and Number of Delays on the Spectra of Ripple-Fired Shots," Earthquake Notes, 34: 1-12.

Russell, L. S., and R. W. Landes, 1940, Geology of Southern Alberta Plains, Canada Geol. Surv. Mem. 221.

Sato, Y., 1956, Analysis of Dispersed Surface Waves; I, II and III, Bull. Earthquake Research Inst., Tokyo Univ., 33: 33-48, 1955; 34: 9-18.

Sato, Y., 1958, Attenuation, Dispersion and the Wave Guide of the G Wave, Bull. Seis. Soc. Am., 48: 231-252.

Sharpe, J. A., 1942, The Production of Elastic Waves by Explosion Pressures, I, Geophysics, 18: 144-154.

Stauder, W., and C. Kisslinger, 1962, Some P and S Wave Studies of the Mechanism of Earthquakes and Small Chemical Explosions, Proceedings of the Colloquium on Detection of Underground Nuclear Explosions, Cal. Inst. of Tech. 125-129.

Vanek, J., 1954, Transitional Zone on the Classical Region for Explosions in Solid Materials, Czech. Jour. Physics, 4: 247.

Warrick, R. E., D. B. Hoover, W. H. Jackson, L. C. Pakiser, and J. C. Roller, 1961, The Specification and Testing of a Seismic Refraction System for Crustal Studies, Geophysics, 26: 820-824.

Werth, G. C. and R. F. Herbst, 1962, Comparison of Amplitudes of Seismic Waves from Nuclear Explosions in Four Media, U. of Calif. Livermore, Lawrence Radiation Lab., UCRL-6962.

Willis, D. E., 1963, A Note on the Effect of Ripple Firing on the Spectra of Quarry Blasts, Bull. Seis. Soc. Amer. 53: 79-85.

AF Cambridge Research Laboratories, Bedford, Mass., Rpt. No. AFCRL-63-701. SEISMIC WAVES GENERATED BY CHEMICAL EXPLOSIONS, Final Report, July 63, 171 p. incl. illus., tables and 34 refs.

Unclassified Report

The spectrum of explosion-generated Rayleigh waves, even at close range, may be so narrow that the source function computed by phase equalization is oscillatory. The data suggest that the medium at the shot and the geologic layering may have more influence on the spectrum than the yield does.

The radiation of Rayleigh waves from a shot distributed in space and time can be explained by single superposition. Delays due to both spatial distribution and the interval between detonations must be taken into account.

The effect of shot depth on body wave properties cannot be separated easily from the effect of changing material properties with depth. The prolonged oscillatory P-motion observed from shots in clay is the result of combining the oscillatory P-wave emanating from the source with reflections from near-surface boundaries.

SH motion is a normal effect of buried explosions. Shots in brittle media produce relatively longer shear waves. The shear energy is radiated in a lobed pattern. Shear waves radiating directly from the shot have been identified vertically above a buried source.

1. Seismic waves
2. Explosion Effects
3. Underground explosions
4. Seismology

I. Project No. 8652
Task No. 865201
II. Contract AF 19(604)-7402
III. St. Louis University, St. Louis, Mo.
IV. Flaslinger, et al
V. In DDC collection

AF Cambridge Research Laboratories, Bedford, Mass., Rpt. No. AFCRL-63-701. SEISMIC WAVES GENERATED BY CHEMICAL EXPLOSIONS, Final Report, July 63, 171 p. incl. illus., tables and 34 refs.

Unclassified Report

The spectrum of explosion-generated Rayleigh waves, even at close range, may be so narrow that the source function computed by phase equalization is oscillatory. The data suggest that the medium at the shot and the geologic layering may have more influence on the spectrum than the yield does.

The radiation of Rayleigh waves from a shot distributed in space and time can be explained by single superposition. Delays due to both spatial distribution and the interval between detonations must be taken into account.

The effect of shot depth on body wave properties cannot be separated easily from the effect of changing material properties with depth. The prolonged oscillatory P-motion observed from shots in clay is the result of combining the oscillatory P-wave emanating from the source with reflections from near-surface boundaries.

SH motion is a normal effect of buried explosions. Shots in brittle media produce relatively longer shear waves. The shear energy is radiated in a lobed pattern. Shear waves radiating directly from the shot have been identified vertically above a buried source.

1. Seismic waves
2. Explosion Effects
3. Underground explosions
4. Seismology

I. Project No. 8652
Task No. 865201
II. Contract AF 19(604)-7402
III. St. Louis University, St. Louis, Mo.
IV. Flaslinger, et al
V. In DDC collection

UNCLASSIFIED